Spring 2022

# The Role of γ-Secretase in Human Papillomavirus Infection

Mac Crite
*Yale University Graduate School of Arts and Sciences*, mac.crite@gmail.com

Abstract

The Role of Gamma Secretase in Human Papillomavirus Infection

Mac Crite

2022

Human papillomaviruses (HPV) are important pathogens that cause 5% of all human cancers worldwide, including essentially all cases of cervical cancer. Prophylactic vaccines against HPV exist, however these are not widely utilized in all communities, cannot cure existing infection, and do not protect against all subtypes. Therefore, study of HPV infection may lead to important new therapeutics to reduce the spread of the virus and disease burden. In addition, thorough investigation of HPV infection is likely to provide new insights into many aspects of cell biology and biochemistry, as the study of viruses has in the past.

HPV requires multiple cellular proteins for proper viral trafficking during virus entry, including both γ-secretase and retromer. γ-secretase is a complex of four cellular transmembrane (TM) proteins that typically binds to and cleaves TM proteins within their TM domain. During HPV infection, γ-secretase binds to the viral capsid protein L2 and facilitates its insertion into the endosomal membrane. As a result of L2 insertion, L2 protrudes into the cytoplasm, a vital step in infection that allows HPV to bind other cellular factors such as retromer. Retromer is a cytoplasmic complex of three proteins that binds to and sorts cellular cargo and HPV into the retrograde trafficking pathway.

In this thesis, we further characterize the interaction between γ-secretase and HPV L2. We show that γ-secretase is required for membrane protrusion of L2 and that L2 associates strongly with the PS1 catalytic subunit of γ-secretase. HPV infection also stabilizes the γ-secretase complex. Mutational studies of a putative TM domain in HPV16 L2 revealed that it cannot be replaced with a foreign TM domain, that infectivity of HPV TM mutants is tightly correlated with γ-secretase binding and stabilization, and that the L2 TM domain is required for protrusion of the L2 protein into the cytoplasm.

Additionally, we show that retromer and γ-secretase interact in infected and uninfected cells, and that both proteins are required for L2 protrusion into the cytoplasm. Retromer binding to L2 is required for the interaction between L2 and γ-secretase and for γ-secretase stabilization. Constitutively active Rab7, which causes retromer to remain associated with L2 on the endosomal membrane, affects complex formation between γ-secretase and L2. Finally, γ-secretase activity is required for the trafficking of a cellular retromer cargo, DMT1-II.

These results provide new insight into the interaction between γ-secretase and L2 and highlight the importance of the native L2 TM domain for proper HPV trafficking during virus entry. They also show that γ-secretase and retromer cooperate to mediate L2 membrane insertion, and suggest that binding to a cytoplasmic protein other than retromer can stabilize L2 in the endosomal membrane. Furthermore, interactions between γ-secretase and retromer may be important for the normal sorting activity of retromer.

Overall, my work in the DiMaio lab highlights the importance of γ-secretase, the HPV L2 transmembrane domain, and the interaction between γ-secretase and retromer in HPV infection. Our results highlight that detailed mechanistic analysis of individual steps in viral entry lead to discoveries that can identify novel functions of proteins that are important for cellular biology.

# The Role of Gamma Secretase in Human Papillomavirus Infection

A Dissertation

Presented to the Faculty of the Graduate School

of

Yale University

in Candidacy for the Degree of

Doctor of Philosophy

By

Mac Crite

Dissertation Director: Daniel DiMaio, MD, PhD

May 2022

# Table of Contents

# List of Figures

# Acknowledgements

I'd like to start by thanking my thesis advisor, the inimitable Daniel DiMaio. Dan, you've taught me what it means to be a scientist and how to investigate research problems not only rigorously but with such creativity and passion. It is so clear that a fantastic thesis advisor is critical to a successful PhD and I know I would not have made it this far without your guidance, suggestions, and thoughtfulness. I am so thankful for the opportunity to work with and for you, and know that the lessons and techniques, both scientific and investigative, that I learned within your lab will follow me as I progress through my career.

Next, to my thesis committee, Walther Mothes, Christopher Burd, and Akiko Iwasaki. Thank you all for pushing me and questioning me and never letting me settle for mediocrity. To Walther, it's been such a pleasure working with you both to make our department more inclusive, as well as within the scientific realm. Thank you for always asking the difficult questions and pushing me to investigate new lines of inquiry while still being supportive. To Chris, thank you for being such a rigorous scientist and fantastic mentor who always asks questions to push me to think about my project in different ways and consider new ideas. To Akiko, I truly appreciate the time you take out of your busy schedule educating the public on virology (not an easy feat!), to meet and discuss my project. I appreciate your genuine kindness, thoughtfulness, and support throughout these long years of the PhD. To all my committee members, I certainly wouldn't be the scientist I am without your help over these last few years and I am so thankful for the opportunity to get to know you all.

To all the members of the DiMaio lab, past and present, thank you from the bottom of my heart for your scientific expertise and collegiality. To Anne Edwards, thank you for always being willing to answer my (stupid) questions and for running the lab with such precision. I've definitely missed your friendship, general presence, and of course all of the dog pictures and talk since you've left the lab. To Lisa Petti, the queen of western blots and cloning, thank you for your thoughtfulness and willingness to always chat about any and all aspects of science. To previous graduate students, Erin Heim and Ross Federman, thank you for creating such a supportive environment in which to be a young graduate student and for showing me the ropes of grad school. It would not have been the same without your exuberance, Erin (or should I say Erin!), and your just general vast scientific (and musical) knowledge, Ross. I truly miss you both. To the current graduate students, Emily Branham and Patrick Buckley, good luck with all of your endeavors, I know you will both be successful in science and your lives as a whole. Finally, to the woman, the myth, the legend Jan Zulkeski, just thank you. You are so, so compassionate, kind, and generous. Thank you so much for all of the dog chats and pets, and just general willingness to listen to me. I miss you and the pups, but I know you're out there saving all the dogs.

To Suzanne Young, Gina Marie Hurley, my 'fellow fellows,' and everyone else at the Poorvu Center for Teaching and Learning, I've sincerely enjoyed every single moment of my time as a CTL fellow and working with you all. Your true passion for our work, willingness to entertain all points of view, and helpfulness has made my time at Yale so much richer. I certainly wouldn't be the educator I am without all of your support and guidance.

To Acadia Kocher, my best grad school friend, thank you for always listening to me complain and offering your commiseration, advice, and encouragement throughout this painful process we call grad school. I definitely couldn't have made it without you. To The Group, Alison Kochersberger, Scott Brown, Severin Uebbing, Alex Lin-Moore, Mark Noble, Cassie Kontur, and Andrew Adams, thanks for movie nights, beer tastings, and genuine friendship. To Chris Lim, Stephen Gaughran, and Celena Gwin, thanks for queering the heck out of Yale with me. Let's Get By (grad school), Together. To my non-scientist friends, Quentin Smith, Audrey Kentner, and John Brown, thanks for good music, good meals, and good chats with good friends. I miss y'all.

To my parents, Greg and Kelly Crite, my brother Mitch, and the rest of the family, thanks for putting up with a 7-year PhD. I love you all to the moon and back and your support means the world to me as I've worked through this difficult phase of my life. Finally, to my partner Alex Rivas, thank you for supporting me and making the big move to New Haven in such a scary and nebulous time. I can't imagine my life without you and I love you and our weirdness so much. I can't wait to see what the rest of our lives will be like together, and hopefully, one day, it'll include more concerts again. Lastly, to my pups Luna (RIP) and Rugby, grad school is hard, but having a happy puppy to come home to makes it so much easier. Grad school definitely would have been a much worse place without your snorty sounds and warm puppy cuddles. Without all of those mentioned above, and countless more who I'd have to write another 200+ page thesis to adequately thank, none of this work would have been completed. Thank you for everything.

# Chapter I: Introduction

## Papillomaviruses

The papovaviridae family was first formed in 1971 in the first report of the International Committee on Taxonomy of Viruses (ICTV) [1]. This family included small nonenveloped dsDNA viruses and two genera, *Polyomavirus* and *Papillomavirus*. The genome structure and icosahedral capsid arrangement of these two virus families are similar, leading them to be grouped together. These viruses are also causative agents of cancer and can cause growths or tumors and papillomas or warts in infected individuals. In 1999, the papovaviridae family was reclassified and split into two families, Polyomaviridae and Papillomaviridae [2]. Papillomaviridae are larger than polyomaviridae, with icosahedral capsids of about 55nm compared to the 45nm capsid of polyomaviruses [3, 4]. Both viral families infect a wide-range of hosts, including mammals and birds for polyomaviruses, and mammals, birds, reptiles and fish for papillomaviruses. Papillomaviruses are classified into over 50 genera and over 420 distinct types [5]. These viruses are highly species specific and typically can only infect one host species. They comprise two subfamilies, firstpapillomavirus and secondpapillomavirus, with only one genus and species present in the secondpapillomavirus subfamily, Sparus aurata papillomavirus 1 [4]. They are classified into subfamilies on the basis of the proteins that the genome encodes. The genome of secondpapillomavirus only encodes a minimal four proteins required for viral replication and capsid formation, while the firstpapillomavirus genome encodes at least one additional accessory protein [4]. The genome of papillomaviridae range from about 6kb to 8kb, with the canine papillomavirus 1 (CPV1)

genome being the largest at 8.6kb. The viral genome encodes four to nine proteins, grouped into two classes, early and late genes. The early genes are important for viral replication and the viral lifecycle within cells, while the late genes, L1 and L2, encode the major and minor viral capsid proteins, respectively [4].

## Human papillomaviruses

According to the International Human Papillomavirus Reference Center (https://www.hpvcenter.se/), there are over 220 distinct types of HPV. These viruses fall into five genera: α-, β-, γ-, μ-, and ν-, with the α- and β-papillomaviruses being the most widely studied [6]. HPVs are classified based on the DNA sequence of the L1 major protein, with genera sharing 60% of L1 sequence [7, 8]. Newly discovered HPVs are considered a distinct type when they share less than 90% sequence identity with already characterized HPVs. HPVs are also classified as high- or low-risk, based on their propensity to cause cancer (high-risk) or warts (low-risk). High-risk HPVs are the causative agent of multiple human cancers including cervical, vaginal, vulvar, penile, anal, and oropharyngeal. Of the ~44,000 cases of cancer that occur in these parts of the body per year in the US, HPVs cause roughly 34,800, or ~80% of these cancers [9]. HPV causes essentially all cases of cervical cancer and can account for approximately 5% of all cancers worldwide [10]. Two alphapapillomavirus types, HPV16 and HPV18 account for 70% of the cases of cervical cancer [9].

There are three licensed vaccines for HPV, all of which block infection by at least HPV16 and HPV18. Gardasil also blocks infection from two wart-causing β-papillomaviruses, HPV6 and HPV11, while Gardasil 9 blocks infection from the same four viruses as Gardasil, along with five other high-risk HPV types, HPV31, HPV33, HPV45,

HPV52, and HPV58 [11-13]. These vaccines are prophylactic and effective at preventing new infections, but they are not therapeutic and cannot be used to treat HPV infection or cancer. There are currently no approved antiviral treatments for HPV infection. The vaccines are expensive which prohibits access to them in developing areas, which typically have the highest rates of HPV infection and account for roughly 85% of new HPV infections. Even in the US, which has access to the vaccine, only 56.1% of adolescents aged 13-17 receive one dose of the vaccine and 45.4% receive the recommended two doses [14]. The high prevalence of HPV infection and low vaccination rate show that the study of HPV entry and progression is vital and may lead to new therapeutics to reduce the spread of the virus and disease burden.

## HPV entry

The HPV capsid is made up of 360 molecules of the L1 major capsid protein arranged into 72 pentameric capsomeres. L1 capsomeres form the outer viral shell. Each viral particle also has up to 72 molecules of the L2 minor capsid protein, with most viral particles having between 12 and 72 copies of L2 [15]. Prior to entry and uncoating, L2 is buried within the L1 shell and only upon multiple conformational changes does L2 become exposed [16, 17]. If expressed together, L1 and L2 self-assemble into viral particles around any piece of either cellular or viral DNA that is less than 8kb, the size of the HPV genome [18]. They can also form VLPs with just L1 and without DNA. However, the assembly of the viral particle with the chromatinized DNA helps to stabilize the particles [19, 20].

The HPV virion takes a complex route to the nucleus to infect cells, and L2 plays a major role in this entry process [19] (Figure 1.1). Initially, the L1 protein of HPV engages with heparan sulfate proteoglycans (HSPGs) on the surface of the cell [21-23]. HSPGs are

found on the surface of most cells in mammals and many viral proteins engage with HSPGs in order to enter cells [24]. The negative charge of heparan sulfate (HS) allows it to interact with various basic residues on the capsid of non-enveloped viruses and with various glycoproteins on the surface of enveloped viruses. HS binding may also be important for concentrating viral particles on the cell surface, which is especially important for HPV as the viral entry process is highly asynchronous [25]. The conformational change that occurs as a result of HPV binding to HSPGs on the surface of basal keratinocytes begins a cascade of conformational changes that prime both L1 and L2 for internalization and further trafficking events [21, 22]. L1 is first cleaved by the kallkrien 8 protease [26]. L2 is then processed by cyclophilins and furin to expose the N-terminal furin cleavage site to furin cleavage [16]. While previous reports had suggested that cyclophilins are important for furin cleavage of L2, the Campos group recently showed that furin cleavage has a minimal dependence on cyclophilins [27]. Regardless, these initial priming steps allow the virion to potentially bind to an unidentified secondary entry receptor and then be internalized into cells.

HPV is internalized via a previously uncharacterized form of endocytosis that does not require clathrin, calveolin, dynamin, or lipid-rafts, but requires actin dynamics [28]. After endocytosis, HPV localizes to early endosomes. A low-pH dependent conformational change to L1 within the endosome causes a portion of the L1 major capsid protein to disassociate from the L2 minor capsid protein and the viral genome. After this, the steps that mediate endosome escape of the sub-viral particle are complex and only now beginning to be characterized. HPV is known to bind multiple proteins localized to the cytoplasm to coordinate trafficking of the virus to the nucleus for infection (eg: [29-33].

To allow binding to these cellular factors, there is a cell penetrating peptide (CPP) in the C-terminus of L2 [34]. Typically, CPPs are thought to act as short segments that can transfer proteins into cells. A well-studied CPP from the HIV Tat protein has been shown to allow Tat to enter cells [35, 36]. Much of the research into this peptide has focused on its therapeutic potential in mediating cellular entry of drugs. In contrast to HIV Tat CPP, whose role in biology is obscure, we believe the CPP from HPV L2 appears to mediate intracellular transfer of protein segments between cellular compartments. The CPP of L2 protrudes through the endosomal membrane which then allows L2 to bind to cellular proteins such as retromer and promote proper trafficking of the virus [34].

After L2 C-terminal protrusion, L2 binds directly to retromer, a cytoplasmic protein complex comprised of three subunits (VPS26, VPS29, and VPS35), to facilitate sorting of HPV into the retrograde pathway [31, 37]. Retromer plays a role in the recycling of many cellular cargoes, and mutations within two subunits, VPS29 and VPS35 are associated with neurodegenerative diseases, such as Alzheimer's disease (AD) [38-40]. Retromer recruitment to the endosomal membrane is regulated by cargo binding as well as the cellular proteins Rab7 and various SNX family proteins. Rab7A and Rab7B are both important for HPV infection and, in contrast to cellular cargo, cycling of Rab7 between its GDP and GTP bound states is vital for productive infection [37, 41-43]. Perturbations to retromer function, such as protein knockdown or chemical inhibition; mutations within the retromer binding site (RBS) or CPP of L2; or alterations to Rab7 function, such as the use of dominant negative or constitutively active forms, or protein knockdown; block HPV infection and cause the virus to accumulate in the endosome at late time points [31, 34, 37, 42, 44]. Additionally, we have shown that a peptide derived from a portion of the C-

terminus of L2 which includes both the CPP and RBS, sequesters retromer away from the virus, causes HPV accumulation in the endosome, and blocks HPV infection [44]. Once HPV successfully binds retromer, the virion is trafficked along the retrograde trafficking pathway inside retrograde transport compartments and transported to the nucleus for productive infection.

Another important cellular protein in HPV entry is the γ-secretase complex [45-47]. γ-secretase is a protein complex comprised of four subunits, all of which have at least one transmembrane (TM) domain. Typically, γ-secretase recognizes and cleaves TM proteins, such as Notch and the amyloid precursor protein (APP), within their TM domain. An siRNA screen from our lab showed that knockdown of any one of the four γ-secretase subunits causes a block in infection by disrupting trafficking, and the use of a chemical inhibitor of γ-secretase, compound XXI, also causes a severe defect in HPV infection [37]. Additionally, mutations within a conserved putative TM domain in HPV L2 block γ-secretase binding, severely inhibit infection, and cause HPV to not traffic properly to the TGN [48, 49]. It has been shown that γ-secretase can cleave within the putative TM domain of L2, but cleavage of L2 does not appear to be required for productive infection. Interestingly, γ-secretase binds to L2 and helps promote stable membrane association of L2 [49]. However, the mechanistic details of membrane insertion, membrane protrusion, and stable membrane association have not fully been elucidated.

Once HPV is bound to retromer after C-terminal protrusion of L2, the sub-viral particle disassociates from retromer and traffics to the trans-Golgi network. Although the arrival of the viral particle at the TGN is important for eventual nuclear entry of L2 and the viral DNA, the distinct role that the TGN plays in HPV infection is not yet known. HPV

requires the onset of mitosis in order to translocate L2 into the nucleus [50]. To assess translocation of HPV L2, the Campos group appended the large 35 kDa BirA biotin ligase to the end of L2 in intact pseudoviral particles. The 15-residue biotin acceptor peptide (BAP) can be biotinylated only by BirA and is expressed in the cytoplasm fused to GFP. If BirA on the C-terminus of L2 can reach the cytoplasm, BAP will be biotinylated, and biotinylation can be detected via western blot with neutravidin. Using this system, it was reported that HPV L2 requires both TGN egress and the progression of mitosis to translocate into the cytoplasm. Blocking the onset of mitosis with chemical inhibitors traps viral particles in the TGN and inhibits biotinylation of BAP, and thus translocation of L2. Additionally, an L2 mutant that is non-infectious and trapped in the TGN does not translocate, again indicating that the viral particle needs to somehow leave the TGN in order to translocation across the membrane. However, the use of a large protein tag on the C-terminus of L2 by Campos may alter the requirements for membrane penetration at this step. Indeed, using a split GFP assay, we saw protrusion of the C-terminus of L2 at very early times post infection (~3h), a time during which the viral particles are in the endosome [34]. Additionally, it is clear that the BAP/BirA translocation system is not measuring endosomal protrusion since the viral particles will have left the endosome many steps prior to reaching the TGN or nucleus. However, it is not known how many of the multiple L2 proteins in each capsid protrude at any given step so it is possible that some L2 molecules may protrude at the endosome to bind retromer, and then other L2 molecules protrude after the TGN for an unknown function.

After egress from the TGN, viral particles have been visualized in the ER through the proximity ligation assay (PLA) and colocalization [47, 51]. A role for the ER has not

been identified and ER localization has been reported by some groups while others fail to see localization. The virus then requires the breakdown of the nuclear envelope, as occurs during mitosis, to gain access to the nucleus where the viral DNA and L2 protein colocalize with PML bodies [52]. Throughout these complex trafficking steps, the genome of the viral particle remains within membrane bound vesicles, as the genomes were inaccessible to small non-membrane permeable dyes until after the completion of mitosis [53, 54]

## HPV L2 Putative Transmembrane Domain

There is evidence that HPV L2 contains a putative transmembrane (TM) domain (Figure 1.2). Several TM prediction algorithms gave high probabilities of a TM domain in the N-terminus of L2 [48]. The different modeling programs give slightly different specific sequences for the amino acids within this putative TM domain, but most center around a region from amino acids 46-67 in the N-terminus of L2. It was also observed that the TM sequence of L2 can tether RFP on HeLa cell membranes, indicating that this sequence can act as a TM domain in mammalian cells [48]. Additionally, this L2 segment can function as a TM domain, which was shown by testing TM functionality and oligomeriztion using the bacterial ToxLuc system [48]. This system measures TM functionality through the addition of a TM domain of interest into a ToxR-MBP (maltose-binding protein) construct. Proper insertion of the TM sequence into the membrane is measured in a bacterial strain that lacks the ability to grow on media with maltose as the sole carbon source. If the TM sequence is properly inserted into the membrane, the MBP on the protein will complement the mutant bacterial strain and allow for growth on medium with maltose as the only carbon source. Additionally, this system measures oligomerization of the TM domain through the ToxR transcriptional activator. This protein requires dimerization to activate luciferase

expression. Therefore, if the TM domain in this ToxR-MBP fusion protein is able to self-associate, luciferase expression can be observed. Through this assay, it was shown that the TM domain of L2 can function as a TM domain and can oligomerize in bacterial membranes [48]. Oligomerization of L2 has not been assessed or reported in mammalian cells.

Antibody staining after selective membrane permeabilization in infected cells also suggests an N-terminal protected region of L2, as epitopes C-terminal of the putative TM domain were accessible to antibody staining, but those N-terminal of the putative TM domain were inaccessible [54, 55]. There is also a highly conserved stretch of glycines in the second half of the TM domain (Figure 1.3). Many TM domains have GXXXG motifs and these could contribute to the dimerization of L2's TM domain or its interaction with γ-secretase. Indeed, mutations at two of these residues, glycine 57 and glycine 61, block HPV infection, association with γ-secretase, and trafficking to the Golgi [48, 49]. Individually, the mutations also block the ability of this TM sequence to oligomerize, as assessed by the ToxLuc system, but do not inhibit the insertion of this sequence into the bacterial membrane, as these mutants can grow on media with maltose as the sole carbon source [48].

Finally, extensive mutational analysis of this N-terminal region was conducted by the Jung group [56]. They generated N-terminal alanine scanning mutations in the region from amino acid 13-78 in HPV16 L2. They found multiple residues within this region to be absolutely required for infection, including C22, C28, D31, and D43. Although none of the required residues are within the putative TM domain, there were seven residues in the TM domain that were labelled as either important or less important for infection, indicating

that their mutation to alanine decreased HPV infection, but did not completely abrogate it. Importantly, these experiments were carried out in CHO-K1 hamster kidney cells, and thus the relevance of these residues to HPV infection in native host cells, such as HeLa and HaCaT cells still needs to be determined. This group also showed that a lipopeptide containing a region N-terminal of the TM domain, from amino acids 13-46, can efficiently block HPV infection by multiple HPV types and in multiple relevant cell lines [56]. They did not determine the mechanism of action of this peptide or convincingly show which step in HPV infection it blocked. They showed that the peptide did not block internalization of HPV and hypothesized that it is acting at an early step in infection.

A TM domain or other membrane spanning region of L2 is likely required for infection. In order to bind to retromer in the cytoplasm, L2 must either gain access to the cytosol completely by being ejected from the membrane and residing entirely in the cytoplasm, or have a membrane anchoring region, which would keep L2 embedded within the membrane and only allow some of the protein access to the cytoplasm. The current literature described above supports the existence of the membrane anchoring region, and not the existence of L2 in a fully soluble state.

## γ-secretase

γ-secretase is a membrane-embedded aspartyl protease that binds to and cleaves type I transmembrane (TM) proteins within their TM domain [57] (Figure 1.4). γ-secretase plays an important role in cleaving substrates and allowing for signaling events that are required during embryonic development, such as the cleavage of the Notch1 intracellular domain. γ-secretase has also been described as a "proteasome of the membrane" because

it removes any membrane stubs that are left behind after ectodomain shedding of substrates [58].

The γ-secretase complex includes four subunits: presenilin 1 (PS1), presenilin enhancer 2 (PEN2), anterior pharynx defective-1 (APH1), and nicastrin, all of which have at least one TM domain [59-61]. PS1 has nine TM domains and is the catalytic subunit of the complex, responsible for the proteolytic cleavage of substrates [62]. Recent structural work has shown that two substrates, Notch and APP, bind directly to the PS1 subunit and it is known that two conserved aspartic acids in the active site of PS1 are vital for substrate cleavage. However, APP and Notch interact with different TM domains within PS1 [63, 64]. This could explain why there is so much heterogeneity in the sequence of γ-secretase substrates, as the substrates can interact with PS1 in different ways. Once the four subunits of the γ-secretase complex come together, PS1 undergoes endoproteolytic cleavage to generate the N-terminal fragment (NTF) and C-terminal fragment (CTF), both of which are incorporated into the mature γ-secretase complex. A GxGD motif within TMD7 of PS1 is important for γ-secretase activity and the "x" residue is thought to be able to discriminate between substrates. A leucine at this position allows for the cleavage of APP and Notch, while a phenylalanine at this position blocks Notch cleavage [65].

The other components of the γ-secretase complex play an important role in substrate recruitment (nicastrin), complex stabilization (APH1), and final complex formation (PEN2) [66]. Nicastrin has one TM domain and a large extracellular domain that binds to and recruits substrates to the complex [67]. Nicastrin also undergoes a maturation process before the γ-secretase complex is fully functional and active. The protein is highly glycosylated and only the highly glycosylated form is stable and incorporated into the

mature γ-secretase complex [68]. APH1 likely acts as a stabilizer and scaffold for the complex and helps mature γ-secretase traffic to the proper subcellular location. APH1 has seven TM domains that interact with PS1 and nicastrin [62]. APH1 forms a pre-complex with the immature nicastrin protein and plays a role in the maturation of nicastrin [69, 70]. This APH1-nicastrin subcomplex is recruited to the immature PS1 protein before maturation of either protein occurs. PEN2 has two TM domains and has been described as the "linchpin" and finalizer of the maturation and assembly of the γ-secretase complex [66]. PEN2 directly binds to PS1 and is recruited to the complex last [61, 71]. Its interactions with PS1 regulate the endoproteolysis of PS1 into the NTF and CTF [61, 72-76]. PEN2 does not only regulate the endoproteolysis of PS1, but also appears to increase the activity of the γ-secretase complex, as co-expressing it with pre-cleaved PS1 NTF and CTF enhances the generation of cleavage products [77]. Once PEN2 has bound to the immature trimeric precomplex, made up of immature nicastrin, the PS1 holoprotein, and APH1, the now complete γ-secretase complex can undergo proteolysis of PS1, and leave the ER where it then traffics to the Golgi for full glycosylation and maturation of nicastrin [78, 79].

Substrate recognition by and recruitment to the γ-secretase complex is complicated and not currently well understood [80, 81]. While the vast majority of γ-secretase substrates are type I TM proteins, with their C-terminus cytoplasmic and their N-terminus extracellular or luminal, one type II TM protein and one polytopic TM protein have been reported to be recognized and cleaved by the γ-secretase complex [82, 83]. Additionally, γ-secretase does not appear to have a substrate recognition binding motif that is present in the known γ-secretase substrates [84]. The known γ-secretase substrates are diverse in their structure, function, and cellular localization, and there are few similarities between

substrates [85]. Many substrates require γ-secretase cleavage to allow for further signaling events, while for others, the role of γ-secretase cleavage has not yet been determined. The only requirement for γ-secretase substrates that has been described is the presence of a short ectodomain, similar to the short N-terminal region of L2 [86-88]. Some substrates have a large ectodomain that is shed in the membrane by membrane proteases such as alpha and beta-secretase prior to γ-secretase engagement, while others have a naturally short ectodomain [89]. The requirement for a short ectodomain can be explained by the structure of the γ-secretase complex and arrangement of nicastrin within it. Nicastrin, which initially interacts with substrates through its large ectodomain, hangs as a "lid" over the top of the γ-secretase complex and blocks the active site [62, 88, 90]. Its large size does not allow for proteins with a large ectodomain to interact properly with it or the γ-secretase complex. While a small ectodomain is critical for γ-secretase cleavage of substrates, it is not sufficient as not all proteins with short ectodomains are substrates of γ-secretase [91]. There is evidence that the juxtamembrane sequences outside of the TM domain can play a role in γ-secretase recognition of substrates and that the conformational flexibility of the substrate TM domain itself could be important for γ-secretase recognition [91, 92]

## γ-secretase and HPV L2

γ-secretase activity is vital for HPV infection. Our group and others have shown that inhibiting the γ-secretase complex blocks the ability of HPV L2 to traffic to the TGN [45-47, 49]. Decreasing protein expression of γ-secretase via siRNA or shRNA knockdowns or CRISPR knockouts, or inhibiting γ-secretase activity through chemical inhibitors completely blocks infection. In fact, the γ-secretase inhibitor XXI is the strongest inhibitor of infection that has been described. γ-secretase recognizes TM proteins which is

consistence with the current hypothesis that there is an N-terminal TM domain within L2 [48].

We have used two approaches to show that γ-secretase binds to HPV L2. First, in a co-immunoprecipitation experiment from cell extracts, where the PS1 subunit of γ-secretase was immunoprecipitated, HPV co-IPs with PS1 and nicastrin (the other γ-secretase subunits were not assessed for binding) [49]. Second, in an in vitro binding assay using purified γ-secretase and a GFP-fusion protein that contained amino acids 13-72 of HPV L2 (which contains the TM domain), L2 co-IPs with PS1, indicating that L2 binds directly to γ-secretase somewhere within this N-terminal segment [49]. γ-secretase can also cleave L2, in or around the TM domain, although cleavage is poor and most of L2 remains uncleaved. Interestingly, L2 cleavage by γ-secretase does not appear to be required for infection. A PS1 mutant (F237I), is a proteolytic mutant that cannot cleave substrates or HPV L2, but can support HPV infection [49]. PS1 KO cells that were reconstituted with the F237I mutant and infected with HPV, allowed for L2 membrane insertion and HPV infection, however L2 was not cleaved. The vital role of γ-secretase in HPV infection appears to be to promote membrane insertion of L2. Stable membrane association is assessed using a carbonate extraction assay, where cells are infected, homogenized, and treated with a high pH buffer to remove non-integral proteins from the membrane, but leave TM proteins within the membrane. A portion of L2 inserts into the membrane, and inhibiting γ-secretase, or decreasing γ-secretase expression blocks membrane insertion of L2 [49]. Thus, it appears that the main role of γ-secretase in HPV infection is to promote stable membrane association of L2, although the mechanism for stable membrane association and insertion has not yet been described.

A recent report from the Tsai and DiMaio labs has provided insight into how HPV is recognized by γ-secretase [93]. There are many γ-secretase adaptor proteins that bring substrates to γ-secretase [84, 94]. One such adaptor protein is p120 catenin, a member of the catenin-cadherin complex, which recruits cadherins at the cell surface to γ-secretase at the endosome for processing [95, 96]. Harwood et al showed that knocking down p120 expression blocks HPV infection, and that there is an interaction between p120 and HPV L2 very early during infection as shown through co-immunoprecipitation experiments [93]. They then went on to show that a mutant γ-secretase that can't bind p120 doesn't support infection, indicating that the interaction between p120 and γ-secretase is important for HPV infection. While this report shows how HPV is targeted to γ-secretase and that a p120 knockdown blocks the association between γ-secretase and HPV, the full viral and cellular requirements for membrane association of L2 and the association between γ-secretase and L2 are not yet understood. One of the main goals of this thesis work is to determine these requirements.

## Retromer

Retromer is a cellular protein complex that regulates the recycling of proteins within the cell, typically from the endosome to the Golgi, but also from the endosome to the plasma membrane [97]. Retromer was first discovered in yeast as an essential cellular component that recycled VPS10 from the endosome to the Golgi [98, 99]. Retromer consists of three proteins: VPS26, VPS29, and VPS35. VPS35 acts as a scaffold that VPS26 and VPS29 bind to, with VPS26 associating with the N-terminus of VPS35 and VPS29 associating with the C-terminus [100, 101]. These three proteins comprise the cargo recognition complex (CRC) and were previously thought to be solely responsible for

directly recognizing and binding to the cargo molecules. However, recent structural evidence suggests that both the CRC and sorting nexins (SNX) are important for cargo binding. An x-ray crystal structure of VPS26, VPS35, SNX3, and part of the retromer cargo DMT1-II shows that there is a binding site for cargo at the interface between VPS26 and SNX3 [102].

Sorting nexins are adapter proteins that help facilitate the recruitment of retromer to membranes and membrane remodeling. In yeast, reports showed that the SNX-BAR dimer made up of VPS5 (SNX1/2 in humans) and VPS17 (SNX5/6 in humans), directly binds to the core retromer trimer and induces membrane remodeling and stabilization of the retromer-SNX complex [98, 103]. However, more recent reports, especially those in higher eukaryotes suggest that the SNX-BAR proteins may not directly bind to retromer and may instead be able to facilitate retrograde trafficking of cargos, such as CIMPR, alone [104, 105]. Indeed, the association between the SNX-BAR dimers and retromer is weak, and high-resolution stimulated emission depletion (STED) microscopy shows that these two protein complexes are in distinct sub-areas of the endosomal membrane [104, 105].

Besides the SNX-BAR dimer, there is evidence that other SNX proteins associate with retromer to perform distinct functions. SNX3 is an adaptor protein that recruits retromer to membranes, and, as mentioned above, binds to cargo along with VPS26 [106-108]. VPS26 undergoes a conformational change to engage with SNX3 and create a binding pocket for the cargo molecule [102]. Although this complex is important for the trafficking of multiple cellular cargos, such as Wntless, DMT1-II, and the transferrin receptor [107, 109, 110], it is not known how this retromer-SNX3 complex accomplishes the formation of transport vesicles or tubules, and thus retrograde trafficking. SXN27 is

another sorting nexin that binds to retromer and helps retromer to facilitate the trafficking of cargo proteins from the cell surface to endosomes. Similar to SNX3, SNX27 binds to VPS26, albeit through a different mechanism than SNX3 [111, 112]. SNX27 may also bind to cargo although this has yet to be sufficiently demonstrated [113]. These various sorting nexin adaptor proteins allow for modulation of the core retromer trimer and for recognition of many different types of substrates that have many different final destinations.

A final set of retromer interactors and regulators includes Rab7 and TBC1D5. Rab7 is a small GTPase that binds directly to an N-terminal region of VPS35 in the core retromer trimer in its GTP-bound form and disassociates from retromer in its GDP-bound form [108, 114]. Rab7-GTP binding to retromer allows for retromer recruitment to the endosomal membrane, and is strongest when Rab7 is in its GTP-bound, active state. TBC1D5 is a Rab7 GTPase-Activating Protein (GAP) that regulates the cycling of Rab7 between its GTP- and GDP- bound forms [115-117]. Cycling of Rab7 is not necessary for cellular cargo to traffic properly through cells, and only the active, GTP-bound Rab7 is necessary for the typical cellular cargo proteins [115]. Overexpression of TBC1D5 causes retromer to disassociate from membranes by hydrolyzing Rab7-GTP into its inactive form, Rab7-GDP [117].

## Retromer and HPV L2

Retromer and many of its associated proteins, such as Rab7, TBC1D5, and multiple sorting nexins are vital for HPV infection [29-31, 37, 41-43]. Perturbing retromer function in any way blocks HPV trafficking to the TGN, and most perturbations cause endosomal accumulation of HPV at late time points post infection [31]. We have shown this through multiple experiments where we decreased retromer expression via knockdown and

performed a proximity ligation assay (PLA), which allows us to localize incoming viral particles to particular cellular compartments. At eight hours post infection (h.p.i.), HPV typically resides in the endosome, regardless of retromer function. At 16 h.p.i., most virus has moved from the endosome to the TGN. When retromer expression is decreased (or perturbed in other ways), HPV accumulates in the endosome at 16 h.p.i [31]. Through multiple co-IP experiments and mutational analysis, we have shown that retromer binds directly to the C-terminus of L2 through FYL and YYML motifs [31, 37]. A canonical retromer binding motif, WLM, can replace the FYL sequence in L2 and allow for retromer binding of L2 and productive infection of this mutant virus. A mutant where both retromer binding motifs are mutated to alanine, termed the double mutant, is defective for infection and also accumulates in the endosome. Additionally, a small peptide that contains the retromer binding site of L2 and the cell penetrating peptide, is internalized into cells, and binds to retromer to sequester it away from incoming viral particles [44]. Treatment with this peptide results in endosome accumulation of HPV and potently blocks infection in both cell culture and animal models, while a similar peptide without the retromer binding site does not inhibit infection. This indicates that blocking retromer binding to L2, and not just the presence of this peptide, is the mechanism by which HPV infection is inhibited.

Rab7 and its associated GAP, TBC1D5, are also necessary for HPV infection [41, 42]. The use of a Rab7 knockdown or catalytic mutants of Rab7 (constitutively active or dominant negative forms) blocks HPV infection and cause accumulation in the endosome. Knocking down TBC1D5 expression, or regulating its function through the use of a small transmembrane protein, also blocks HPV infection and causes endosomal accumulation [42]. Through the use of the dominant negative and constitutively active forms of Rab7,

we have shown that Rab7 cycling is essential in allowing retromer to disassociate from the incoming viral particles and promote proper trafficking, as the use of either mutant form of Rab7 blocks infection and causes endosomal accumulation [42]. The constitutively active form of Rab7 causes increased retromer binding, likely because it cannot disassociate from the membrane. The dominant negative form of Rab7, on the other hand, blocks retromer binding to HPV entirely, likely because this mutant of Rab7 does not recruit retromer to the membrane.

Various sorting nexins are also important for HPV infection. The Banks group has shown that HPV L2 interacts with SNX17, a retrograde sorting protein, through a conserved NPxY motif in the middle of L2 [29]. Knocking down SNX17 expression decreases HPV infection and causes a defect in late-trafficking steps. Consistent with a role in retrograde trafficking of the viral particle from the endosome to the TGN, blocking SNX17 activity does not affect the arrival of HPV at the endosome. Furthermore, the related sorting nexin protein, SNX27 also binds to HPV and contributes to infection, although to lesser degree than SNX17 [30]. Overall, this abundance of data shows that retrograde trafficking, retromer regulation by accessory proteins, and retromer binding to HPV L2 is important for infection and perturbing these interactions in any way blocks HPV entry and infection.

## Retromer and γ-secretase

While retromer and γ-secretase act at different steps in HPV infection, both are necessary for endosomal escape of HPV. This suggested that there might be a coordination between these two proteins to allow for HPV infection. Previous reports in the literature show that mutations within both protein complexes, as well as within their accessory

proteins, such as the sorting nexin adaptor family for retromer, are associated with the development of various neurodegenerative diseases, such as Alzheimer's disease (AD) and Parkinson's disease (PD) [38-40, 118-121]. AD pathogenesis occurs as a result of improper γ-secretase mediated cleavage of the amyloid precursor protein (APP) and increasing production of the amyloidegenic AB-42 peptide [122]. Less is known about PD pathogenesis, but it is characterized by a decrease in dopaminergic neurons [123].

Unsurprisingly, many mutations within all four subunits of the γ-secretase complex are associated with AD pathogenicity [121]. Most of these mutations are in the PS1 subunit, which is consistent with its role as the catalytic subunit of γ-secretase. Mutations within VPS35 are associated with increased AD pathogenicity and with late-onset PD [40, 124, 125]. Multiple separate single-amino acid mutations in VPS35 are found associated with PD patients. Additionally, both VPS26 and VPS35 expression are reduced in the brains of AD patients [126]. Mutations in patients that alter the function of various SNX family members can either increase or decrease the pathogenicity of AD, depending on the SNX protein that was targete [127]. Both SNX17 and SNX27 are involved in AD progression. SNX27 interacts with γ-secretase to inhibit improper processing of APP [128]. SNX27 can also associate with another retromer cargo protein, SORLA, and with it, regulate the trafficking of APP [129]. SNX17 directly binds to APP and decreasing SNX17 levels in cells decreases APP levels [130].

Outside of their role in AD and PD pathogenesis, the retromer complex and γ-secretase complexes interact. A previous report shows that VPS35 and PS1 co-IP both in cells and in mice [131]. Additional reports show that both γ-secretase and APP traffic through the retrograde trafficking pathway in order to be recycled, although it is not clear

if they traffic through the retromer-dependent retrograde trafficking pathway [132]. These associations between γ-secretase and retromer could be hijacked by HPV in order to leave the endosome, traffic to the nucleus, and efficiently infect cells.

## Cell-penetrating peptides (CPPs)

Cell-penetrating peptides (CPPs) are short protein sequences that can penetrate cellular membranes and deliver attached cargo into cells. The first two CPPs that were discovered were in the HIV Trans-Activator of Transcription (Tat) protein and in the antennapedia homodomain, a transcription factor from *Drosophilia melanogaster*. Both proteins were shown to efficiently enter cells, and the shortest sequence that mediated cellular uptake was identified and described as a cell-penetrating peptide. For HIV Tat, this sequence is RKKRRQRRR, and for the antennapedia homodomain, the CPP is called penetratin and has the sequence RQIKIWFQNRRMKWKK [35, 36, 133, 134]. These sequences represent basic, or cationic CPPs, however CPPs that are hydrophobic, ampipathic, and anionic have also been discovered [135, 136].

While CPPs have been isolated and characterized from a variety of organisms, the biological role of only a few of these CPPs is known. For example, one role that has been described for the CPP of the antennapedia homodomain is to enter neuronal cells and promote neuronal differentiation [137], although this result is disputed. The HIV Tat protein, on the other hand, regulates viral transcription, but it has not been shown whether this regulation is from secreted Tat that reenters cells, or if it is from Tat that is produced inside a particular cell [138]. Our results described below imply that CPPs may have other activities entirely, namely to transfer proteins between different cellular compartments and possibly to convert soluble proteins into TM proteins. The majority of the research into

CPPs focuses on their potential role in drug delivery, as opposed to their normal biological functions. The ability of CPPs to efficiently enter into cells while attached to either large or small cargo molecules makes them attractive candidates for drug development. Researchers have developed CPPs for a variety of biomedical applications, including delivery of dyes for imaging [139] and delivery of drugs for therapeutic applications, such as targeting tumors [140], or destabilizing prion formation [141].

The mechanism of action for CPPs is not known, and due to the chemical diversity of the penetrating sequences, it's likely that they function in different ways. One hypothesis for cationic CPPs is that there could be electrostatic interactions between the positively charged amino acids and negatively charged proteoglycans on the surface of cells [142]. The CPP would then be internalized through endocytosis after these initial interactions. It is unclear if endocytosis or another type of cellular uptake is the mechanism by which CPPs are taken up by cells. Other groups have proposed direct penetration of the CPP, pore-formation or micelle-formation by the CPP, and receptor- or transporter- mediated uptake with interactions between unknown receptors or transporters and the CPP, among others [143-147]. No clear mechanism has been described that encompasses the internalization of the vast variety of CPPs that have been discovered or engineered.

Another hurdle for CPPs is endosomal escape. Once internalized CPPs typically reside in the endosome and must escape to perform their desired function within the cell. Again, due to the wide variety of CPPs, there are likely multiple mechanisms that these short peptides use to access the cytoplasm. One aspect that is generally accepted as being important for endosomal escape is concentration of the peptide [148, 149]. Direct penetration of the CPP from the endosome to the cytoplasm has been seen for some CPPs,

but only once they reach a high enough concentration on the membrane [148]. It has also been suggested that high concentrations of CPPs in the endosome can cause "endocytic leakage" which eventually causes rupture of the endosome [150, 151]. The rupturing of endosomes would be highly toxic to cells, therefore other mechanisms are likely involved for CPPs that do not cause obvious cytotoxicity [147]. Additionally, for therapeutic applications, cellular toxicity is not ideal, so other mechanisms that allow for cytoplasmic localization are likely involved and important for these CPPs.

## Assays to measure endosomal escape of CPPs

Many methods have been developed to measure cellular penetration of CPPs [147]. For CPPs, the two most relevant categories of assays include those that measure total cellular uptake and those that measure cytosolic localization. It is important to differentiate between total cellular uptake and cytosolic location because assays that measure total cellular uptake measure CPPs and cargo that are still membrane-embedded and those that remain trapped within the endosome, as well as those that have escaped into the cytoplasm [147]. Many CPPs that are attached to cargo will perform their function in the cytosol, such as CPPs attached to drugs that have cytosolic targets, and thus they must escape from the endosome. In these cases, measuring total cellular uptake is important, but insufficient to properly characterize and optimize such CPPs.

One method that can be used to measure endosomal escape is ultracentrifugation followed by western blotting or other quantitative assay such as mass spectrometry [152, 153]. In a cell uptake assay, where CPP internalization is measured by performing western blotting or quantitation on cell lysates, a major drawback is that the cell lysate includes everything within the cell. However, if the cytosolic fraction is separated from the other

fractions using ultracentrifugation, the amount of CPP-cargo complex localized to the cytosol can be assessed. This can be compared to the amount of CPP-cargo complex in the total cell lysate to get a measure of cytosolic localization, and thus endosomal escape. A caveat to this type of assay is that complete subcellular fractionation is difficult, time intensive, and it is hard to confirm separation of the different cell fractions [147]. Assays have also been developed that rely on the generation of cytosolic fluorescence. For example, a pH-sensitive dye, such as napthofluorescein could be conjugated to the CPP-cargo complex [154, 155]. Napthofluorescein is not fluorescent at the lower pHs found in the endosome (~pH 5 or 6), but fluoresces when it reaches the neutral pH of the cytosol. One caveat to this method is that fluorescence would be generated in any neutral cellular compartment, as well, and this would therefore need to be distinguished from cytosolic fluorescence, perhaps through microscopy [147]. Another way to measure endosomal escape is through expression or fluorescence of a reporter protein. One of these assays is the split reporter protein assay, where a fragment of a protein, such as GFP or luciferase, is added to the CPP-cargo complex [156, 157]. The other portion of the protein is expressed in the cytoplasm. If the CPP-cargo complex is able to escape the endosome and access the cytosol, it will complement the protein fragment in the cytosol and produce fluorescence or protein expression [156-158]. Lastly, assays have been developed that measure direct cytosolic interaction with a protein, such as the farnesylation penetration assay and the biotin ligase assay [159, 160]. In the biotin ligase version of this assay, the short biotin acceptor peptide (BAP) is appended to the CPP-cargo complex and BirA, a biotin ligase, is expressed in the cytoplasm [161]. The BAP is not biotinylated by eukaryotic biotin ligases, and can only be biotinylated by BirA if the CPP-cargo complex can access the

cytoplasm [162, 163]. Biotinylated proteins can be visualized by western blotting to assess cytoplasmic localization. Each of these assays have advantages and disadvantages and it is likely that multiple assays should be used to assess endosomal localization of a particular CPP-cargo complex.

## CPPs and HPV L2

A "membrane-destabilizing peptide" exists at the C-terminus of L2 which is important for infection and endosomal exit of HPV, and has been described as a cell-penetrating peptide after extensive characterization [34, 164]. All known HPVs have a similar basic CPP region with at least four basic residues, typically a combination of lysine (K) and arginine (R), terminating in the three residue stretch RKR. Many of these CPPs appear in multiple sequenced papillomavirus L2 proteins; the most abundant sequence is KRRKR, found in 17 papillomavirus L2 proteins and the second most abundant sequence is RKRRKR, found in 16 papillomavirus L2 proteins including HPV16 L2. There are over 160 different CPPs found in at least one papillomavirus L2 protein, all of which likely have different cell-penetrating efficiencies due to their chemical differences. The HPV16 CPP can be replaced by other cationic CPPs, such as that from HIV Tat, and the resulting virus retains wild-type levels of infection and proper subcellular trafficking [34]. In HPV16 at least, the native cationic CPP cannot be replaced by an ampipathic or hydrophobic CPP, and the CPP sequence requires at least four arginine residues, as a three-arginine mutant is noninfectious. This is consistent with the fact that all sequenced papillomaviruses have at least four basic residues in their CPP region.

This CPP region mediates the protrusion of HPV L2 into the cytoplasm. Using a split-GFP assay [157, 165], our group showed that the basic region is vital for L2 protrusion

into the cytoplasm, in order to bind retromer [34]. In this assay, seven copies of GPF11 are appended to the C-terminus of L2 in intact viral particles, and GFP1-10 is expressed in the cytoplasm of cells. Alone, these two components do not fluoresce. However, if the C-terminus of L2 is able to protrude into the cytoplasm upon infection, GFP will be able to self-assemble into an active, fluorescent protein that can be observed using live-cell confocal microscopy. Through this experiment, we showed that the C-terminus of L2 protrudes to the cytoplasm to produce reconstituted fluorescence at early time points post-infection. This protrusion step occurs by three hours post infection, a time during which incoming viral particles reside in the endosome. Without this protrusion step, L2 is unable to access retromer in the cytoplasm or traffic to the TGN. In the absence of a CPP in L2, HPV accumulates in the endosome, which is the same phenotype caused by other viral mutations that block retromer binding. We also showed that short peptides and fusion proteins containing both the CPP and some of the surrounding L2 sequence are able to enter cells, thus this sequence can act as a CPP in the absence of full-length L2 [34, 44]. C-terminal protrusion of L2 is essential for retromer to bind L2, and is therefore indispensable for HPV infection. While we know that L2 protrudes into the cytoplasm and that this protrusion step requires a basic region at the C-terminus of L2, we do not have the full picture of what protrusion requires. CPPs are typically thought to work without help from chaperones or other proteins, however there could be other proteins important for HPV infection that play a role in mediating protrusion of L2. One major goal of this thesis is to determine the requirements for endosomal protrusion of L2 and determine if other proteins in HPV infection, such as retromer or γ-secretase, are important for protrusion.

## Figures

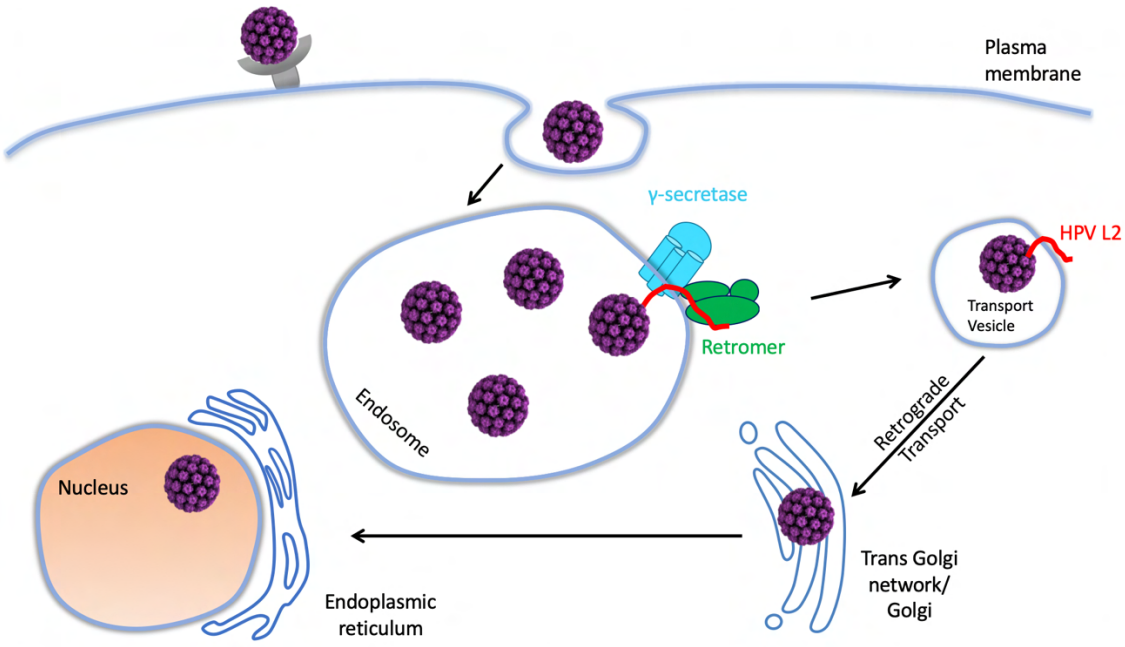


***Figure 1.1: HPV Entry***

Human papillomavirus takes a complex route to the nucleus. Upon binding to heparan sulfate proteoglycans on the surface of a cell, HPV is internalized into the endosome. Once in the endosome, through the action of a cell penetrating peptide on the C-terminus of the L2 protein, L2 protrudes through the endosomal membrane in order to bind retromer, which sorts the viral particle into the retrograde trafficking pathway. The γ-secretase complex plays an important, yet undefined role in this process. Once out of the endosome, HPV traffics to the trans-Golgi network, and eventually the nucleus to infect a cell.

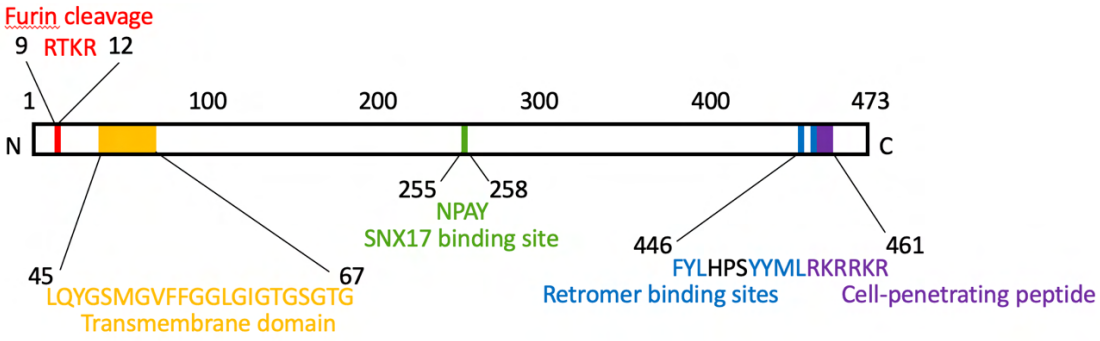


***Figure 1.2: Schematic of HPV L2 protein***

A schematic of the HPV16 L2 protein depicting important motifs such as the furin cleavage site (red) and putative transmembrane domain (orange) in the N-terminus of L2. The retromer binding site (blue) and a cell-penetrating peptide (purple) are found in the C-terminus.

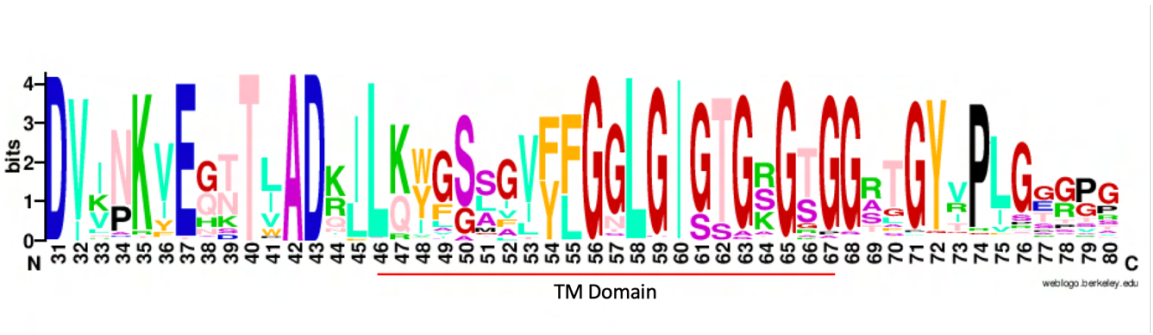


***Figure 1.3: Conservation of the L2 transmembrane domain***

A sequence logo showing conservation of residues in and around the putative transmembrane domains from over 300 papillomavirus types. The putative TM domain is underlined in red. Note that the stretch of highly conserved glycines at the C-terminus of the TM domain is unusual, as is the fact that the TM domain is less hydrophobic than typical TM domains.

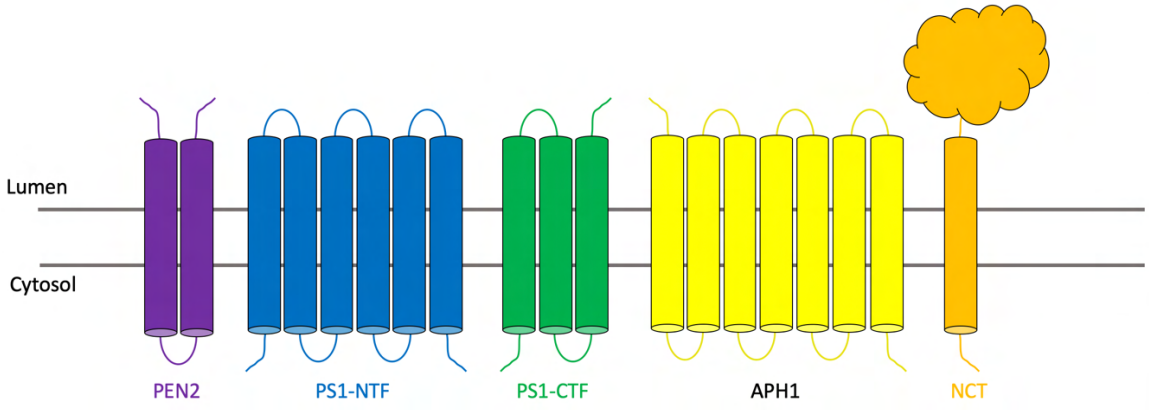


***Figure 1.4: The γ-secretase complex***

A schematic of the γ-secretase complex showing all four components of the complex. PEN2 binds directly to the N-terminal fragment of PS1 and APH1 binds to both the C-terminal fragment of PS1 and nicastrin. Nicastrin has a large ectodomain thought to be important for substrate recognition. Once the four components of the complex associate, PS1 undergoes endoproteolysis between the 6$^{th}$ and 7$^{th}$ TM domains to form the PS1-NTF and PS1-CTF. PEN2 – purple, PS1-NTF – blue, PS1-CTF – green, APH1 – yellow, nicastrin – orange

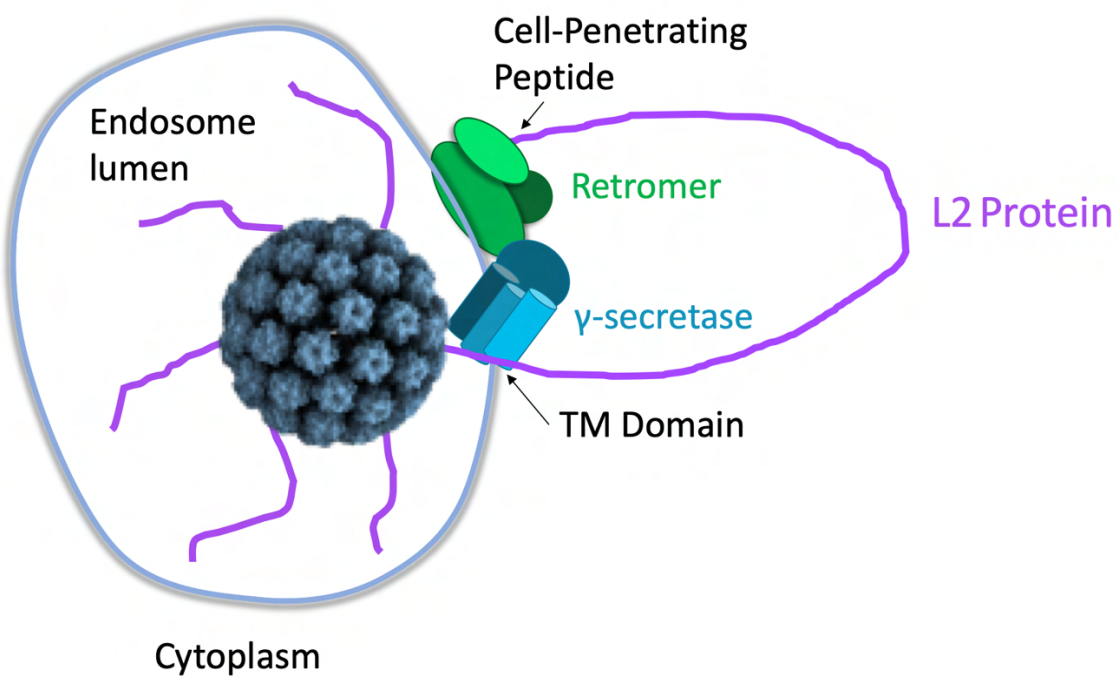


***Figure 1.5: HPV L2 C-terminal protrusion model***

A model of the protrusion of HPV L2 into the cytoplasm once HPV is in the endosome. C-terminal protrusion is vital for allowing HPV to bind to cellular factors in the cytoplasm, such as retromer.

# Chapter II: Characterization of the interaction between γ-secretase and HPV L2, and its role in mediating HPV infection

## Introduction

The γ-secretase complex is indispensable for HPV infection. γ-secretase is a transmembrane protease that typically binds to and cleaves within the TM domain of proteins. This allows the resulting cleaved protein to perform its function, typically in signal transduction or activating other signaling events. Many groups have reported that γ-secretase is necessary for HPV infection at an early step [45-47, 49]. Our group showed that γ-secretase binds to and promotes proper trafficking of HPV through the retrograde transport pathway [47, 49]. In the absence of γ-secretase function, HPV is able to bind to and be internalized into cells, localizing to the endosome at 8 hours post infection (h.p.i.), but the viral particles are unable to traffic to the TGN or bind to retromer. It is not known where the virus localizes when γ-secretase activity is inhibited or γ-secretase binding to L2 is blocked, but we do know that the virus does not accumulate in the endosome, as is seen under conditions when the viral particle cannot bind retromer [31, 49]. Additionally, although γ-secretase cleaves HPV L2, the main role of γ-secretase in HPV infection appears to be somehow promoting membrane association of HPV L2, although this role could be direct or indirect [49]. Inhibiting γ-secretase blocks membrane association of L2,

which subsequently blocks the ability of retromer to bind and properly sort HPV into the retrograde pathway [49].

A recent report from our collaborators in Billy Tsai's lab at the University of Michigan describes an important role for p120-catenin, a γ-secretase adaptor protein that brings substrates to γ-secretase [93]. In HPV infection, the function of p120 is to deliver the viral particle to γ-secretase at early time points. If p120 expression is knocked down, HPV infection is blocked and L2 can't bind to either p120 or γ-secretase. A mutant PS1 protein that cannot bind to p120 does not support HPV infection. This shows that p120 binding to both HPV and γ-secretase is important for HPV infection.

One of the main goals of this thesis work is to determine the role that γ-secretase plays in HPV infection and the mechanisms by which it accomplishes this role. While we know that γ-secretase is important and appears to assist in a membrane association step of HPV L2, there are still many unanswered questions. We do not know, for example, if HPV associates with only a few subunits of the γ-secretase complex or all four subunits. Association with only a few subunits would be unlikely, as the proteins within the γ-secretase complex are unstable if not in the complex, however it is a possibility. While *in vitro* work has shown that residues 13-72 in L2 are able to bind to purified γ-secretase, and we would predict that the putative TM domain (residues 46-67) would bind to γ-secretase because γ-secretase binds and cleaves within the TM domain of its other substrates, we have not narrowed down the amino acids that are important for γ-secretase association with L2 [48, 49]. Importantly, we do not know if γ-secretase is directly promoting the membrane association of HPV or if there are accessory proteins that are playing a role in this process.

Additionally, we have not yet fully characterized the protrusion step in infection. We know that protrusion occurs early in infection (~3 h.p.i., as shown with a split-GFP assay), is mediated by the CPP on the C-terminus of L2, and replacing the RKRRKR CPP sequence with RRR (3R mutant) blocks infection and protrusion [34]. We know that blocking protrusion with the 3R mutant causes endosomal accumulation and the inability of viral particles to access or bind to retromer. We hypothesize that γ-secretase would play a role in protrusion since γ-secretase activity is important for membrane association of L2, however this hypothesis has not yet been tested.

## Results

### Characterization of the interaction between γ-secretase and HPV L2

Previous work from our lab showed that L2 binds to γ-secretase and that inhibiting γ-secretase activity blocks infection and trafficking of the viral particle to the TGN [47, 49]. We used both in vivo and in vitro coimmunoprecipitation experiments to show that the γ-secretase subunits PS1 and PEN2 bind directly to HPV L2 [49]. The binding of the other subunits of γ-secretase was not assessed. Here, I used a co-IP to assess binding of all four subunits to HPV PsV. HPV PsV contains the L1 and L2 capsid proteins encapsidating a reporter gene of choice. Quantitation of reporter gene expression is used as a proxy for infection, and interaction between HPV and cellular factors can be assessed using a FLAG tag on L2. HeLa cells were infected with HPV16 PsV for 16 hours. Cells were lysed in a lysis buffer containing the mild detergent, decyl maltose neopentyl glycol (DMNG), which solubilizes membranes but maintains transmembrane (TM) protein complexes. L2 was immunoprecipitated using an antibody that recognizes the FLAG tag on its C-terminus. Samples were then subjected to SDS-PAGE and western blotting using antibodies that

recognize the subunits of γ-secretase. Figure 2.1 shows that all four subunits are found in the immunoprecipitates from infected, but not uninfected cells. This shows that HPV is in a complex with all four subunits of γ-secretase, an expected result as the γ-secretase complex is unstable if any subunit in it is not present.

I then asked if the interaction between HPV and γ-secretase required the HPV L2 protein. Previous *in vitro* binding experiments using purified γ-secretase and a GFP fusion protein containing a short segment of the N-terminus of L2 suggested that L2 alone was sufficient for γ-secretase binding [49], however we wanted to know if the interaction between HPV and γ-secretase required the L2 protein during infectious viral entry. HPV virus-like particles (VLPs) can be generated using a plasmid that only contains L1 and GFP. This plasmid is packaged by L1 as the viral genome and also used to produce the L1 capsids. HeLa cells were infected with L1-only VLPs for 16 hours. They were lysed in a lysis buffer containing 1% n-dodecyl-β-D-maltoside (DDM) buffer and immunoprecipitated using an antibody that recognizes PS1. DDM is another mild detergent that maintains TM protein interactions while still permeabilizing membranes. Samples were analyzed by SDS-PAGE and western blotting for HPV and γ-secretase subunits. As shown in Figure 2.2, L1-only particles do not bind to γ-secretase, suggesting that L2 is necessary for the interaction between γ-secretase and HPV.

We then wanted to explore the interaction between γ-secretase and HPV more extensively and assessed which γ-secretase subunits bound most tightly to HPV16 L2. In these experiments, cells were lysed in a lysis buffer containing varying concentrations of mild (DDM) and more stringent (NP40) detergents. Previously published work has shown that the γ-secretase complex can be disassociated through the use of different detergents

[166].The complex first disassociates into two subcomplexes of APH1/Nicastrin and PS1/PEN2. Under the most stringent conditions used, the complex will disassociate into the four individual subunits. I infected HeLa cells with HPV16 PsV for 16 hours and then lysed them in a lysis buffer containing varying concentrations of less stringent (DDM) and more stringent (NP40) detergents. Cells were lysed in one of three lysis buffers: 0.3% NP40 and 0.7% DDM, 0.4% NP40 and 0.6% DDM, or 0.5% NP40 and 0.5% DDM. I immunoprecipitated HPV using the FLAG tag and subjected the samples to western blot analysis using antibodies for the γ-secretase subunits and HPV. After quantifying the relative densities of the bands (Figure 2.3), it is evident that PS1 is IPed in the lysis buffer containing 0.3% NP40 and 0.7% DDM and in the buffer containing 0.4% NP40 and 0.6% DDM. The other subunits are depleted in these same buffers, implying that PS1 is more tightly bound to HPV L2 than the other components of the γ-secretase complex. This suggests that PS1 binds directly to HPV L2 which is consistent with recently published crystal structures of Notch and APP bound to γ-secretase. In these structures, both Notch and APP are directly bound to PS1, although they interact with different TM helices of PS1 [63, 64].

## HPV infection stabilizes the γ-secretase complex

I next wanted to confirm the interaction between γ-secretase and HPV by doing a reciprocal co-IP: immunoprecipitating a γ-secretase subunit and assessing HPV binding to γ-secretase. Cells were mock infected or infected with wild type HPV16 PsV for 16 hours and lysed in 1% DDM lysis buffer. The PS1 subunit of γ-secretase was immunoprecipitated and samples were analyzed using western blot for γ-secretase subunits and HPV. In cells infected with HPV, the other three subunits of γ-secretase co-immunoprecipitated with PS1

and HPV, as expected (Figure 2.4). However, in the mock-infected cells, the other subunits did not co-IP with PS1. This suggest that under these lysis conditions, PS1 is associated with the other subunits of γ-secretase only in infected cells. A similar result was observed when an antibody to another γ-secretase subunit, APH1, was used (Figure 2.4). The γ-secretase subunits only co-immunoprecipitated with APH1 in cells that were infected with HPV and not in cells that were mock infected, suggesting that HPV infection stabilizes the γ-secretase complex.

HPV might induce the formation of the complex or alter the arrangement of γ-secretase subunits in a preexisting complex in such a way as to strengthen the interactions between the γ-secretase subunits. To characterize the γ-secretase complex in the presence and absence of HPV infection, we performed PS1 IPs in weak (CHAPSO), intermediate (DDM), and strong (NP40) detergents. In the presence of mildest detergent CHAPSO, anti-PS1 immunoprecipitated the other components of the γ-secretase complex in both infected and uninfected cells, showing that the complex exists in the absence of HPV infection (Figure 2.5). In the presence of the intermediate strength detergent DDM, anti-PSI immunoprecipitated the other components of the γ-secretase complex only in cells infected by HPV as shown above. In the presence of the strong detergent NP40, anti-PS1 did not immunoprecipitate the other components of the complex, regardless of HPV infection (Figure 2.5). These results suggest that HPV alters the preexisting γ-secretase complex to produce a complex that is resistant to dissociation by the intermediate strength detergent.

I next wanted to characterize the stabilization phenotype for HPV infection. I found that stabilization occurs at many multiplicities of infection (MOIs). I infected HeLa cells with HPV PsV at varying MOIs from 5 to 100 and see that a small amount of γ-secretase

subunits co-IP with HPV and PS1 at low MOIs and this increases as the MOI increases (Figure 2.6). These results imply that HPV stabilizes the γ-secretase complex in a dose-dependent manner. I also performed anti-PS1 co-IPs in HaCaT cells and found that HPV stabilizes the γ-secretase complex in these cells, also in a dose-dependent manner (Figure 2.7). Notably, HPV is around 10x less infectious in HaCaT cells than in HeLa cells, and we start seeing stabilization around a MOI of 50. HaCaT cells are human keratinocytes, which are cells that HPV typically infects, and have never been exposed to HPV before, unlike the more commonly used HeLa cells, which are derived from an HPV18-induced cervical carcinoma. I also found that stabilization requires L2, as L1 only VLPs do not stabilize the γ-secretase complex (Figure 2.2). Additionally, I showed that stabilization of γ-secretase occurs in cells infected with HPVs from both the α-papillomavirus (HPV16) and β-papillomavirus (HPV5) families, which infect genital mucosa and skin, respectively (Figure 2.8). Finally, in a time course experiment with anti-PS1 immunoprecipitation, I show that the L2-γ-secretase interaction is first observed at 4 h.p.i., followed shortly thereafter by stabilization at 6 h.p.i., which increased at 8 h.p.i. (Figure 2.9). Although we do not yet know the role of γ-secretase stabilization in HPV infection, this data shows that the stabilization phenotype is reproducible, dose-dependent, depends on L2, and occurs in multiple cell types and with multiple types of HPV.

## Membrane association of HPV L2

During infection, HPV L2 associates with the endosomal membrane [49]. To assay membrane insertion, I used the carbonate extraction method, which allows us to classify proteins as either TM or non-TM based on sodium carbonate incubation and subsequent ultracentrifugation, with the integral membrane proteins being present in the final pellet

(P2) (Figure 2.10). Cells were infected with HPV16 PsV for 12 hours and then mechanically homogenized until roughly 80% of cellular membranes were ruptured. The membrane fraction was separated using high-speed ultracentrifugation at 100k xg for 30 minutes. This membrane fraction was then incubated with a solution of urea and sodium carbonate. This high pH solution should extract non-TM proteins while leaving TM proteins embedded in the membrane. After another high-speed ultracentrifugation, the soluble proteins are in the supernatant and the TM proteins are in the pellet. Samples are then analyzed via western blot for cellular markers and HPV proteins. BAP31 immunoblotting is used as a marker for TM proteins, and PDI is a marker for luminal proteins. As is shown in Figure 2.11, in the final pellet fraction, a portion of L2 associates with the membrane. Treating with the γ-secretase inhibitor, XXI, prior to infection blocks the ability of L2 to associate with the membrane. These data confirm previous results from our collaborators that γ-secretase activity is necessary for membrane association of HPV L2.

## γ-secretase plays a role in membrane protrusion of HPV L2

L2 protrudes through the endosomal membrane in order to bind to cytoplasmic proteins, such as retromer and the SNX proteins, and traffic through the retrograde pathway to infect cells [34]. Protrusion and membrane association are thought to be linked, as the L2 protein presumably needs to associate with the membrane in order to protrude through it. Protrusion is measured using a split GFP assay. In this assay, we express GFP1-10 with a nuclear export signal in the cytoplasm of HaCaT cells. In addition, tandem copies of GFP11 are appended to the C-terminus of L2 in intact viral particles; this PsV is infectious and traffics similarly to wild-type PsV [34]. Alone, GFP1-10 and GFP11 do not fluoresce.

However, if the C-terminus of L2 protrudes through the cellular membrane to reach the cytoplasm, GFP11 and GFP1-10 will associate and produce reconstituted GFP fluorescence that can be observed using live cell confocal microscopy. We have used this assay to show that the CPP sequence in the C-terminus of L2 is important for and mediates protrusion [34]. The first question I wanted to ask was whether L2 protrusion during HPV infection required γ-secretase activity. HaCaT cells expressing cytoplasmic GFP1-10 were treated with XXI γ-secretase inhibitor or DMSO control for 30 minutes prior to infection with GFP11-tagged PsV or FLAG-tagged PsV (as a control). Three h.p.i., the cells were stained with Hoescht 33342 for cellular DNA and imaged for reconstituted fluorescence using confocal microscopy. As is shown in Figure 2.12, cells infected with FLAG-tagged PsV do not produce reconstituted fluorescence, showing no background GFP1-10 fluorescence. In contrast, DMSO treated cells infected with GFP11-tagged PsV did fluoresce, indicating that L2 can protrude through the membrane in these cells. In contrast, treatment with the γ-secretase inhibitor eliminated reconstituted fluorescence, indicating that γ-secretase activity is necessary for membrane protrusion of L2. The effect of mutations in L2 and other cellular perturbations on viral protrusion will be discussed in future chapters (Chapters III and IV).

## Discussion

I have shown that HPV associates with all four components of the γ-secretase complex and that infection appears to stabilize the complex. This was an entirely unexpected result as γ-secretase stabilization has not been reported by others examining the association between γ-secretase and its substrates. However, groups have reported that γ-secretase is stabilized when it is inhibited. It has been shown that γ-secretase inhibitors

both stabilize the γ-secretase complex and block cleavage of substrates [167]. We know that HPV is not cleaved well by γ-secretase [49], so it is possible that HPV infection is inhibiting γ-secretase activity, thereby causing stabilization of the complex. We investigated this possibility by looking at the cleavage of Notch after infection and did not see much change in Notch cleavage (data not shown, d.n.s.). However, we did not investigate the cleavage of other γ-secretase substrates after HPV infection, so it is still possible that HPV infection inhibits the ability of γ-secretase to cleave its substrates. Future experiments could look at this phenomenon more carefully by examining the effect of HPV infection on APP and ErbB4 cleavage, for example, or on other γ-secretase substrates.

γ-secretase stabilization may also function to allow HPV to stably associate with the membrane. A potential model is that the cell penetrating peptide on the C-terminus of L2 reversibly inserts into and out of the membrane until it is "locked" in place by something, such as a cytoplasmic protein. A possible role of the γ-secretase complex, then, could be to bind the TM domain of L2 once the CPP has penetrated the membrane. In this way, γ-secretase would stabilize L2 within the membrane and L2 could reciprocally stabilize γ-secretase.

It is also possible that the role of γ-secretase may be to recruit another factor that allows L2 to stably associate with the membrane. The γ-secretase complex may allow for L2 to remain within the membrane until another protein can anchor it in the cytoplasm. There are many proteins that are important for HPV infection that could fulfill this role, such as retromer or Rab7. These questions will be explored in Chapter IV.

While we do not know the role of γ-secretase stabilization by HPV in infection, it would be interesting to investigate if expressing the HPV L2 protein alone would allow for

γ-secretase stabilization. We know that we can observe binding of purified γ-secretase to a portion of L2 as a GFP fusion protein, but it could be that γ-secretase stabilization only occurs as a result of L2 protruding through the endosome. If stabilization does not occur when expressing L2 alone, this could provide evidence that L2 requires γ-secretase to stabilize it within the membrane in order to bind another cellular factor, as mentioned above.

Finally, I also began examining how HPV infection affects γ-secretase localization. The γ-secretase complex can be found in many membranes, including both endosomal and TGN membranes. Through initial immunofluorescence experiments, I preliminarily found that HPV infection doesn't affect γ-secretase localization, however this was not investigated in depth and could be examined more carefully. HPV infection and the stabilization phenotype do not increase absolute levels of the γ-secretase components, as assessed by western blot, but HPV infection could re-localize γ-secretase to the viral particle. Additionally, we see γ-secretase binding at both early (8 hpi) and late (16 hpi) time points, as assessed by co-IP. It is possible that the γ-secretase complex is trafficking with HPV from the endosome to the TGN. This could be investigated through testing HPV/γ-secretase association with PLA at different times post infection. PLA is advantageous in this instance because it allows us to look at individual cells and more discrete instances of localization between γ-secretase and HPV.

## Figures

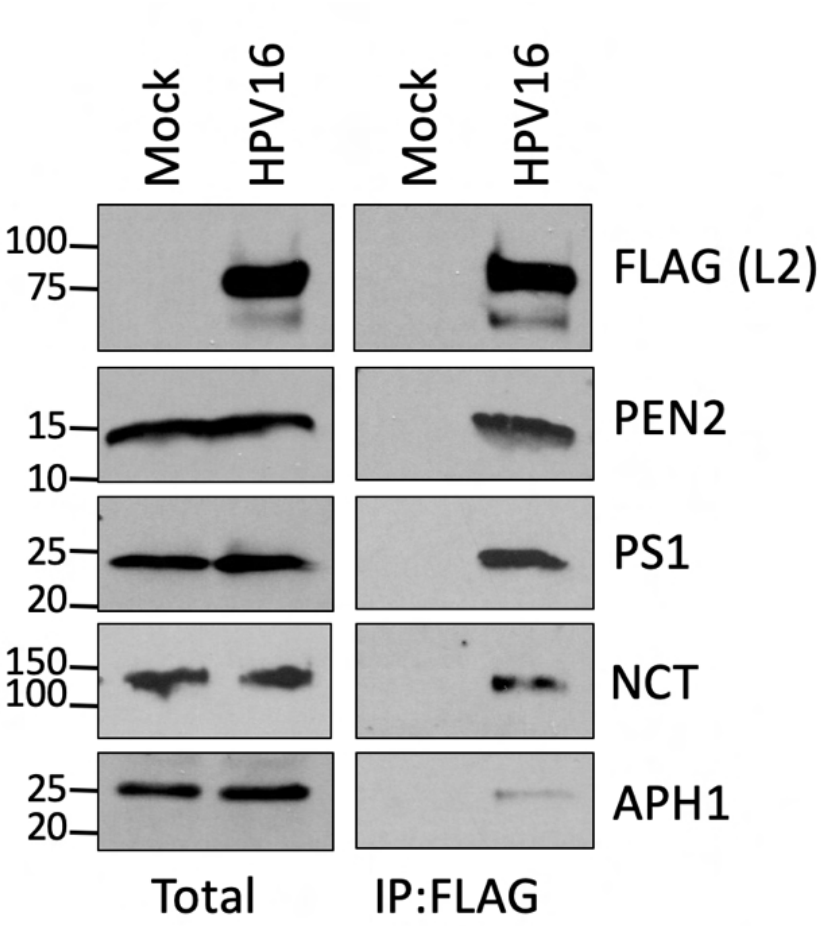


***Figure 2.1: HPV L2 associated with all four components of γ-secretase***

HeLa cells were infected with HPV containing FLAG-tagged L2 for 16 hours or mock infected. Cell lysates were collected in 1% DMNG lysis buffer, immunoprecipitated with FLAG antibody, and immunocomplexes were captured with protein G magnetic beads. Samples were washed in TBS-T, eluted from the beads, and analyzed by SDS-PAGE and immunoblotted from the indicated γ-secretase subunit and HPV.

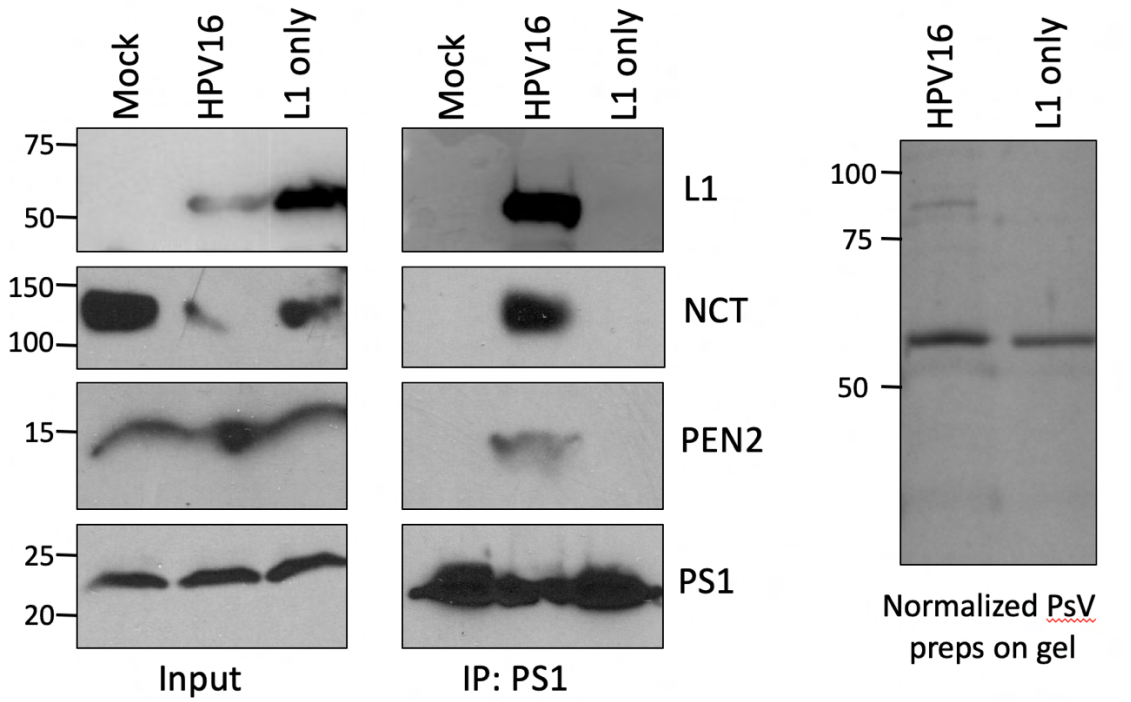


***Figure 2.2: The stabilization interaction between γ-secretase and HPV requires the L2 protein***

HeLa cells were infected with L1-only VLPs for 16 hours or mock infected. Cell lysates were collected in 1% DDM lysis buffer, immunoprecipitated with PS1 antibody, and immunocomplexes were captured with protein G magnetic beads. Samples were washed in TBS-T, eluted from the beads, analyzed by SDS-PAGE, and immunoblotted for the indicated γ-secretase subunit and HPV.

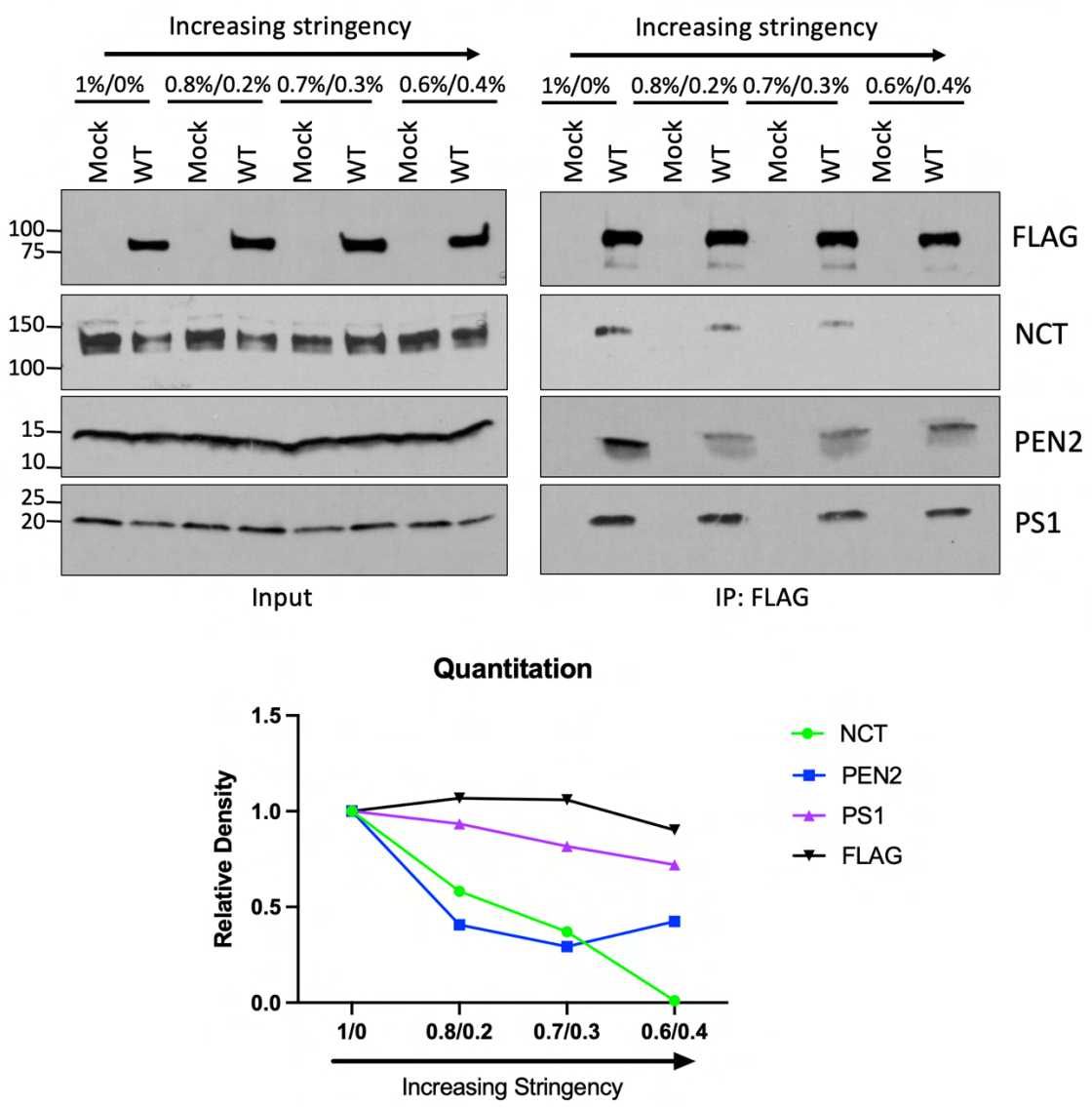


***Figure 2.3: FLAG IP in different detergents suggests HPV binds directly to PS1***

(Top) HeLa cells were infected with HPV16 PsV for 16 hours or mock infected. Cell lysates were collected in the indicated lysis buffer, which contains varying concentrations of mild (DDM) and more stringent (NP40) detergents. Cell lysates were incubated with FLAG antibody, and immunocomplexes were captured with protein G magnetic beads. Samples were washed in cold lysis buffer, eluted from the beads, analyzed by SDS-PAGE and immunoblotted for the indicated γ-secretase subunits and HPV. Note that PS1 remains more abundantly bound than the other subunits in multiple lysis buffers. (Bottom) Quantitation of blots on the top.

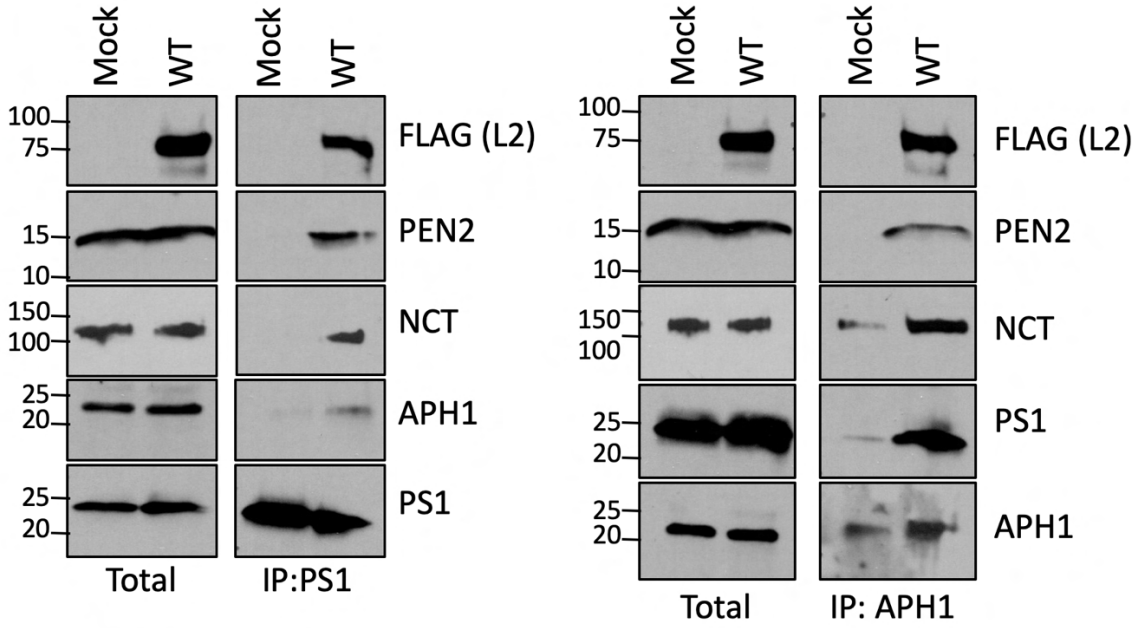


***Figure 2.4: HPV infection stabilizes the γ-secretase complex***

HeLa cells were infected with HPV16 PsV for 16 hours or mock infected. Cell lysates were collected in 1% DDM lysis buffer, immunoprecipitated with PS1 (left) or APH1 (right) antibody, and immunocomplexes were captured with protein G magnetic beads. Samples were washed in TBS-T, eluted from the beads, analyzed by SDS-PAGE, and immunoblotted for the indicated γ-secretase subunit and HPV. Note that the other components of the γ-secretase complex only co-immunoprecipitated in the HPV infected samples.

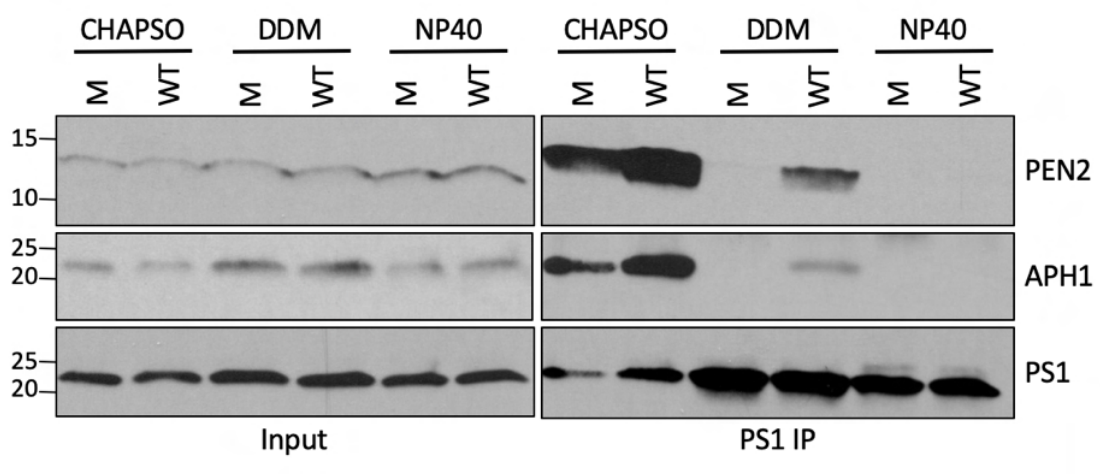


***Figure 2.5 HPV infection stabilizes a preexisting γ-secretase complex***

HeLa cells were infected with HPV16 PsV for 16 hours or mock infected. Cell lysates were collected in 1% CHAPSO, DDM, or NP40 lysis buffer, as indicated. Sampels were immunoprecipitated with anti-PS1 antibody, and immunocomplexes were captured with protein G magnetic beads. Samples were washed in TBS-T, eluted from the beads, analyzed by SDS-PAGE, and immunoblotted for the indicated γ-secretase subunit.

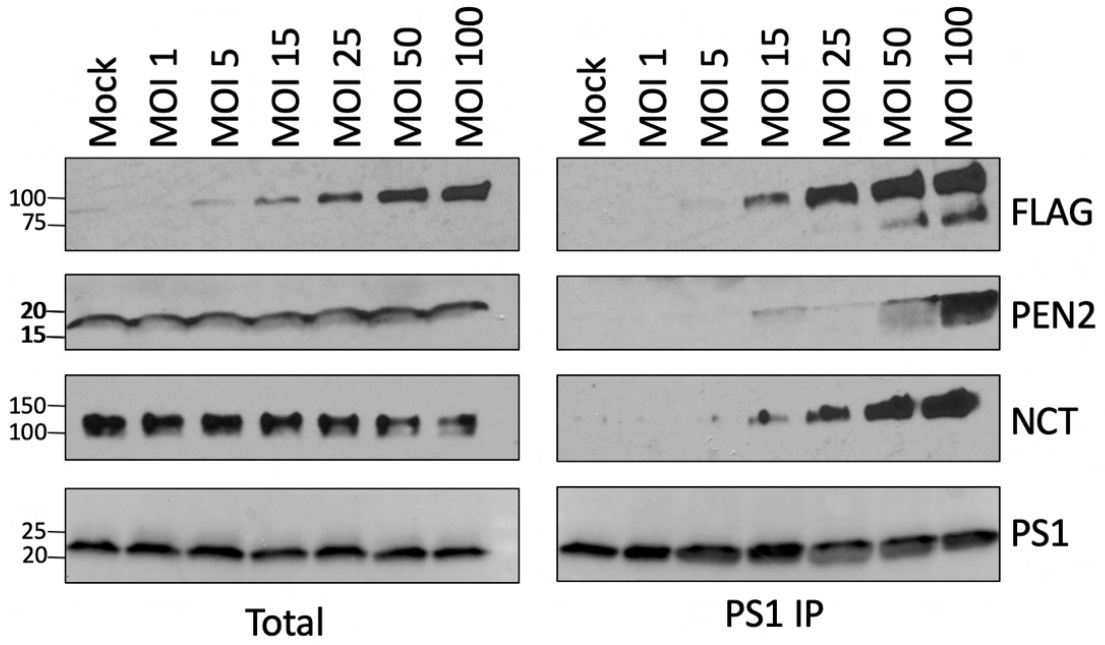


***Figure 2.6: HPV infection stabilizes the γ-secretase complex at multiple MOIs***

HeLa cells were infected with HPV16 PsV at varying MOIs for 16 hours or mock infected. Cell lysates were collected in 1% DDM lysis buffer, immunoprecipitated with PS1 antibody, and immunocomplexes were captured with protein G magnetic beads. Samples were washed in TBS-T, eluted from the beads, analyzed by SDS-PAGE, and immunoblotted for the indicated γ-secretase subunit and HPV.

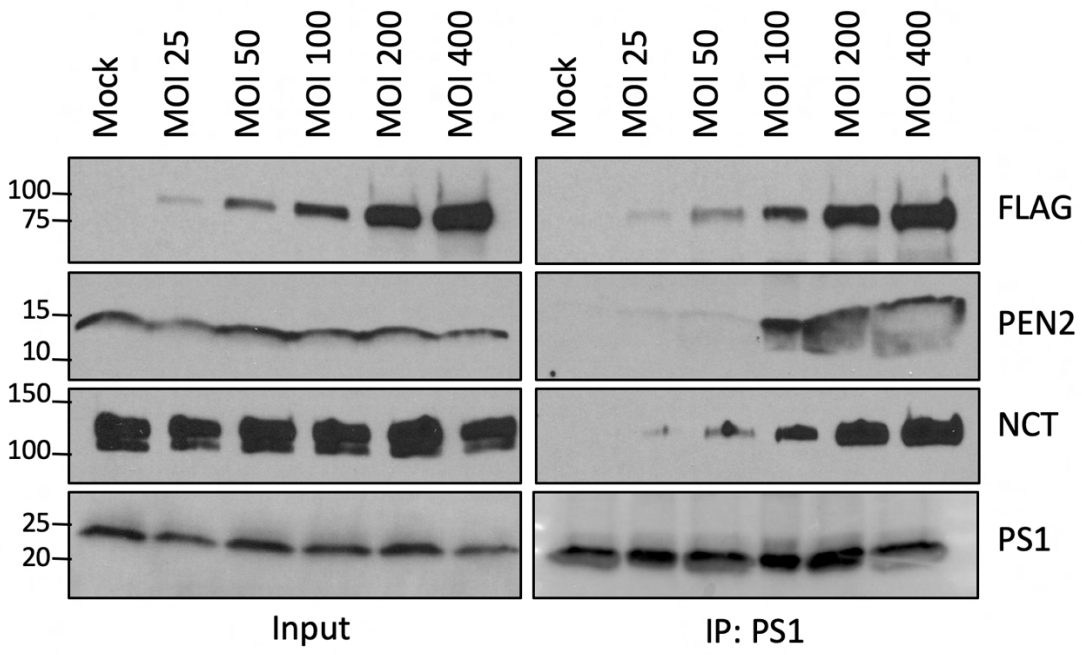


***Figure 2.7: HPV infection stabilizes the γ-secretase complex in HaCaT cells***

HaCaT cells were infected with HPV16 PsV at varying MOIs for 16 hours or mock infected. Cell lysates were collected in 1% DDM lysis buffer, immunoprecipitated with PS1 antibody, and immunocomplexes were captured with protein G magnetic beads. Samples were washed in TBS-T, eluted from the beads, analyzed by SDS-PAGE, and immunoblotted for the indicated γ-secretase subunit and HPV.

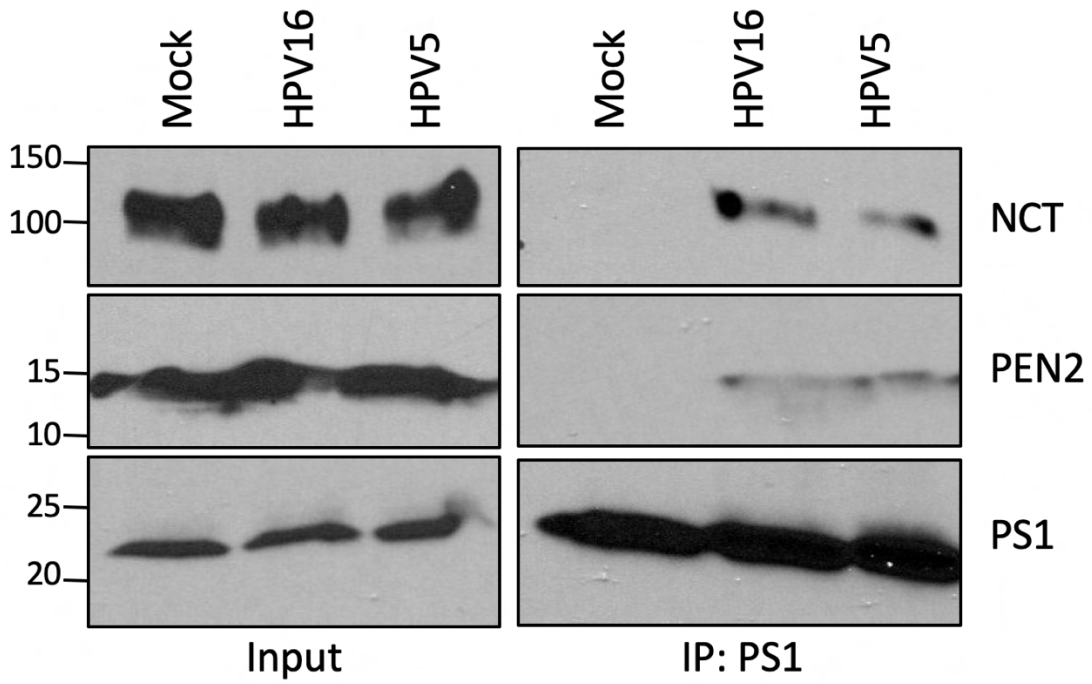


***Figure 2.8: α-papillomavirus and β-papillomavirus subtypes both stabilize the γ-secretase complex***

HeLa cells were infected with HPV16 or HPV5 PsV for 16 hours or mock infected. Cell lysates were collected in 1% DDM lysis buffer, immunoprecipitated with PS1 antibody, and immunocomplexes were captured with protein G magnetic beads. Samples were washed in TBS-T, eluted from the beads, analyzed by SDS-PAGE, and immunoblotted for the indicated γ-secretase subunit and HPV.

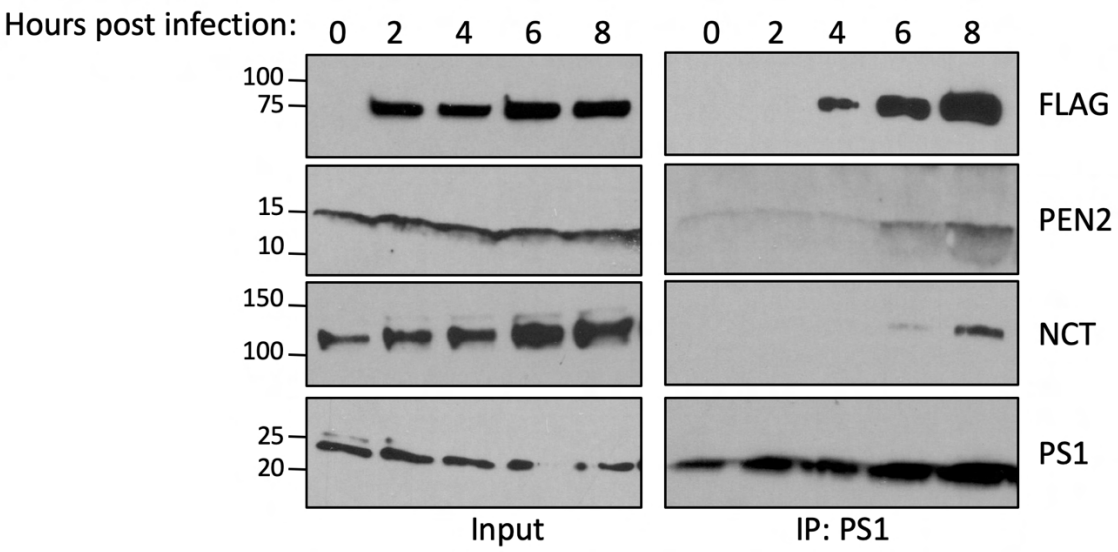


***Figure 2.9: Time course of HPV-γ-secretase interaction and stabilization***

HeLa cells were infected with HPV16 for the indicated time. Cell lysates were collected in 1% DDM lysis buffer, immunoprecipitated with PS1 antibody, and immunocomplexes were captured with protein G magnetic beads. Samples were washed in TBS-T, eluted from the beads, analyzed by SDS-PAGE, and immunoblotted for the indicated γ-secretase subunit and HPV.

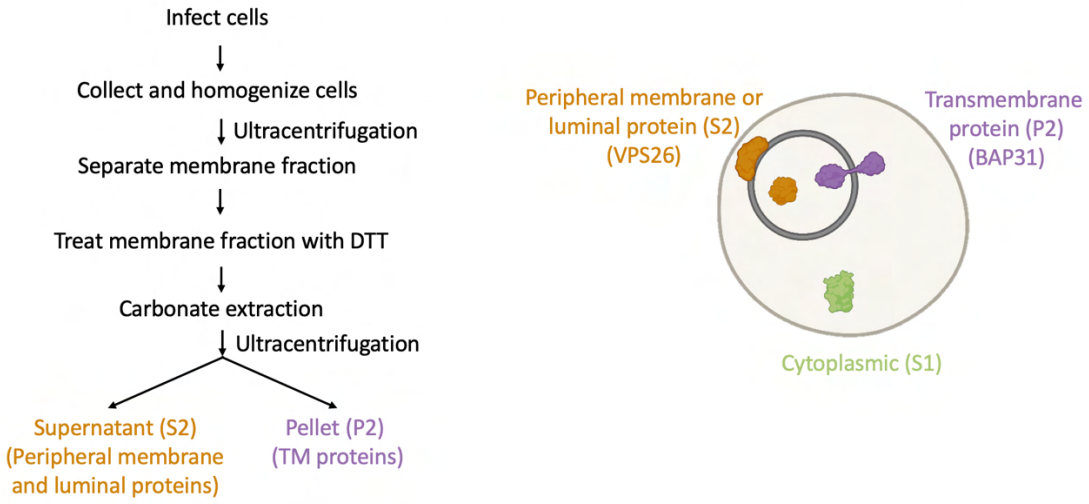


***Figure 2.10: Schematic of carbonate extraction***

(Left) Flow chart depicting the experimental set up of the carbonate extraction. First, cells are infected with HPV PsV then homogenized using mechanical homogenization. A high speed ultracentrifugation step then separates the membrane fraction from the cytoplasmic fraction (S1). The membrane fraction is then treated with DTT followed by the carbonate incubation. Following the carbonate extraction, the sample is centrifuged again in the ultracentrifuge to separate luminal (S2) and transmembrane proteins (P2). (Right) Schematic of the location of luminal and peripheral membrane, transmembrane, and cytoplasmic proteins during the carbonate extraction experiment.

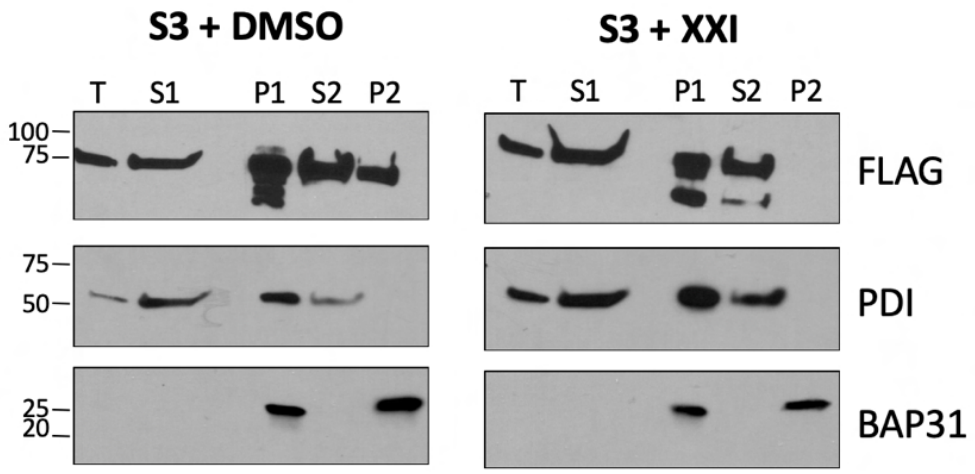


***Figure 2.11: γ-secretase is required for HPV to stably associate with the membrane***

HeLa cells were treated with 1μM XXI γ-secretase inhibitor or vehicle and for 30 minutes prior to infection with HPV PsV for 12h. The cells were mechanically homogenized and the membrane fraction was separated by ultracentrifugation. The total membrane fraction was incubated with 0.1M sodium carbonate and 4.2M urea to extract non-TM proteins. The resulting supernatant and pellet fractions were analyzed by SDS-PAGEs and immunoblotted for L2 (FLAG), and cellular markers for luminal (PDI) and transmembrane (BAP31) proteins. T = Total; S1 = cytoplasmic proteins; P1 = membrane fraction; S2 = luminal proteins; P2 = transmembrane proteins.

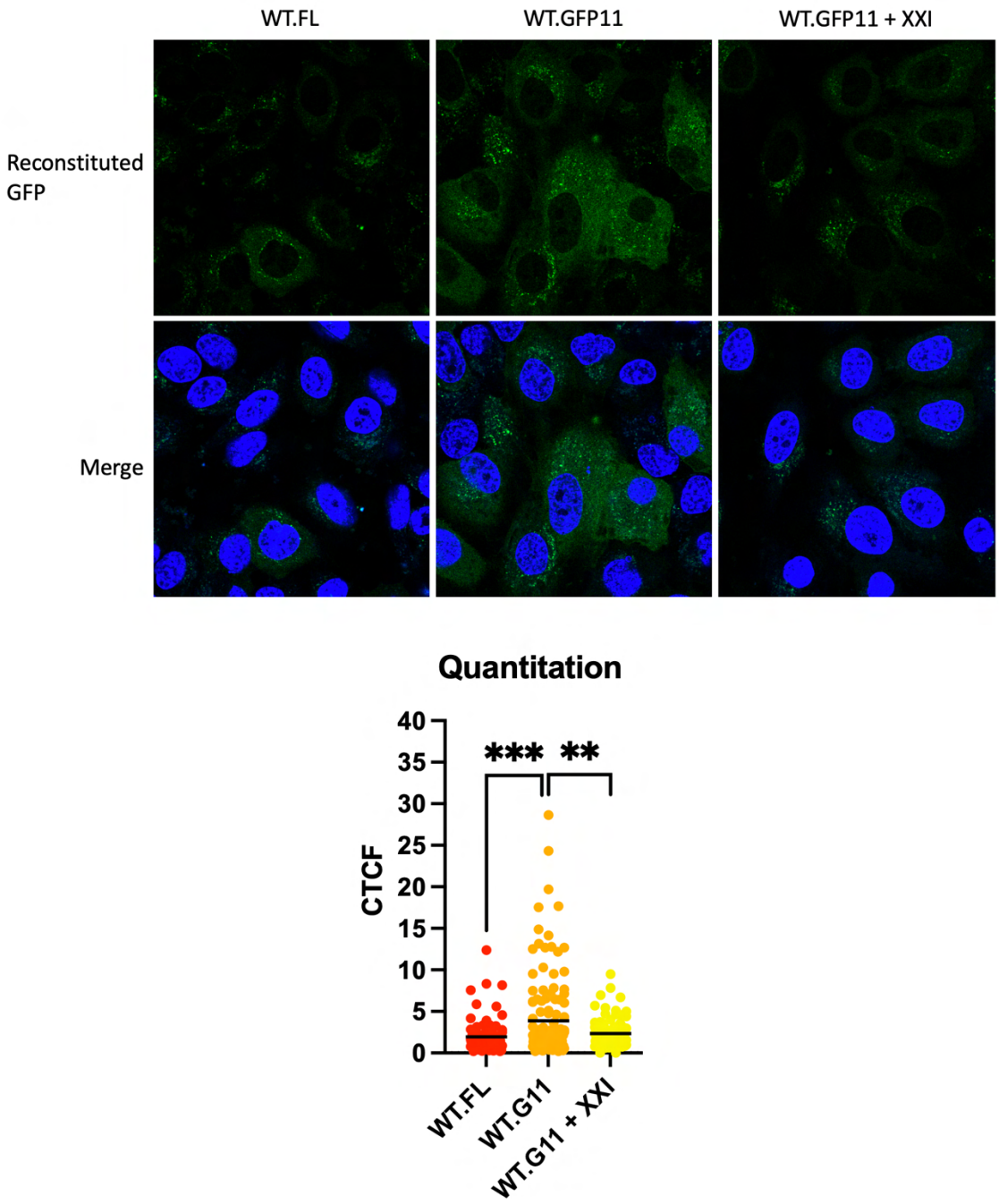


***Figure 2.12: L2 membrane protrusion requires γ-secretase activity***

(Top) Clonal HeLa M cells expressing GFP1-10 were treated with 1μM XXI or DMSO control for 30 minutes prior to infection with FLAG-tagged HPV (control) or GFP11 tagged HPV. 3hpi, cells were stained with Hoechest 33343 and reconstituted GFP fluorescence due to cytoplasmic protrusion of L2 was observed in live cells using a Leica SP5 confocal microscope. (Bottom) Quantitation of corrected total cellular fluorescence from the top panel. ** $p \leq 0.01$; *** $p \leq 0.001$

# Chapter III: Mutations within the putative transmembrane domain of HPV L2 affect infection and association with γ-secretase

## Introduction

There is abundant evidence that there is a transmembrane (TM) domain near the N-terminus of the HPV L2 protein [48, 54, 56]. Multiple modeling programs predict that L2 has a TM domain [48]. This TM sequence can functionally act as a TM domain, because the Campos group showed that it can tether a protein to a membrane [48]. They also showed that this sequence can act as a TM domain in the bacterial ToxLuc system. The Sapp group has shown that there is a trypsin protease protected fragment N-terminal to the TM domain and that the portion of L2 C-terminal of the TM domain is not protected from digestion with trypsin [54]. Finally, the Jung group carried out mutational analysis in this region of HPV16 L2 and identified a few residues that are necessary for infection, however they used CHO cells to test the infectivity of their mutants, a non-relevant cell type for HPV, and mutated the residues to alanine, which is not a typical TM domain residue [56]. It is also important to note that while this segment appears to function as a TM domain, this sequence does not look like typical TM domains, in that it is less hydrophobic and has a very high glycine content, particularly in the C-terminal half of the TM domain (Figure 1.3).

Two of the most interesting results presented in the previous chapter are that HPV infection appears to stabilize the γ-secretase complex and γ-secretase function is necessary for membrane protrusion of the L2 protein. We therefore sought to determine the role of

the TM domain of L2, which is the most likely portion of L2 to associate with γ-secretase since γ-secretase binds to the TM domains of its substrates. There are many unanswered questions related to the TM domain such as the following: Is the TM domain necessary for γ-secretase binding and stabilization? Is the TM domain necessary for membrane association and protrusion of L2? Can the TM domain be replaced with TM domains from other proteins, or is there something specific about the L2 TM sequence that is important for infection? Which specific residues in the TM domain are important for infection and γ-secretase association or stabilization? We started to ask these questions by generating mutants within the TM domain and assessing their infectivity, trafficking, and association with γ-secretase.

## Results

## TM mutant generation

We generated mutations within the putative N-terminal TM domain of HPV L2 and the surrounding sequence. The analysis of these TM mutants would allow us to determine if specific aspects of the TM domain, such as γ-secretase binding, or particular residues within the TM domain were important for HPV infection. These TM mutants were designed to fall within a few categories to test particular characteristics of the L2 TM domain and will be discussed within these broad categories in individual sections below. All TM mutants were generated in the same way. First, we used site-directed mutagenesis to insert a silent AvrII restriction site into L2 N-terminal of the TM domain in the p16SheLL pseudovirus packaging plasmid, which encodes for HPV16 L1 and L2 proteins. This plasmid was then used as the backbone to generate the rest of the TM mutants. There was no infectivity defect for WT PsV containing the AvrII backbone, as assessed by flow

cytometry. There is an XbaI restriction site in p16SheLL immediately upstream of the start codon for L2. gBlocks were ordered from IDT that had the XbaI restriction site, the N-terminal portion of L2, (a) mutation(s) within the TM domain, and the AvrII restriction site. gBlocks are synthetic fragments of double stranded DNA that can readily be used for cloning. Both the gBlock and the p16SheLL AvrII plasmid were digested with XbaI and AvrII, ligated, transformed, and colonies were selected to test for successful insertion of the mutant TM domain.

After confirmation of the mutant plasmid sequence, plasmid DNA was grown, purified, and then used to generate HPV PsV in the same way as with wild type p16SheLL plasmid [18, 168, 169]. This is done by transfecting the mutant packaging plasmid along with HcRed or GFP reporter plasmid into 293TT cells. 72h post transfection, cell lysates were collected and capsids were harvested. Capsids were allowed to mature overnight at 37°C in a water bath and the resulting mature capsids were purified by centrifugation through an iodixanol (Optiprep) gradient the following day. 10 fractions were collected and the purity of the PsV fractions was assessed by gel electrophoresis and Coomassie staining. The fractions with the highest levels of L1 and L2 for each mutant were combined (Figure 3.1 as an example).

Titering of the mutant viral stocks was done in one of two ways, through capsid protein level or qRT-PCR for reporter plasmid content. Protein level is assessed via gel electrophoresis and Coomassie staining of Optiprep-purified viral stocks. An equal volume of wild type and mutant PsV was analyzed on an SDS-PAGE gel and stained with Coomassie Brilliant Blue. Levels of L1 were compared in both samples, and then used to determine a relative titer for the mutant virus, compared to the amount of capsid protein in

a wild-type PsV stock of known infectious titer. The infectious titer of the wild-type PsV was determined using flow cytometry. HeLa S3 cells were infected with wild-type PsV at varying dilutions for 48 hours. Cells were collected and assessed for reporter gene expression using flow cytometry. qPCR was also used to titer and to assess packaging of the viral genome in pseudovirus stocks containing the mutant L2 proteins. 5 □L of mutant or wild-type PsV was digested with DNAse I to remove any cellular DNA stuck to the capsids. The capsids were then digested with proteinase K, followed by purification of the viral genome. The samples were then analyzed by qRT-PCR and compared to a standard curve of the control plasmid in order to calculate the number of genomes/mL of viral stock. It is important to assess packaging of PsV both ways, to ensure that the mutant PsV is not altered in its ability to package the genome, as this could alter the interpretation of infectivity results.

## L2 mutants without a functional TM domain

The first subset of TM mutants includes one mutant in which we altered the ability of the TM sequence to act as a TM domain (GV mutant) and another mutant in which we removed the TM domain completely (Null mutant). The GV mutant, described previously [48, 49], has glycine 57 and glycine 61 in the TM domain mutated to valine. This mutant is unable to infect cells, but it is internalized and localizes to the endosome at early times post infection. This mutant does not bind to γ-secretase and cannot traffic to the TGN [49].

The null TM mutant is a mutant I generated that has the TM sequence of L2 removed. We used this mutant to test if the TM domain of L2 was required for infection. This mutant is packaged properly, as assessed by qRT-PCR for genomes and western blotting for L1 and L2 (FLAG) levels in PsV (Figure 3.2). Flow cytometry for reporter

gene expression showed that, this mutant is noninfectious, even at high MOI (Figure 3.3). This shows that the TM domain of L2 is vital for infection, which is unsurprising considering that this portion of L2 is conserved and is the portion that is most likely associating with γ-secretase.

I then tested where the block in infection was for the null mutant. I first used immunofluorescence to determine if the mutant PsV was able to enter cells. Cells were infected with wild-type or Null mutant PsV for 8 hours and then cells were permeabilized and processed for immunofluorescence using an antibody that detects L1. There was a similar level of bright staining for L1 for both the wild-type and Null mutant, indicating that this mutant is internalized (Figure 3.4). I then performed the proximity ligation assay (PLA) to determine which trafficking step in infection was blocked. PLA is an immune-based detection technique that allows us to localize incoming viral particles to particular cellular compartments. PLA uses complementary probes that recognize primary antibodies specific for the target antigen, in this case one is for a cellular marker and one is for a viral protein. The probes can only associate and, after amplification, produce fluorescence if they are within 40nm of one another and thus will only show signal if the incoming viral particle is close to the cellular marker. Here, I performed PLA for HPV and either an endosome marker, EEA1, or TGN marker, TGN46. Cells were infected with wild-type or Null mutant PsV for 8 or 16 hours and then processed for PLA. At 8 h.p.i., wild-type PsV is found in the endosome, as evidenced by bright green EEA1/L2 PLA signal, and traffics to the TGN next, by 16 h.p.i., as shown by the TGN46/L2 PLA signal. The null mutant is localized to the endosome at 8 h.p.i. (Figure 3.5), but fails to reach the TGN at 16 h.p.i.

(Figure 3.6). This indicates that the block in infection for this mutant is related to intracellular trafficking.

We next assessed whether the Null and the GV mutants could associate with and stabilize the γ-secretase complex. Cells were infected, lysed in buffer containing 1% DDM, and lysates were immunoprecipitated with an antibody that recognizes the γ-secretase subunit, PS1. In cells infected with wild-type HPV16 PsV but not mock-infected cells, the other components of the γ-secretase complex immunoprecipitated with the PS1 subunit, demonstrating the expected stabilization. However, in cells infected with either the GV or the Null mutant, the other components of the γ-secretase complex were not immunoprecipitated, indicating that neither of these mutants stabilizes the γ-secretase complex (Figure 3.7). Similar results were obtained using an antibody that recognizes a second γ-secretase subunit, APH1 (Figure 3.8). These results show that a functional L2 TM domain is necessary for γ-secretase binding and stabilization.

Finally, we tested these mutants for their ability to protrude through the membrane using a split GFP assay. Here, GFP1-10 expressing cells were infected with FLAG-tagged wild-type PsV, or GFP11-tagged wild-type or mutant PsV. If GFP11 on L2 can access GFP1-10 in the cytoplasm, reconstituted fluorescence will be observed. 3 h.p.i., cells were processed for confocal microscopy. In cells infected with wild-type FLAG tagged PsV, no reconstituted fluorescence was observed, but in cells infected with the wild-type GFP11 tagged PsV, reconstituted fluorescence was observed. Cells infected with either the Null mutant or the GV TM mutant do not fluoresce (Figure 3.9), indicating that the C-terminus of L2 cannot access the cytoplasm when the TM domain is altered. This shows that

membrane protrusion of L2 requires a functional TM domain, which is consistent with the lack of γ-secretase binding for these mutants.

## L2 mutants with a TM domain from a general TM protein

We next tested mutants where the L2 putative TM domain was replaced by that of a canonical TM protein. The two proteins that we chose were the platelet derived growth factor receptor (PDGFR) TM domain and the glycophorin A (GlyA) TM domain. The PDGFR TM domain was chosen because it is a well-studied TM domain and we wanted to see if replacing the L2 TM domain with that of any TM domain would support infection. The GlyA TM domain was chosen because it has a single GXXXG motif that is important for dimerization of the GlyA protein [170]. We reasoned that if dimerization of L2 was important and mediated by the GXXXG motifs, the GlyA TM mutant might be able to support infection.

Both the GlyA-L2 and PDGFR-L2 TM mutants package properly as assessed by levels of encapsidated genomes and by L1 and L2 levels via western blot (Figure 3.10 and 3.11). Neither mutant is infectious, even at high MOI, as assessed by flow cytometry for reporter gene expression (Figure 3.12 and 3.13). This shows that simply replacing the TM domain of L2 with a TM domain from another protein is not sufficient for infection. Additionally, the ability of the TM domain to dimerize or the presence of the GXXXG motif is not sufficient for supporting infection.

These mutants were next tested to identify the block in infection. Immunofluorescence results also show that the PDGFR-L2 mutant is internalized into cells. Cells were stained with antibodies recognizing EEA1 and HPV L2 and there is a similar level of L2 staining for both the wild-type and the PDGFR-L2 mutant (Figure 3.14).

I investigated the trafficking of the PDGFR-L2 mutant further using PLA. At 8 h.p.i., I performed PLA for L2 and the early endosome marker, EEA1. As shown in Figure 3.15, the PDGFR-L2 mutant is decreased in its endosome localization at this early time point. Additionally, using PLA for L2 and the TGN marker TGN46, at 16 h.p.i. the PDGFR-L2 mutant is not located in the TGN, unlike wild-type L2 (Figure 3.16). This indicates that this mutant likely has a block in reaching the endosome and does not traffic to the T2N. Immunofluorescence results show that the GlyA-L2 mutant is internalized, but unlike wild-type PsV doesn't reach the TGN as there is little co-localization between the TGN marker, TGN46 and HPV L2 (stained with FLAG), at 16 h.p.i., PsV (Figure 3.17).

Finally, I tested the ability of these mutants to bind to γ-secretase. Cells were infected with wild-type, GlyA-L2, or PDGFR-L2 TM mutant PsV for 16 hours. Cells were lysed in buffer containing 1% DMNG and immunoprecipitated with an antibody recognizing the FLAG tag on L2. The γ-secretase subunits immunoprecipitated with wild-type L2, but not with either of the mutants (Figure 3.18), indicating that these mutants do not bind to γ-secretase. Thus, there is a specific aspect of the L2 TM domain that is vital for infection and γ-secretase association. Simply replacing the TM domain with another TM domain, even with one that shares some features of the L2 TM domain is not sufficient to support infection.

## L2 mutants with a TM domain from a γ-secretase substrate

The next subset of TM mutants has the TM domain of L2 replaced with the TM domain from the canonical γ-secretase substrates, Notch and APP. There are multiple lines of reasoning behind making these TM mutants. Because γ-secretase association with HPV L2 likely occurs through the TM domain, we wanted to see if the presence of a canonical

γ-secretase substrate TM domain in L2 could support infection. Additionally, the TM domain of L2 has many overlapping GXXXG motifs (Figure 1.3) that could be important for oligomerization of L2 as well as TM functionality. While the Notch TM domain does not have any GXXXG motifs (sequence: FMYVAAAAFVLLFFVGCGVLLS), the APP TM domain does (sequence: GAIIGLMVGGVVIATVIVITLVML). We reasoned that if the GXXXG motifs were important, perhaps the GXXXG motifs in the APP TM domain could support infection.

After generating the mutant PsV, I first checked to see if the virus packaged properly. The Notch-L2 mutant PsV packages properly, as assessed by western blot of L1 and L2 (FLAG) levels in intact PsV particles and by the levels of encapsidated genomes as measured by qRT-PCR (Figure 3.10). The APP-L2 mutant packages properly when looking at encpasidated genomes, but has a lower L1:L2 ratio than wild-type virus (Figure 3.11). To test infectivity of these mutants, I infected HeLa S3 cells at multiple MOIs, based on encapsidated genome number, and performed flow cytometry for reporter gene expression two days later. Even at high MOI, both of these mutants were noninfectious (Figure 3.12 and 3.13). This indicates that another feature of the L2 TM domain, besides γ-secretase recognition, is important for infection.

We next tested if the block in infection was due to the viral particles being unable to enter cells. Cells were infected with wild-type or Notch-L2 mutant PsV for 8 hours and then processed for immunofluorescence using an antibody that recognizes L1. We observed L1 staining in cells infected with either wild-type and the Notch-L2 mutant PsV, indicating that this mutant is able to enter cells (Figure 3.14). I also performed a similar experiment with the APP-L2 mutant. Here, cells were infected with wild-type or APP-L2

mutant PsV for 16 hours and processed for immunofluorescence using an antibody that recognizes either TGN46 or the FLAG tag on the C-terminus of L2. For both the wild-type virus and the APP-L2 mutant PsV, we observed staining, again indicating that this mutant PsV is internalized (Figure 3.17), even though the capsids have less L2 than wild-type capsids.

For the Notch-L2 mutant, I used PLA to assess the ability of the PsV to traffic through the retrograde transport pathway. Cells were infected with wild-type or Notch-L2 mutant PsV for 8 or 16 hours, and then processed for PLA using antibodies that recognize L2 and either the endosomal marker, EEA1, or the TGN marker, TGN46. At 8 h.p.i., wild-type PsV was in the endosome, but Notch-L2 mutant PsV was not (Figure 3.15). This indicates that the Notch-L2 mutant blocks trafficking prior to endosome entry. Unsurprisingly, the Notch-L2 mutant viral particles also did not reach the next step in the retrograde transport pathway, the TGN, as assessed by the lack of L2-TGN46 PLA signal at 16 h.p.i., which is when wild-type PsV is in the TGN (Figure 3.16).

Finally, for both mutants, I assessed γ-secretase binding. Cells were infected with wild-type or mutant PsV for 16 hours, lysed in buffer containing 1% DMNG, and immunoprecipitated with an antibody that recognizes the FLAG tag on the C-terminus of L2. The γ-secretase subunits associated with wild-type but not the mutant L2 (Figure 3.18). This is consistent with the trafficking data outlined above, as γ-secretase binding occurs on the endosomal membrane and the Notch-L2 mutant does not reach the endosome.

## L2 mutants with a fusion peptide as the TM domain

Although the sequence of the putative TM domain from L2 differs from a typical TM sequence, it closely resembles the sequence of a fusion peptide from an enveloped

virus. Many enveloped viruses have fusion proteins that are responsible for mediating fusion between the viral membrane and the host membranes [171]. The fusion peptide is a portion of an enveloped virus fusion protein that inserts into the host membrane and brings it in close proximity with the viral membrane so that fusion can occur. These fusion peptides are masked in the fusion protein until activated by a particular cellular process, such as low pH or receptor binding [172, 173]. This could be similar to the HPV L2 protein, which would need to be both TM and non-TM at different points in the viral entry process. For example, "activation" of the TM domain may occur after the viral particle encounters low pH in the endosome. Fusion peptides are typically around 22 amino acids long, have a high glycine/alanine content which allows them conformational flexibility, and have multiple overlapping GXXXG motifs. The L2 TM domain is 22 amino acids long, has a 39% glycine/alanine content, and multiple GXXXG motifs that are vital for infection, so we reasoned that the sequence of the TM domain might be able to be replaced by that of a fusion peptide and still support infection. I replaced the L2 TM domain with the fusion peptide from Dengue virus ENV protein (sequence: VVDRGWGNGCGLFGKGGVVTCAK) or the fusion peptide from influenza H1N1 HA protein (sequence: GLFGAIAGFIEGGWTGMVDGWYG).

After making the constructs to make these mutant viruses, I first checked if they were packaged properly. As assessed by western blot, it appears that the Flu HA-L2 TM mutant packages properly, however the DENV EnV-L2 TM mutant does not (Figure 3.19). The levels of L2 in this mutant pseudovirus are much lower than expected compared to the level of L1 in these particles. Even though the DENV EnV-L2 mutant does not package properly, the infectivity of both mutants was tested by flow cytometry for reporter gene

expression. Even at high MOI, neither mutant was infectious (Figure 3.20), indicating again that there is something specific about the natural L2 TM domain that is vital for productive infection.

## L2 mutants with the pHLiP sequence as the TM domain

As mentioned above, the sequence for the L2 putative TM domain does not resemble that of a typical TM domain. The L2 TM domain may be "activated" by some external factor, such as the low pH that the viral particle would encounter as the endosome matures. The pH (low) insertion peptide (pHLiP) is a hydrophobic peptide that interacts only weakly with membranes at neutral pH, however at low pH, the peptide will insert into membranes and become a stable TM helix [174]. This technology was developed to target the acidic environment of tumors in order to deliver therapeutics directly to the cancerous cells. However, if L2 is triggered by low pH to form a TM protein, it is possible that a pHLiP sequence can replace this function of L2 and support infection.

I generated three TM mutants with different pHLIP sequences based on a mutational analysis of the pHLiP sequence [175]. Variant 3 (sequence: ACDDQNPWRAYLDLLFPTDTLLLDLLW) was chosen because it was the best variant at targeting tumors, and thus low pH, and inserted with fast dynamics. Variant 7 (sequence: ACEEQNPWARYLEWLFPTETLLLEL) was chosen because it is shorter, closer to the natural TM length of HPV L2, and quickly inserts into acidic membranes. Finally, variant 12 (sequence: ACEDQNPWARYADLLFPTTLAW) was chosen as it is the same length the natural L2 TM domain, yet could still function adequately as a pHLiP and insert into membranes at low pH. The mutant viruses with the pHLiP sequences were first assessed by Coomassie staining to determine if the levels of L1 and L2 in the intact viral particles

were similar to wild-type HPV. As Figure 3.21 shows, the levels of L1 and L2 are similar between the mutant viruses, indicating that they are properly packaged. They also package genomes at similar levels as wild-type HPV, as assessed by qRT-PCR for genome number. Infection was measured at multiple MOIs for all three mutants using flow cytometry. Even at high MOI, none of the three pHLiP mutants were infectious (Figure 3.22). Clearly, there is something specific about the L2 putative TM domain that makes it suitable for infection and difficult to replace with similar TM domains.

## L2 chimeric and point TM mutants

The results presented above indicate that there is something specific about the L2 putative TM domain that allows it to support infection. Therefore, we started to approach the generation of TM mutants from a different perspective. Instead of trying to replace the TM domain with those from other proteins that share similar characteristics as the L2 TM domain, we wanted to determine which portions of the TM domain were important for infection. In order to do this, we first generated chimeric mutants where half (BR11-L2) or just the first six (BR6-L2) amino acids of the L2 TM domain were replaced with those from the PDGFR TM domain. We chose to replace the N-terminal region of the TM domain first because the C-terminal half is more well conserved and has the overlapping GXXXG motifs that we know are important for infection.

Both of the chimeric mutants package properly, as assessed by Coomassie staining and western blot for L1 and L2 (Figure 3.23). These mutants are both noninfectious at even the highest amount of virus tested, indicating that some residue, or combination of residues, in the first six amino acids is important for infection (Figure 3.24). These mutants were also tested for their ability to bind γ-secretase and did not bind to or stabilize the γ-secretase

complex (Figure 3.25), providing additional evidence that the TM domain is important for γ-secretase binding and stabilization.

Because the BR6-L2 chimeric mutant had only six amino acids replaced and still didn't infect cells, I went on to make single mutations in these first six amino acids: L46A, Q47L, Y48L, G49L, S50L, M51L. G49L and S50L. These mutants packaged lower amounts of genomes, as assessed by qRT-PCR, but after normalizing to genome numbers, had similar levels of L1 as wild-type pseudovirus. This suggests that although the titer of these mutants was lower, they still package properly (Figure 3.26). These mutants were tested for infectivity with the help of a rotation student, Cathy Garcia, and displayed varying levels of infection. The L46A, G49L, and S50L mutants were most drastically reduced, being roughly 50-fold less infectious than wild-type virus (Figure 3.27). The Q47L, Y48L, and M51L mutations all decreased infection, but did not inhibit infectivity as severely as the other mutations. These mutants infected at roughly 40-50% of wild-type levels. This indicates that residue 46, 49, and 50 are vital for infection, and that residues 47, 48, and 51 are important, but not strictly necessary for infection. The L46A, Q47L, and Y48 mutants were also tested for binding to cells. Wild-type or mutant PsV was added to HeLa cells and incubated at 4°C for 2 hours. This incubation allows the virus to bind to cells, but not to be internalized. After 2 hours, cells were kept on ice and either scraped off the plate, or lysed in trypsin. The trypsin treatment serves as a negative control, as it should remove all virus bound to the cells. The samples were then collected and analyzed via western blotting for L1 to assess binding. Similar to wild-type HPV PsV, all three mutants bound robustly to cells (Figure 3.28). This shows that the reduction in infection was not due to an inability to bind to the HeLa cells.

These mutants were then tested for their ability to bind to and stabilize the γ-secretase complex. Cells were infected with wild-type or mutant PsV for 16h, lysed in buffer containing 1% DDM, immunoprecipitated with a PS1 antibody, and analyzed by western blot for L1 and γ-secretase. As expected, in cells infected with wild-type PsV, both L1 and the other components of the γ-secretase complex immunoprecipitated with PS1 (Figure 3.24). In cells infected with the noninfectious point mutants, the γ-secretase complex was not stabilized and the mutant viruses were drastically reduced in their ability to bind γ-secretase, as is evidenced by the low levels of L1 that immunoprecipitated with PS1. On the other hand, cells that were infected with the less defective mutants robustly bound to PS1 and stabilized the γ-secretase complex. This correlation between infectivity and γ-secretase binding and stabilization suggests that, although we do not yet know the role that stabilization of γ-secretase plays in infection, the stabilization phenotype itself is important for infection.

## L2 mutants with point mutations predicted to affect pH dependence

We also considered the possibility that the sequence surrounding the TM domain may play a role in the function of the TM domain. Immediately N-terminal of the TM domain, there are three acidic residues that could play a role in a pH-dependent step for HPV infection (Figure 1.3). D31, E17, and D43, where D is aspartic acid and E is glutamic acid, are absolutely conserved among the over 300 different papillomavirus species, indicating that they may be playing an important role for infection. We chose to then investigate the role that these three amino acids could be playing in infection by mutating them to asparagine (N). Asparagine is similar in size and chemical structure to aspartic acid, but is a neutral amino acid and thus its side-chain is not protonated or deprotonated

based on pH. Asparagine, unlike aspartic acid and glutamic acid, can't be protonated as a result of low pH in the endosome, and thus a protein with aspartic acid and glutamic acid residues mutated to asparagine would no longer have the same pH dependence as the natural protein.

The D31N, E37N, D43N, and the 3M mutant (all three residues simultaneously mutated to asparagine), all packaged properly, as assessed by a Coomassie blue stain of the capsid protein after PsV purification and gel electrophoresis (Figure 3.29). All four mutants have similar levels of L1 and L2 as wild-type PsV. As assessed by flow cytometry, all of the mutants show a defect in infection as compared to wild-type PsV (Figure 3.30). At an MOI of 1 or higher, the E37N mutant is the most infectious, but still has a severe infectivity defect. As shown by infection at the higher MOI of 25, both the D31N and D43N mutants were roughly 25-fold impaired compared to wild-type pseudovirus. The 3M mutant, which one might expect to have the most severe infectivity defect, was noninfectious even at the highest MOI tested, a MOI of 100. These residues are therefore important for infection, although I did not follow up to determine where the block in infection occurred.

## L2 insertion mutants

The final set of TM mutants that I made contained mutations immediately C-terminal of the putative TM domain. These mutants have either an epitope tag or a protease cleavage site inserted at residue 72. They were constructed in order to allow us to determine which portions of the L2 protein were able to access the cytoplasm. They can also be used to determine if L2 can tolerate a large insertion and still be infectious. The thrombin protease cleavage site (sequence: LVPRGS) was inserted into one of the mutants. With this mutant, we would infect cells that express thrombin through an inducible promoter, with

HPV, collect the samples and analyze by a western blot to determine if there was a size shift in the L2 protein as a result of thrombin cleavage. This would indicate that the portion C-terminal to the TM domain is accessible to the cytoplasm and thrombin protease. Two other mutants were made that have either the V5 epitope tag (sequence: GKPIPNPLLGLDST) or an HA epitope tag (sequence: YPYDVPDYA). These mutants can also be used to determine which portions of L2 access the cytoplasm through selective permeabilization and immunofluorescence. Cells would be infected with the mutant viruses, selectively permeabilized using digitonin [54, 55], and processed for immunofluorescence using either V5 or HA antibodies. Any visible signal would indicate that this portion of L2 was accessible to the cytoplasm.

These mutants are slightly altered in their ability to package genomes, as assessed by qRT-PCR and western blotting after normalizing the virus amount based on genome packaging. All of the mutants do package both L1 and L2, but the L2 levels are decreased compared to the L1 levels for the 72V5-L2 mutant (Figure 3.31). At low MOIs, the mutants are quite impaired for infectivity, but they are able to infect at higher MOIs (Figure 3.32). The 72HA-L2 mutant is least impaired for infectivity and is roughly 10X less infectious than wild-type virus. The 72V5-L2 and 72Th-L2 mutants are more severely impaired for infection, being roughly 25X less infectious than wild-type. This indicates that although the PsV can tolerate these mutations, they are quite disruptive. These mutants, then, are likely not the best tool to use to study the protrusion of L2 into the cytoplasm and new mutants that have less detrimental effects on HPV infectivity need to be generated in order to study this question.

## Discussion

The study of the TM mutants led to many interesting conclusions. First, the TM domain of L2 cannot be replaced with those from other proteins, even if they share similar characteristics as the L2 TM domain, such as binding to γ-secretase, a dependence on pH, or the presence of GXXXG motifs. We had hypothesized that one of the categories of TM domains, when inserted into the L2 protein, would support infection. However, from both the TM replacement mutants and the TM point mutants, it is clear that the actual sequence of the L2 TM domain must remain relatively intact in order to support infection. Indeed, even some of the point mutants, such as G49L and S50L, were almost entirely blocked for infection, even though there was only a single amino acid substitution within the TM domain, and the residue was not absolutely conserved among all of the sequenced papillomaviruses (Figure 1.3). This indicates that the specific sequence itself, as opposed to individual sequence elements, of the L2 TM domain is what is necessary for infection. Interestingly, it appears that the sequence context is also important. Residue 49 in the HPV16 L2 protein is a glycine residue and the G49L mutation almost entirely blocked infection (Figure 3.27). However, as can be seen from the sequence logo, there are some L2 proteins that naturally have a leucine at position 49, which suggests that both the amino acid itself and the residues around that particular amino acid are important. Future experiments could determine if the HPV L2 proteins that naturally have a leucine at position 49 could tolerate a glycine at this position, or if the HPV16 L2 protein could tolerate full TM domains from other HPV proteins.

Interestingly, we found different critical residues for infection than have previously been reported [56]. The Jung group performed mutational analysis of the N-terminal region

of L2 by mutating residues to alanine and assessing infectivity of the resultant PsV in CHO-K1 cells. Similar to my results, the Jung group found that D31 and D43 were critical for infection. However, their mutational analysis did not identify E37 as an important residue. Additionally, they found that L46, Q47, and Y48 were similarly important for infection, and that G49, S50, and M51 weren't important. My results show that L46, G49, and S50 are critical for infection, and Q47, Y48, and M51 are less important. There are a few critical differences between the two studies that could contribute to these conflicting results. Importantly, the Jung group assessed infectivity of their mutants in CHO-K1 hamster kidney cells, a cell line that is non-relevant to HPV infection. Different residues could be important for infection in these cells than cell types that HPV typically infects, such as the HeLa cells that we used in this study. Additionally, the Jung group replaced the residues with alanine and we replaced them with either asparagine (for charged residues, as asparagine is similar in size and shape to the basic residues) or leucine (for residues within the TM domain, as leucine is the most commonly found residue within TM domains). The different substitutions clearly have different effects on infection. We also used flow cytometry for GFP or HcRed expression, and the Jung group used Lucia levels, which could lead to different results. Finally, in the Jung lab's report, it is unclear how the mutant PsV preps were normalized to the wild-type PsV preps, so it is possible that the amount of mutant virus added to the cells in their report was not equivalent to the wild-type PsV.

Additionally, the TM domain of L2 is necessary for binding to and stabilization of γ-secretase. I showed that the TM domain (and γ-secretase activity as was shown in Chapter II) is also important for protrusion of L2 into the cytoplasm to bind to cytoplasmic cellular entry factors. The L2 proteins from both the null and the GV mutant were unable to bind

to γ-secretase, stabilize γ-secretase or protrude through the membrane. This shows that the presence of the functional L2 TM domain is important for these steps in infection. This is not surprising, since in order to stably insert into a membrane, proteins presumably would require a TM domain. Even though the L2 TM domain does not look like a typical TM domain, this could actually be used to the virus's advantage. The L2 TM domain is less hydrophobic than typical TM domains and this could allow L2 to move into and out of the membrane as necessary for proper viral trafficking. L2 would stably associate with the membrane to bind retromer, but could also be released from membrane association in order to traffic to distal retrograde compartments, like the TGN. However, this has not been demonstrated, so it is also possible that L2 remains embedded within different membranes throughout infection. Future experiments can examine HPV L2 membrane association at different times after infection.

Another important take away from these experiments is that membrane protrusion and association, as well as γ-secretase binding and stabilization, are tightly correlated with one another. For example, I was unable to find a mutant that bound to γ-secretase without stabilizing γ-secretase, or a mutant that associated with the membrane but didn't bind to γ-secretase. Indeed, through the study of the chimeric and point mutants, we observed that infectivity, γ-secretase binding, and γ-secretase stabilization were all highly linked. Perhaps γ-secretase is acting as a master regulator of these important steps and coordinates the recruitment of other proteins to assist in membrane association, protrusion, and stabilization of γ-secretase, rather than being directly involved in these steps. It would be interesting to determine if γ-secretase stabilization by HPV L2 is absolutely necessary for HPV infection. Perhaps there is a mutation in an HPV capsid protein or a mutation in a γ-

secretase subunit could support infection, but would not allow L2 to stabilize the γ-secretase complex. Indeed, previous work has shown that pathogenic γ-secretase mutations destabilize the interaction between γ-secretase and its substrates, in this case APP [176]. These mutant forms of the PS1 subunit of γ-secretase could be expressed in PS1 KO cells, infected with HPV, and a co-IP would be used to determine whether or not γ-secretase stabilization occurs. If a mutant could be found that supports infection, but blocks γ-secretase stabilization, for example, that would indicate that γ-secretase stabilization is not absolutely necessary for HPV infection. Some of these possibilities are explored in the following chapter, Chapter IV.

## Figures

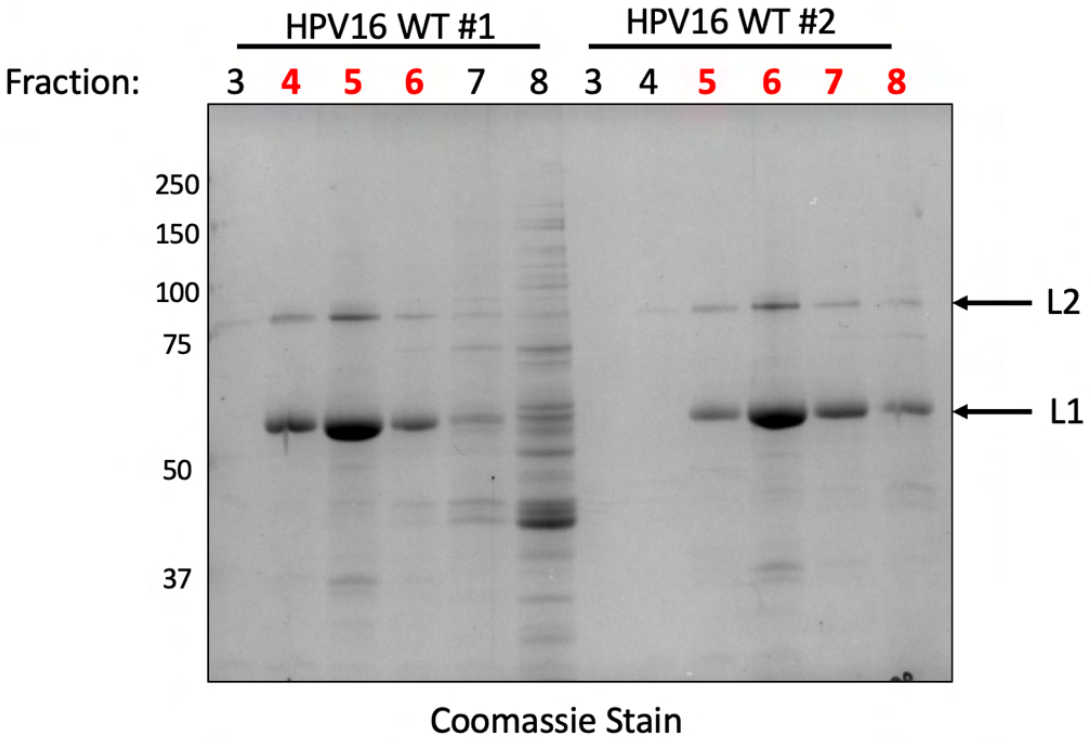


***Figure 3.1: L1 and L2 levels in PsV fractions***

The packaging and reporter plasmids were transfected into 293TT cells. 72 hours post transfection, cell lysates were collected, capsids were matured overnight and subsequently purified using an iodixonol gradient and ultracentrifugation. 10 200µL fractions were collected and 10µL of Fractions 3-8 for two different WT PsV preps were analyzed on an SDS-PAGE gel with Coomassie Brilliant Blue staining. The red numbers indicate the fractions that were pooled as the viral stock. L1 = 50kDa, L2 = 75kDa

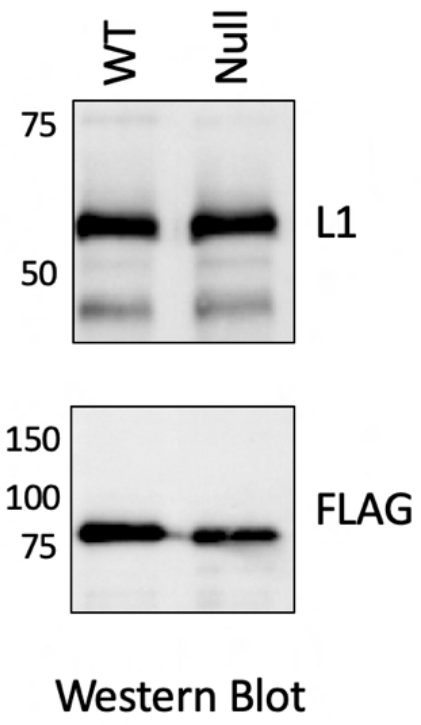


***Figure 3.2: Characterization of Null TM mutant***

Purified PsV was normalized by qRT-PCR for genome content and analyzed by SDS-PAGE followed by western blotting for L1 and L2 (FLAG).

```
Wild-type L2  …ADQILQYGSMGVFFGGLGIGTGSGTGGRTG…
Null-L2       …ADQI----------------------GRTG…
```

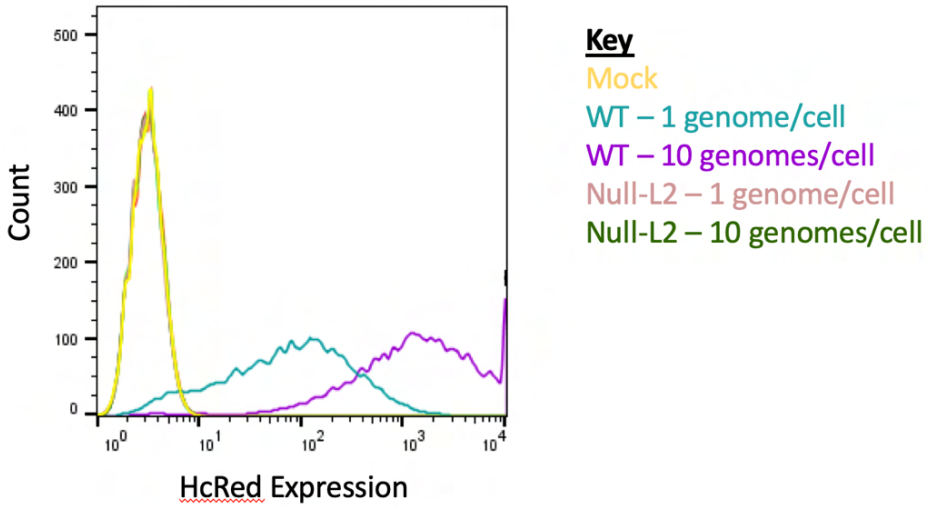


***Figure 3.3: TM Null mutant is noninfectious***

(Top) Sequence of wild-type L2 protein and Null mutant. (Bottom) HeLa S3 cells were infected with normalized amounts of wild-type or Null PsV as indicated. 48 hours post infection, samples were collected and analyzed for HcRed reporter gene expression. A shift to the right indicates successful infection.

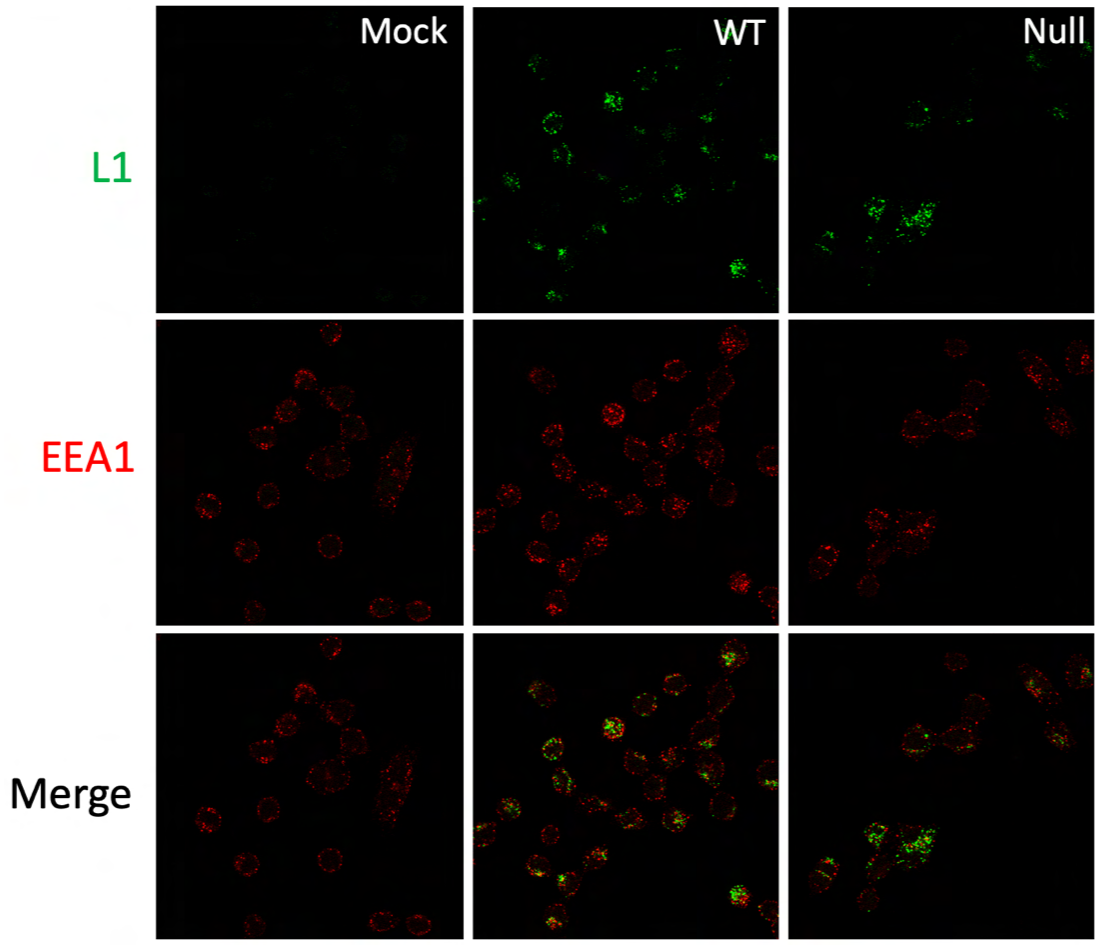


***Figure 3.4: Internalization of Null TM mutant***

HeLa Sen2 cells were infected with wild-type or mutant PsV for 8 hours. Samples were fixed using 10% formalin, permeabilized with 1% saponin and processed for immunofluorescence using an antibody that detects L1 (green) and EEA1 (red).

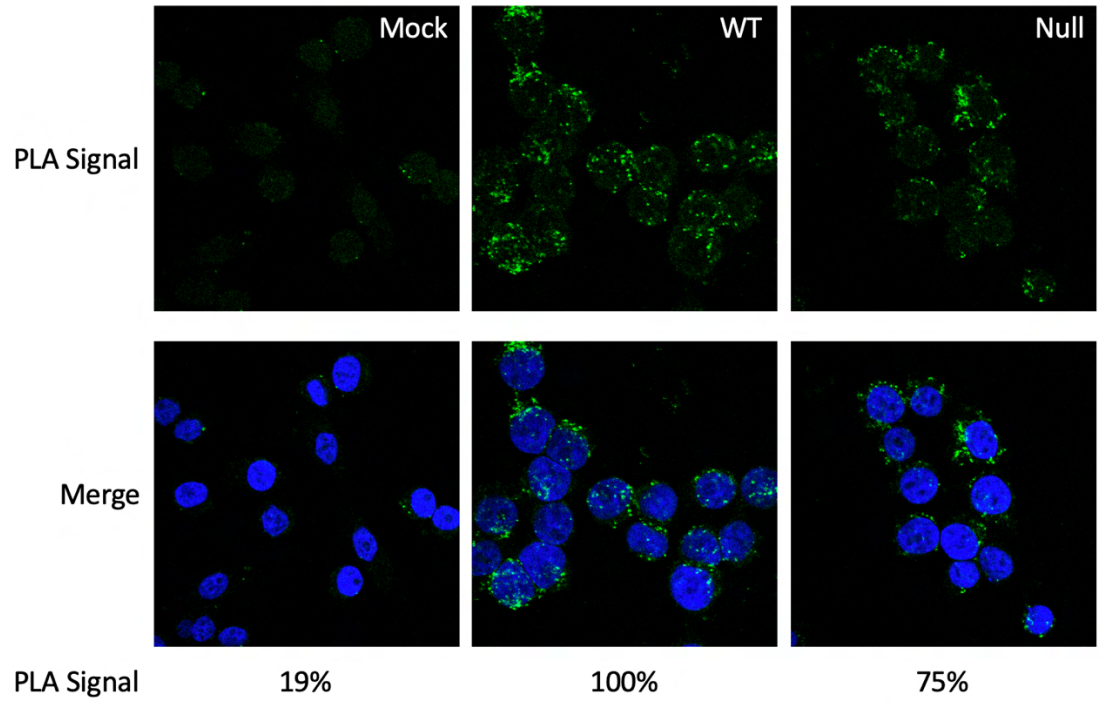


***Figure 3.5: Null TM mutant localizes to the endosome at 8hpi***

HeLa Sen2 cells were infected with wild-type or null mutant PsV at an MOI of 50. 8 hours post infection, samples were fixed in 10% formalin, permeabilized with 1% saponin, and processed for the proximity ligation assay. Briefly, samples are incubated with primary antibodies recognizing a EEA1 and HPV. Samples are then incubated with probes that recognize the primary antibodies, the probes are ligated and amplified and signal can be observed using a confocal microscope. Note that PLA only produces signal if the two markers are within 40nm of each other. PLA signal was quantitated using BlobFinder software. DAPI - blue, PLA signal - green

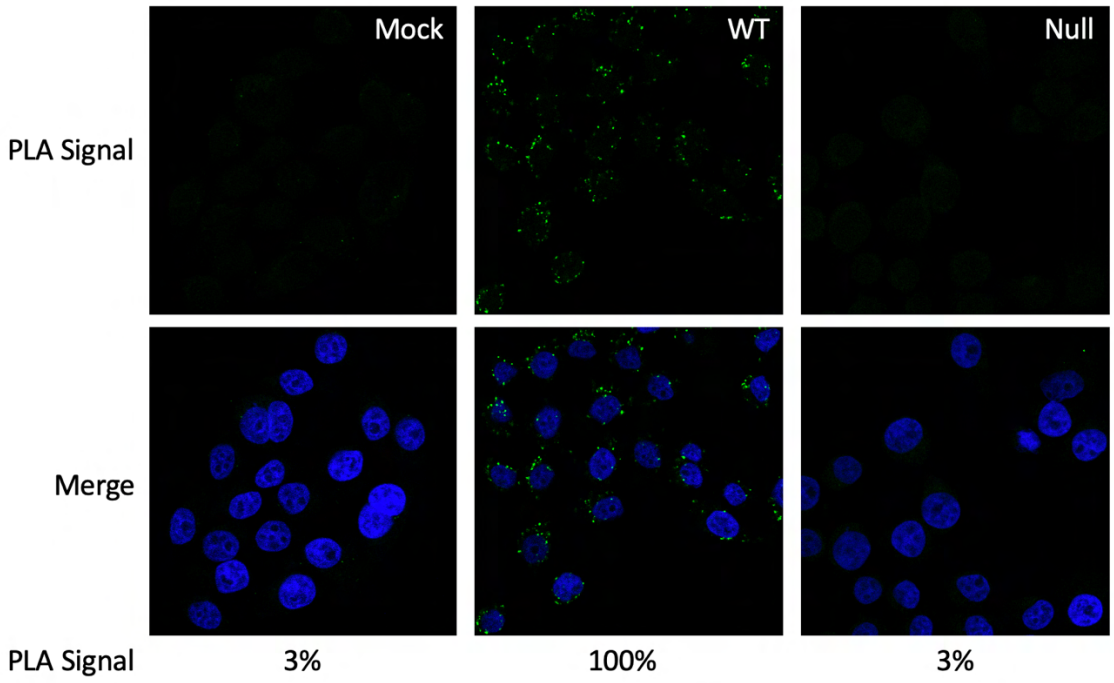


***Figure 3.6: Null TM mutant fails to reach the trans-Golgi network***

HeLa Sen2 cells were infected with wild-type or null mutant PsV at an MOI of 50. 16 hours post infection, samples were fixed in 10% formalin, permeabilized with 1% saponin, and processed for the proximity ligation assay. Briefly, samples are incubated with primary antibodies recognizing TGN46 and HPV. Samples are then incubated with probes that recognize the primary antibodies, the probes are ligated and amplified and signal can be observed using a confocal microscope. Note that PLA only produces signal if the two markers are within 40nm of each other. PLA signal was quantitated using BlobFinder software. DAPI - blue

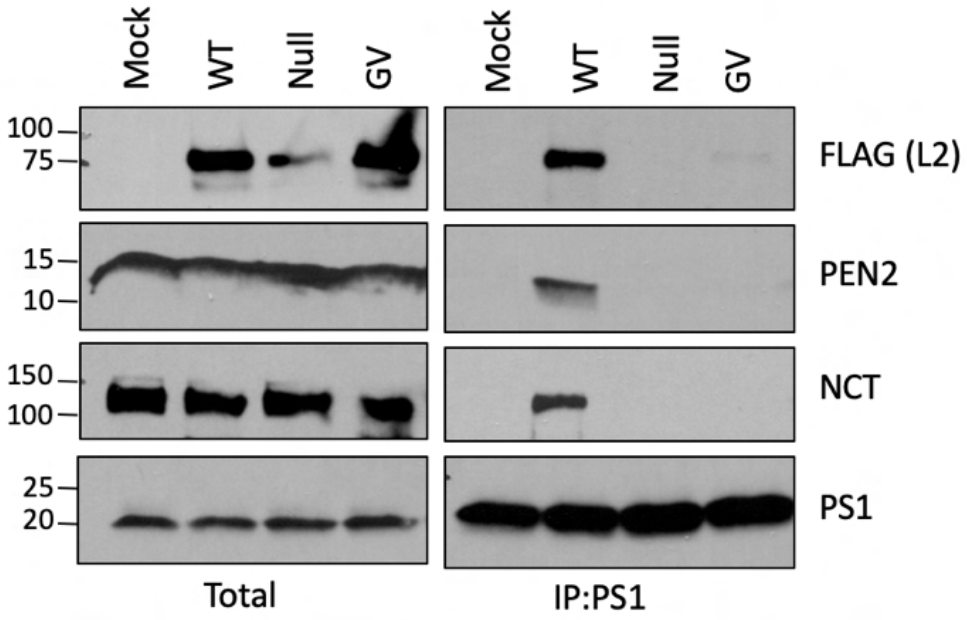


***Figure 3.7: Null and GV mutants do not stabilize γ-secretase***

HeLa S3 cells were infected with wild-type, Null, or GV mutant PsV for 16 hours. Cells lysates were collected in 1% DDM lysis buffer and incubated with an antibody recognizing the PS1 subunit of γ-secretase. Samples were incubated with protein G magnetic beads overnight and subsequently washed with TBS-T. Samples were eluted from the beads using sample buffer and analyzed via SDS-PAGE and western blotting for the indicated antibodies.

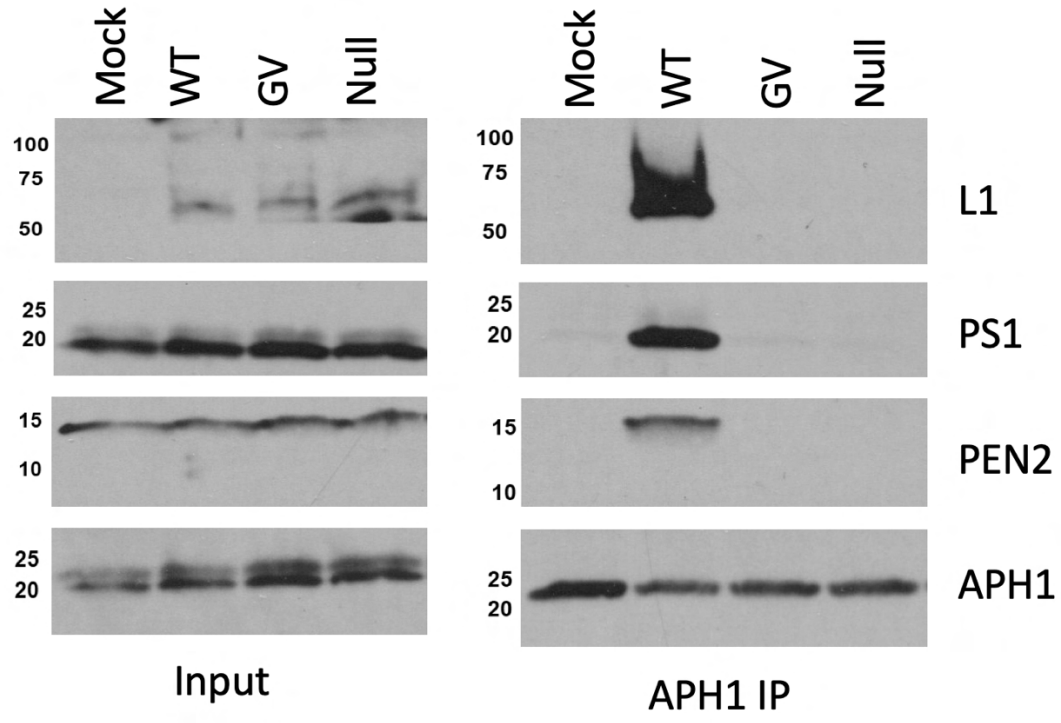


***Figure 3.8: Null and GV mutants do not stabilize γ-secretase***

HeLa S3 cells were infected with wild-type, Null, or GV mutant PsV for 16 hours. Cells lysates were collected in 1% DDM lysis buffer and incubated with an antibody recognizing the APH1 subunit of γ-secretase. Samples were incubated with protein G magnetic beads overnight and subsequently washed with TBS-T. Samples were eluted from the beads using sample buffer and analyzed via SDS-PAGE and western blotting for the indicated antibodies.

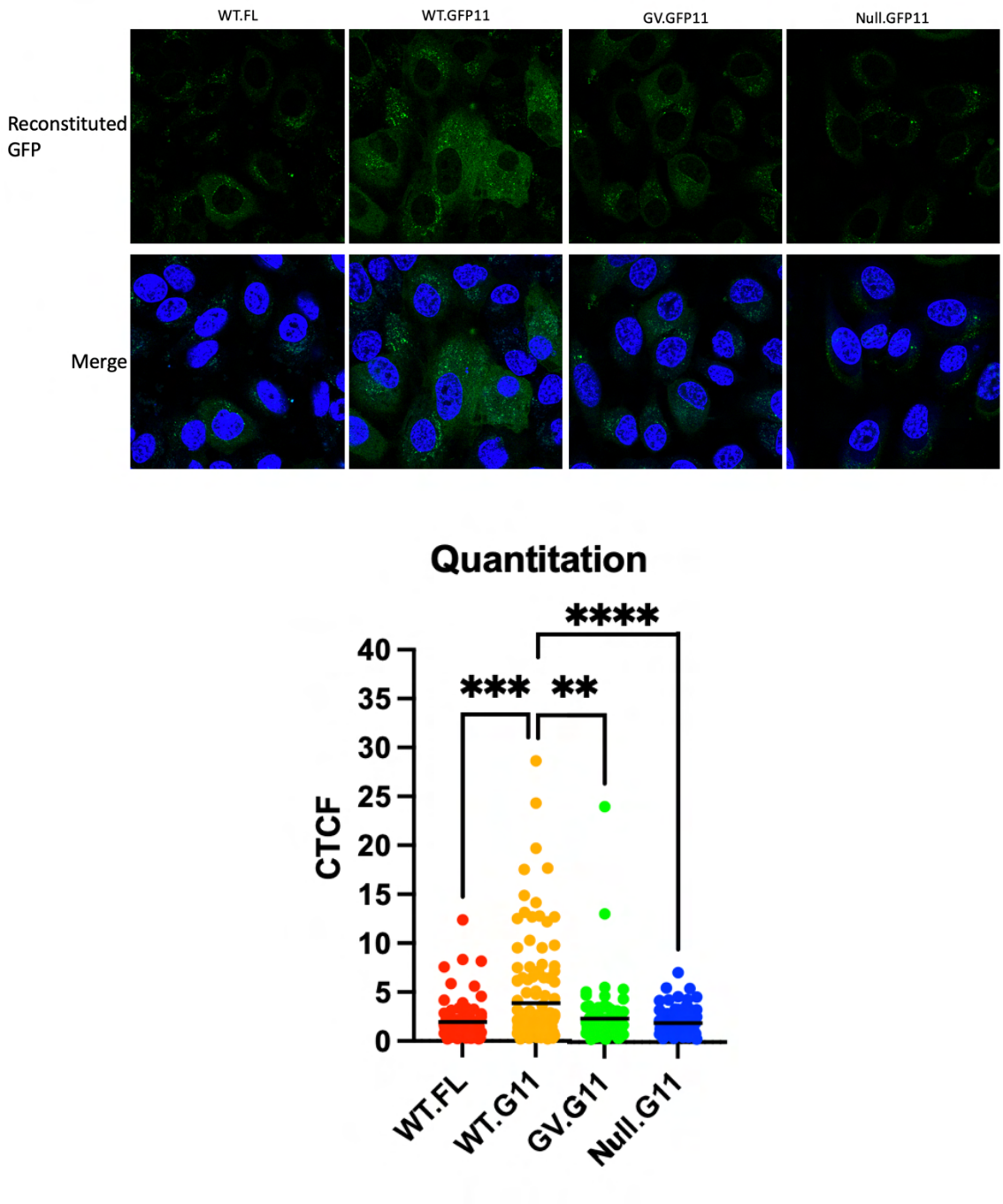


***Figure 3.9: Null and GV mutants do not protrude***

(Top) Clonal HeLa M cells expressing GFP1-10 were infected with FLAG-tagged HPV (control) or GFP11 tagged wild-type or mutant HPV16 PsV. 3hpi, cells were stained with Hoechest 33343 and reconstituted GFP fluorescence due to cytoplasmic protrusion of L2 was observed in live cells using a Leica SP5 confocal microscope. (Bottom) Quantitation of corrected total cellular fluorescence from the top panel. ** $p \leq 0.01$; *** $p \leq 0.001$; **** $p \leq 0.0001$

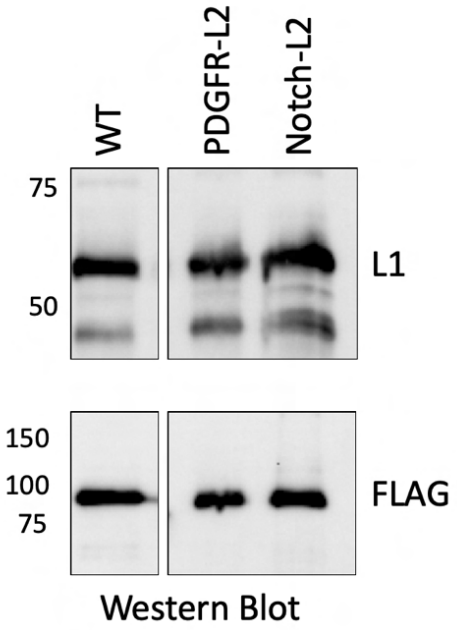


***Figure 3.10: Characterization of PDGFR-L2 and Notch-L2 mutants***

Purified PsV was normalized for genome content and analyzed by SDS-PAGE followed by western blotting for L1 and L2 (FLAG). An extraneous lane was removed between WT and PDGFR-L2 mutants, all samples were analyzed on the same gel.

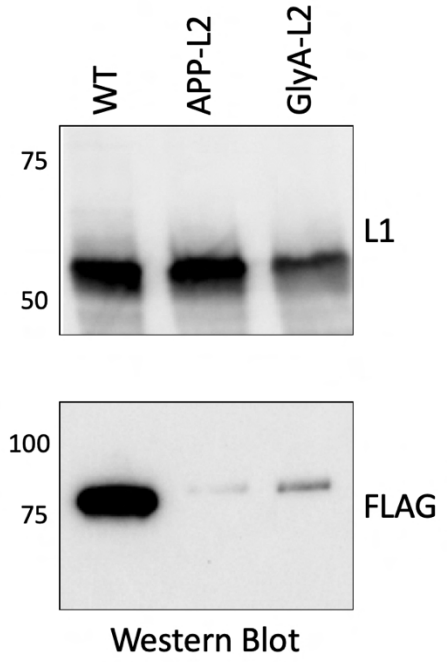


***Figure 3.11: Characterization of GlyA-L2 and APP-L2 mutants***

Purified PsV was normalized for genome content and analyzed by SDS-PAGE followed by western blotting for L1 and L2 (FLAG).

```
Wild-type L2  …ADQILQYGSMGVFFGGLGIGTGSGTGGRTG…
PDGFR-L2      …ADQIVVVISAILALVVLTVISLIILIGRTG…
Notch-L2      …ADQIFMYVAAAAFVLLFFVGCGVLLSGRTG…
```

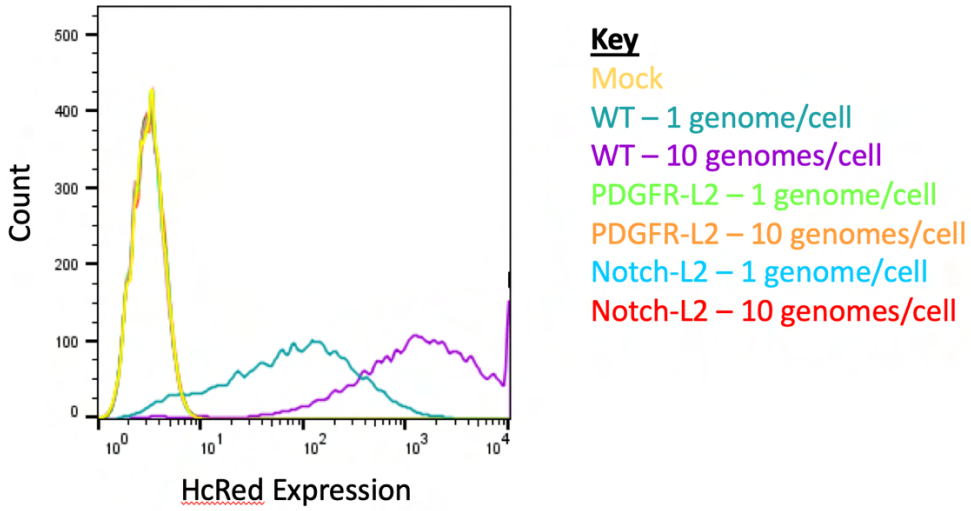


***Figure 3.12: PDGFR-L2 and Notch-L2 mutants are noninfectious***

(Top) Sequence of wild-type L2 protein and mutant proteins. (Bottom) HeLa S3 cells were infected with normalized amounts of wild-type or mutant PsV as indicated. 48 hours post infection, samples were collected and analyzed for HcRed reporter gene expression. A shift to the right indicates successful infection.

Wild-type L2 …ADQI**LQYGSMGVFFGGLGIGTGSGTG**GRTG…

GlyA-L2 …ADQI**ITLIIFGVMAGVIGTILLISYGI**GRTG…

APP-L2 …ADQI**GAIIGLMVGGVVIATVIVITLVML**GRTG…

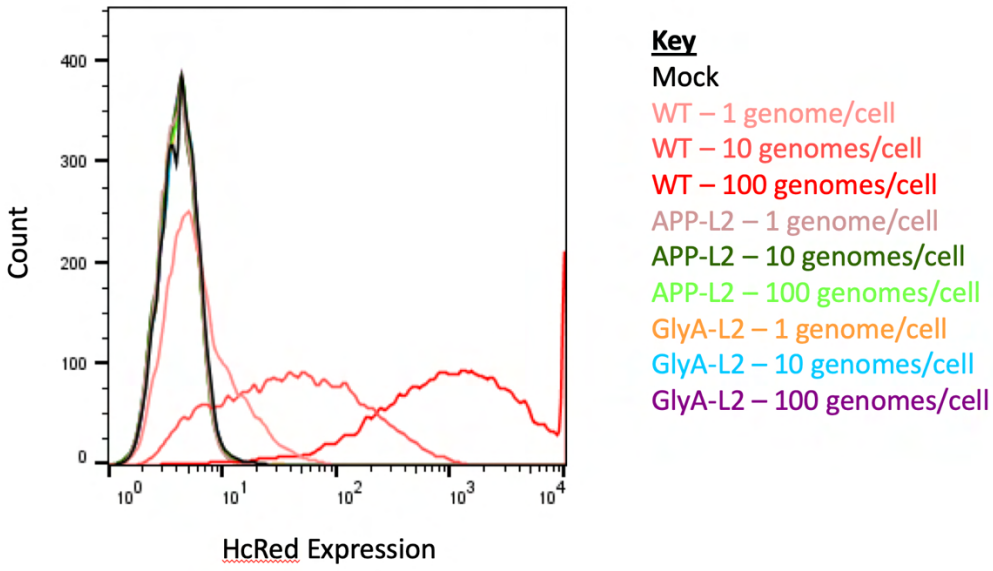


***Figure 3.13: GlyA-L2 and APP-L2 mutants are noninfectious***

(Top) Sequence of wild-type L2 protein and mutant proteins. (Bottom) HeLa S3 cells were infected with normalized amounts of wild-type or mutant PsV as indicated. 48 hours post infection, samples were collected and analyzed for HcRed reporter gene expression. A shift to the right indicates successful infection.

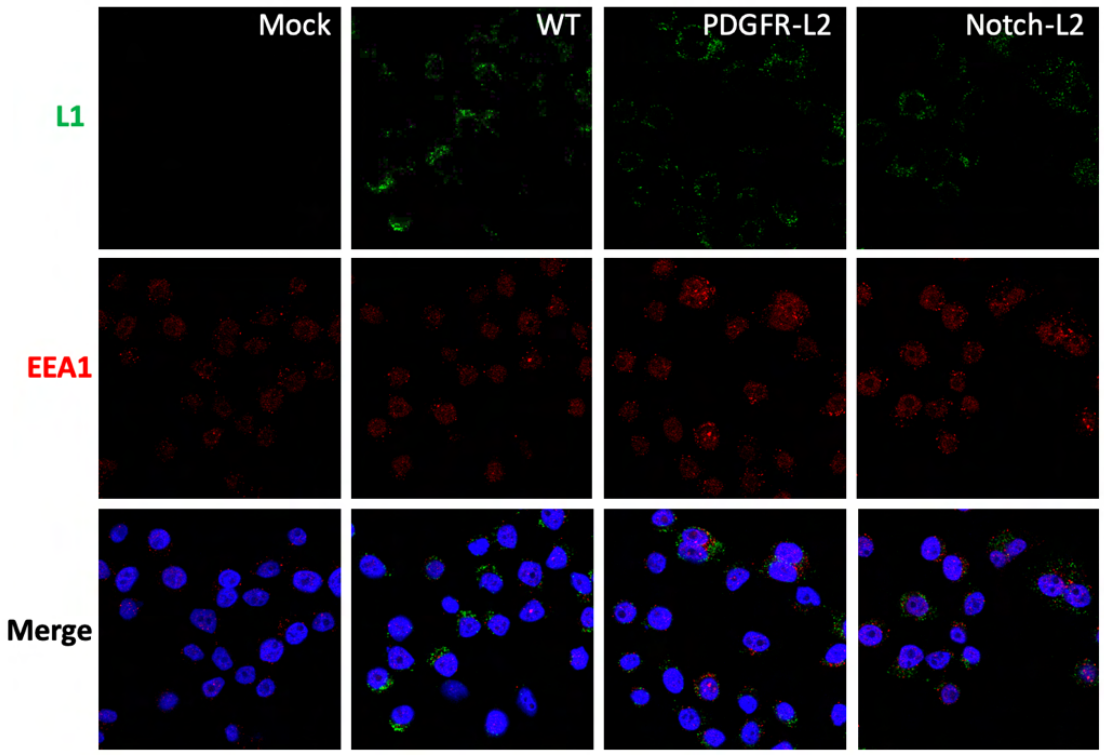


***Figure 3.14: Internalization of PDGFR-L2 and Notch-L2 mutants***

HeLa Sen2 cells were infected with wild-type or mutant PsV for 8 hours. Samples were then fixed using 10% formalin, permeabilized with 1% saponin and processed for immunofluorescence using an antibody that detects L1 (green) and EEA1 (red). DAPI - blue

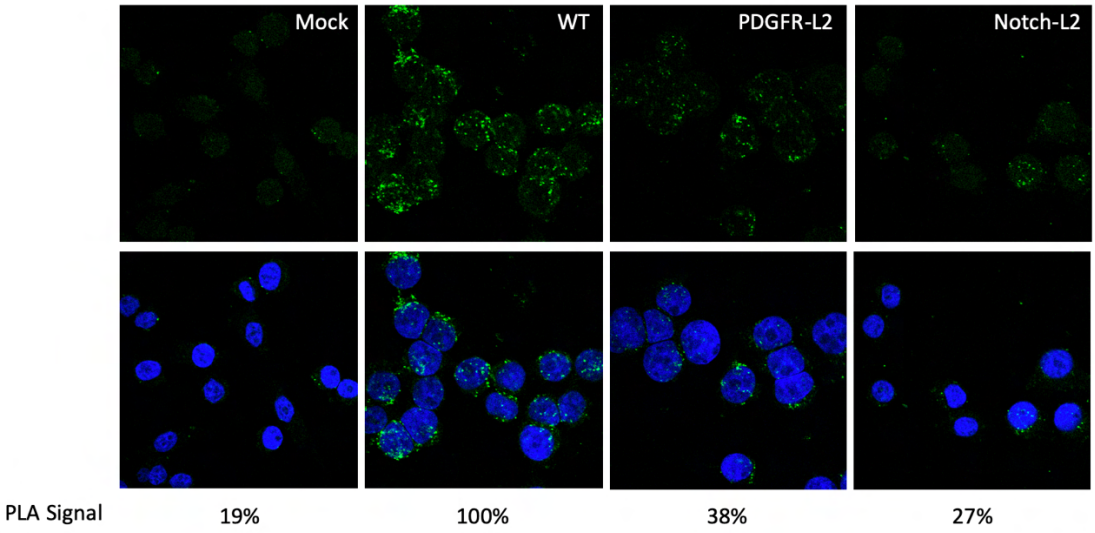


***Figure 3.15: PDGFR-L2 and Notch-L2 are decreased for endosome localization***

HeLa Sen2 cells were infected with wild-type or mutant PsV at an MOI of 50. 8 hours post infection, samples were fixed in 10% formalin, permeabilized with 1% saponin, and processed for the proximity ligation assay. Briefly, samples are incubated with primary antibodies recognizing a EEA1 and HPV. Samples are then incubated with probes that recognize the primary antibodies, the probes are ligated and amplified and signal can be observed using a confocal microscope. Note that PLA only produces signal if the two markers are within 40nm of each other. PLA signal was quantitated using BlobFinder software. DAPI - blue

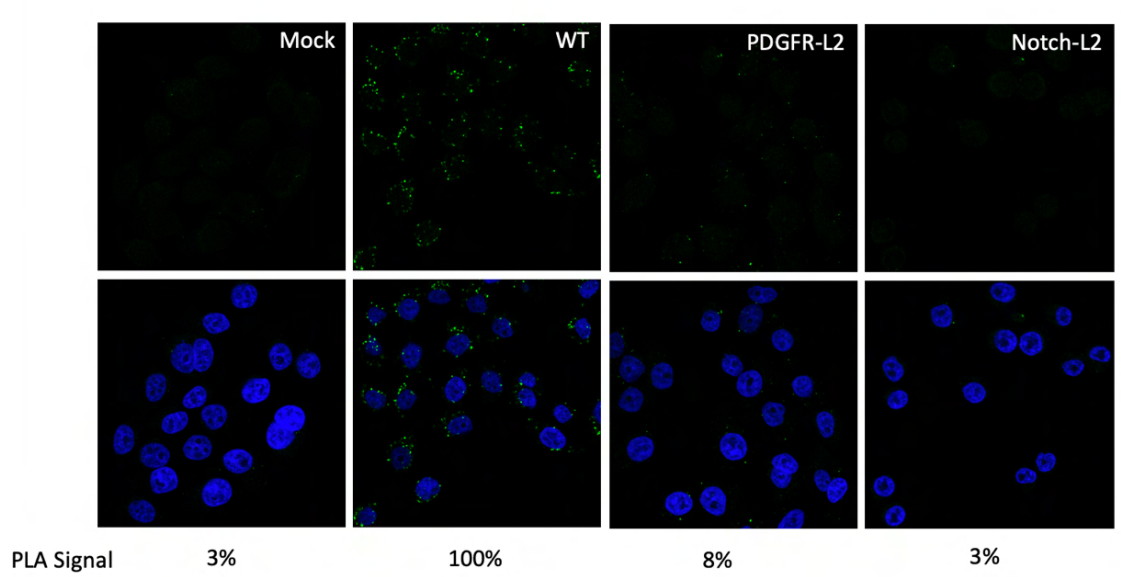


***Figure 3.16: PDGFR-L2 and Notch-L2 TM mutants fail to reach the trans-Golgi network***

HeLa Sen2 cells were infected with wild-type or mutant PsV at an MOI of 50. 16 hours post infection, samples were fixed in 10% formalin, permeabilized with 1% saponin, and processed for the proximity ligation assay. Briefly, samples are incubated with primary antibodies recognizing TGN46 and HPV. Samples are then incubated with probes that recognize the primary antibodies, the probes are ligated and amplified and signal can be observed using a confocal microscope. Note that PLA only produces signal if the two markers are within 40nm of each other. PLA signal was quantitated using BlobFinder software. DAPI - blue

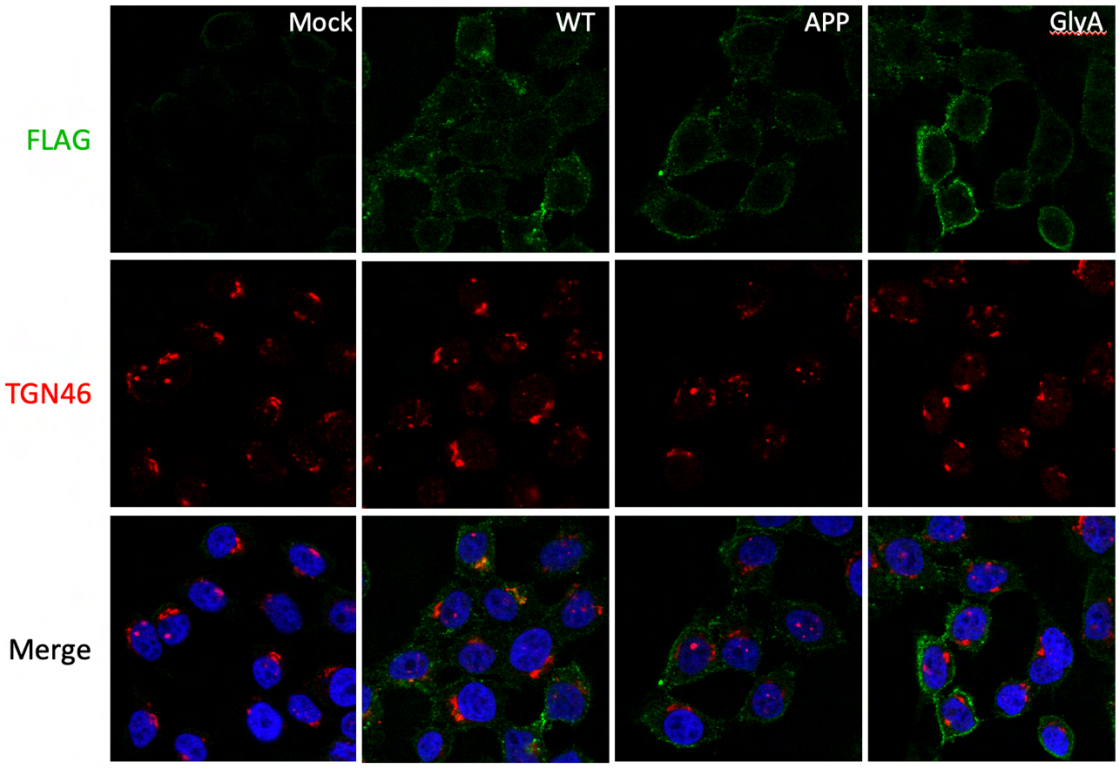


***Figure 3.17: Localization of GlyA-L2 and APP-L2 mutants***

HeLa Sen2 cells were infected with wild-type or mutant PsV for 16 hours. Samples were then fixed using 10% formalin, permeabilized with 1% saponin and processed for immunofluorescence using an antibody that detects FLAG for L2 (green) and TGN46 (red). DAPI - blue.

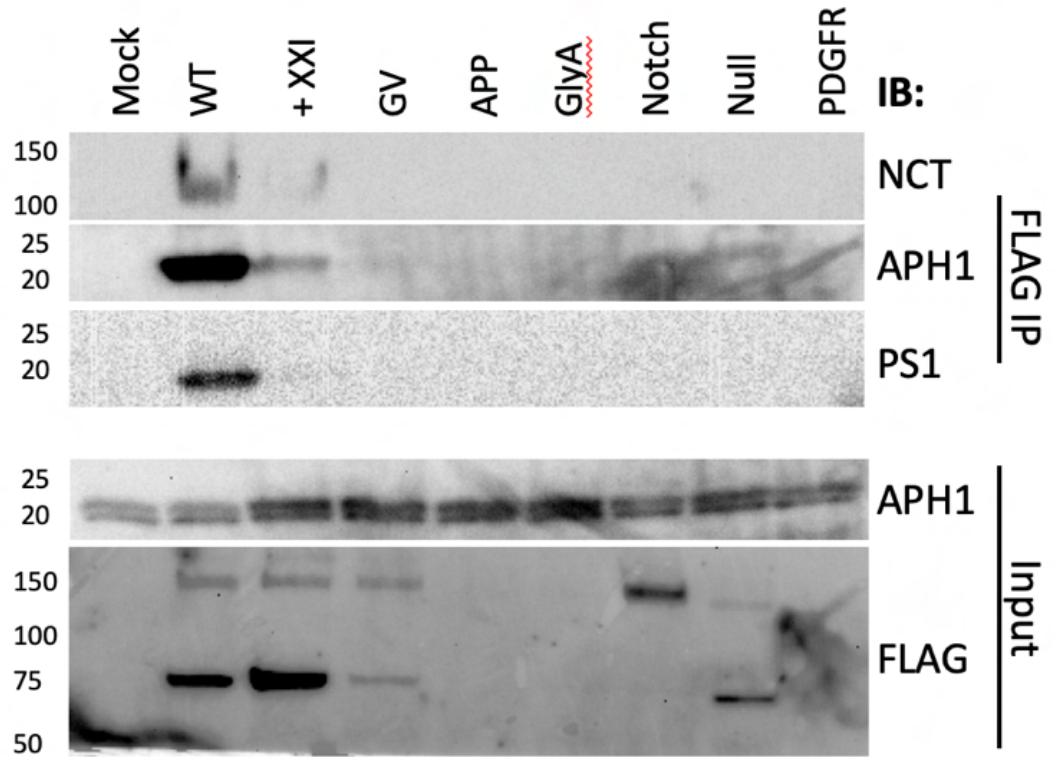


***Figure 3.18: TM mutants do not bind γ-secretase***

HeLa S3 cells were infected with wild-type or mutant PsV for 16 hours. Cells lysates were collected in 1% DMNG lysis buffer and incubated with an antibody recognizing the FLAG tag on the C-terminus of L2. Samples were incubated with protein G magnetic beads overnight and subsequently washed with TBS-T. Samples were eluted from the beads using sample buffer and analyzed via SDS-PAGE and western blotting for the indicated antibodies.

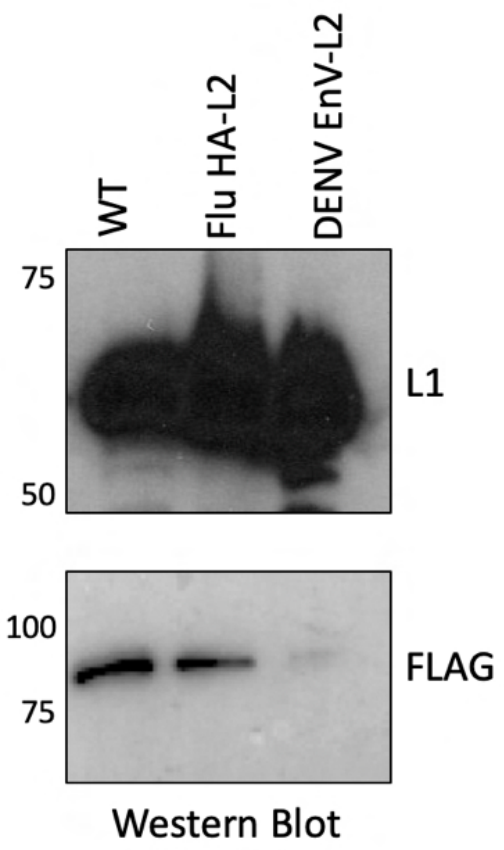


***Figure 3.19: Characterization of DENV-L2 and Flu HA-L2 mutants***

Purified PsV was normalized for genome content and analyzed by SDS-PAGE followed by western blotting for L1 and L2 (FLAG).

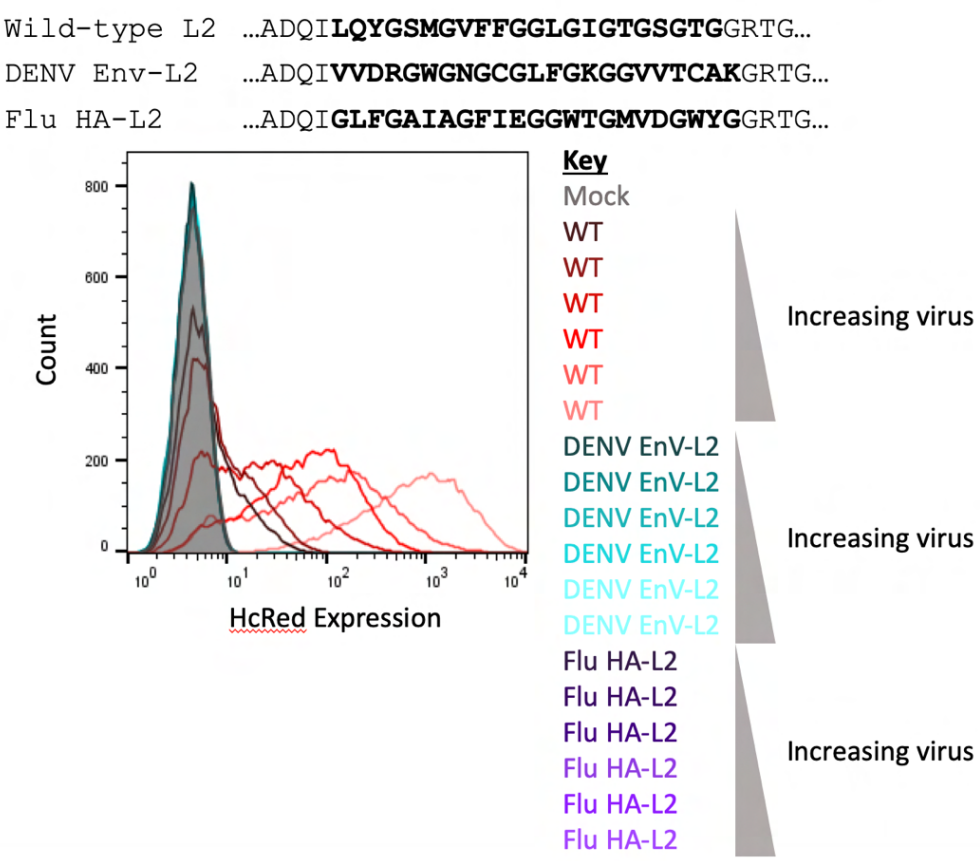


***Figure 3.20: DENV-L2 and Flu HA-L2 mutants are noninfectious***

(Top) Sequence of wild-type L2 protein and mutant proteins. (Bottom) HeLa S3 cells were infected with normalized amounts of wild-type or mutant PsV as indicated. 48 hours post infection, samples were collected and analyzed for HcRed reporter gene expression. A shift to the right indicates successful infection.

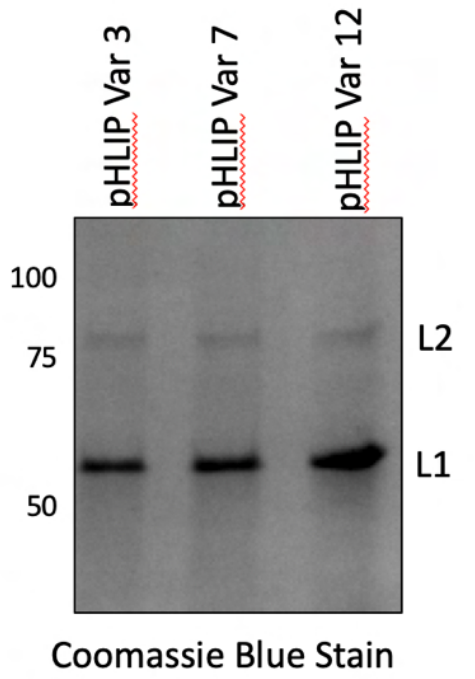


***Figure 3.21: Characterization of pHLiP TM mutants***

Purified PsV was normalized for genome content and analyzed by SDS-PAGE followed by Coomassie Blue staining. L1 = 50kDa, L2 = 75kDa

Wild-type L2 …ADQI**LQYGSMGVFFGGLGIGTGSGTG**GRTG…

pHLiP var 3 …ADQI**ACDDQNPWRAYLDLLFPTDTLLLDLLW**GRTG…

pHLiP var 7 …ADQI**ACEEQNPWARYLEWLFPTETLLLEL**GRTG…

pHLiP var 12 …ADQI**ACEDQNPWARYADLLFPTTLAW**GRTG…

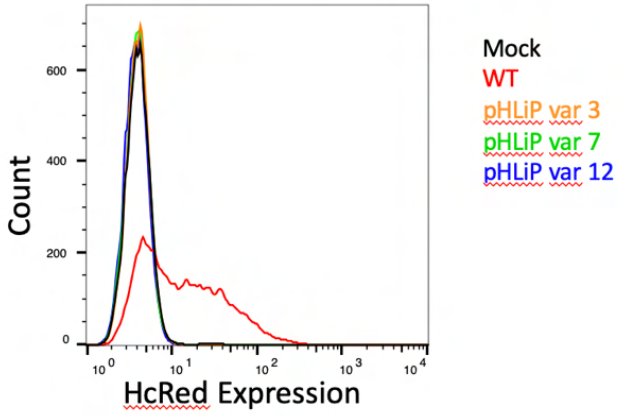


***Figure 3.22: pHLiP TM mutants are noninfectious***

(Top) Sequence of wild-type L2 protein and mutant proteins. (Bottom) HeLa S3 cells were infected with normalized amounts of wild-type or mutant PsV as indicated. 48 hours post infection, samples were collected and analyzed for HcRed reporter gene expression. A shift to the right indicates successful infection.

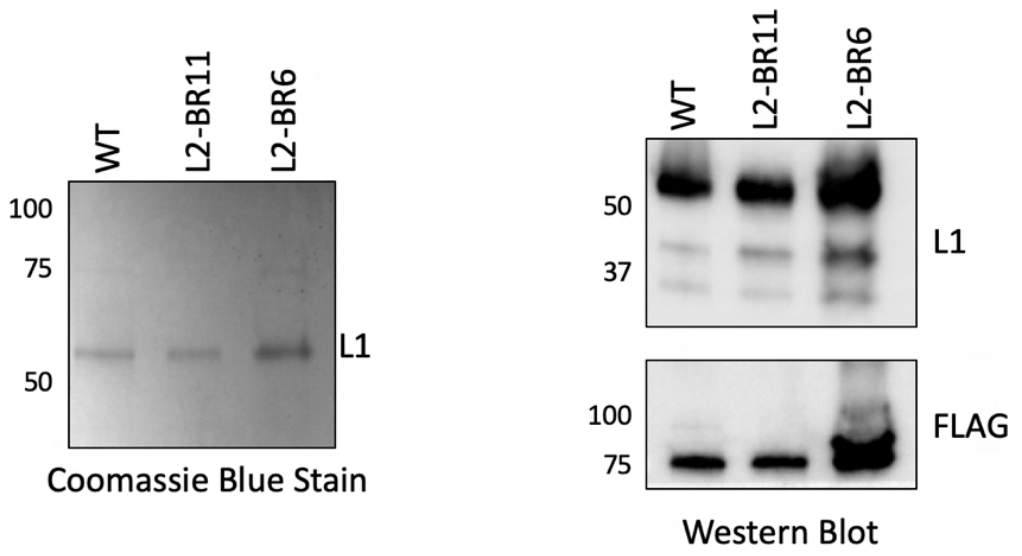


***Figure 3.23: Characterization of chimeric mutants***

Purified PsV was analyzed by SDS-PAGE followed by Coomassie Blue staining (left) or western blotting for L1 and L2 (FLAG) (right).

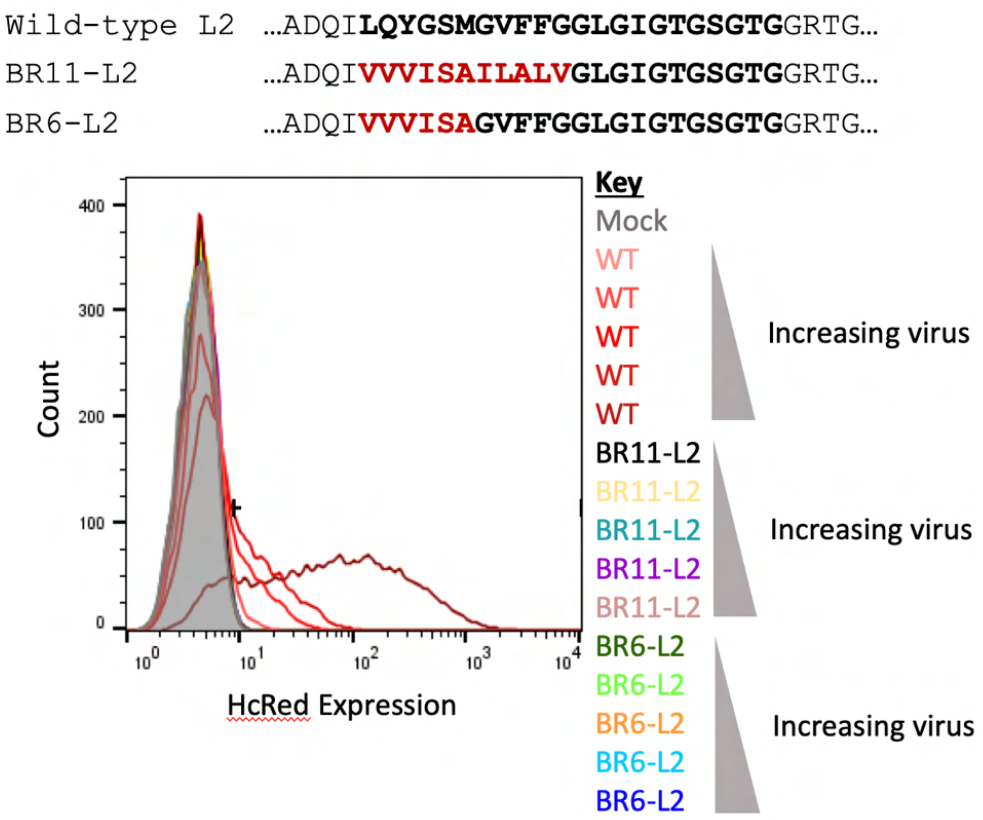


***Figure 3.24: Chimeric mutants are noninfectious***

(Top) Sequence of wild-type L2 protein and mutant proteins. (Bottom) HeLa S3 cells were infected with normalized amounts of wild-type or mutant PsV as indicated. 48 hours post infection, samples were collected and analyzed for HcRed reporter gene expression. A shift to the right indicates successful infection.

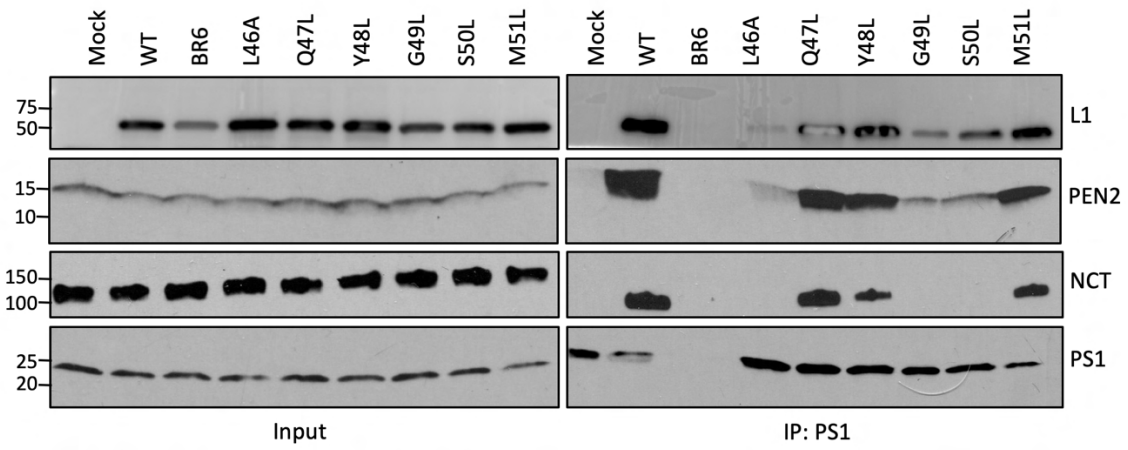


***Figure 3.25: Chimeric and point mutants do not stabilize γ-secretase***

HeLa S3 cells were infected with wild-type or mutant PsV for 16 hours. Cells lysates were collected in 1% DDM lysis buffer and incubated with an antibody recognizing the PS1 subunit of γ-secretase. Samples were incubated with protein G magnetic beads overnight and subsequently washed with TBS-T. Samples were eluted from the beads using sample buffer and analyzed via SDS-PAGE and western blotting for the indicated antibodies.

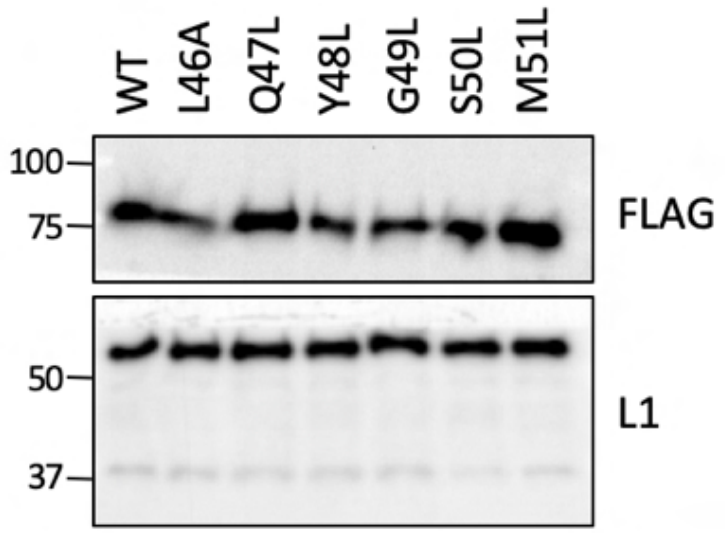


***Figure 3.26: Characterization of TM mutants***

Purified PsV was analyzed by SDS-PAGE followed by western blotting for L1 and L2 (FLAG).

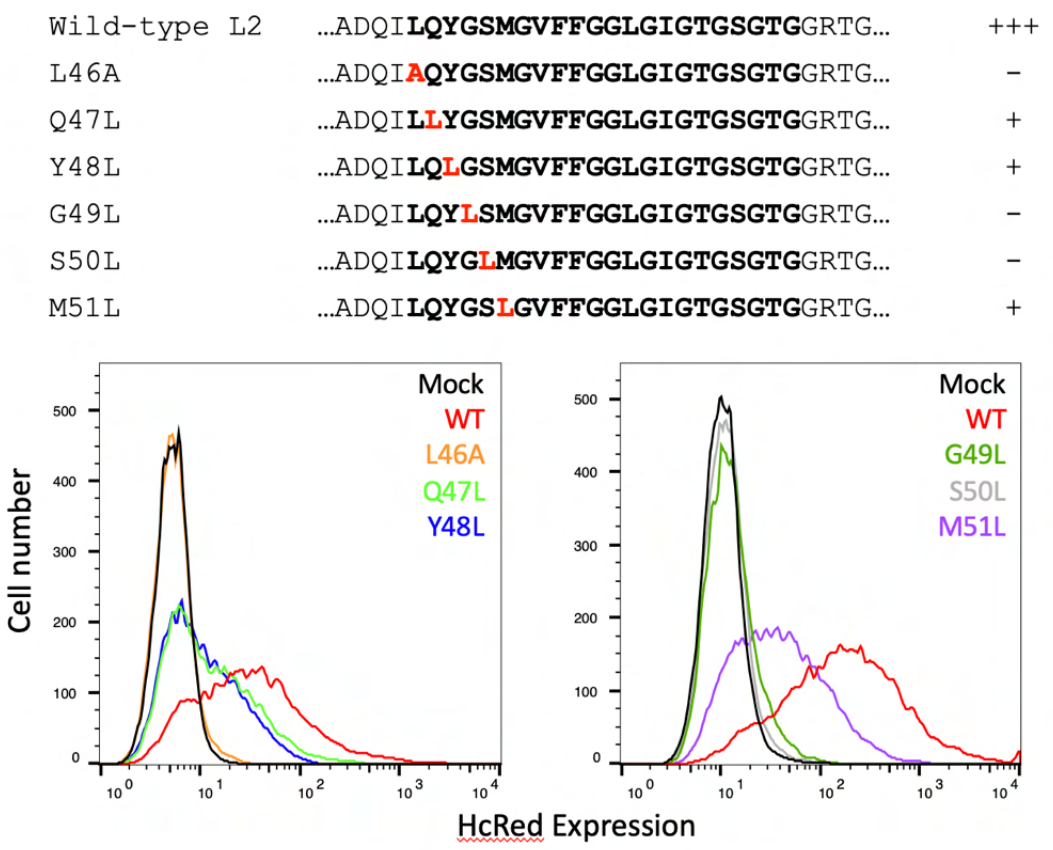


***Figure 3.27: TM mutants have varying infectivity***

(Top) Sequence of wild-type L2 protein and mutant proteins. The plus (+) and (-) signs refer to infectivity relative to wild-type HPV16. (Bottom) HeLa S3 cells were infected with normalized amounts of wild-type or mutant PsV as indicated. 48 hours post infection, samples were collected and analyzed for HcRed reporter gene expression. A shift to the right indicates successful infection.

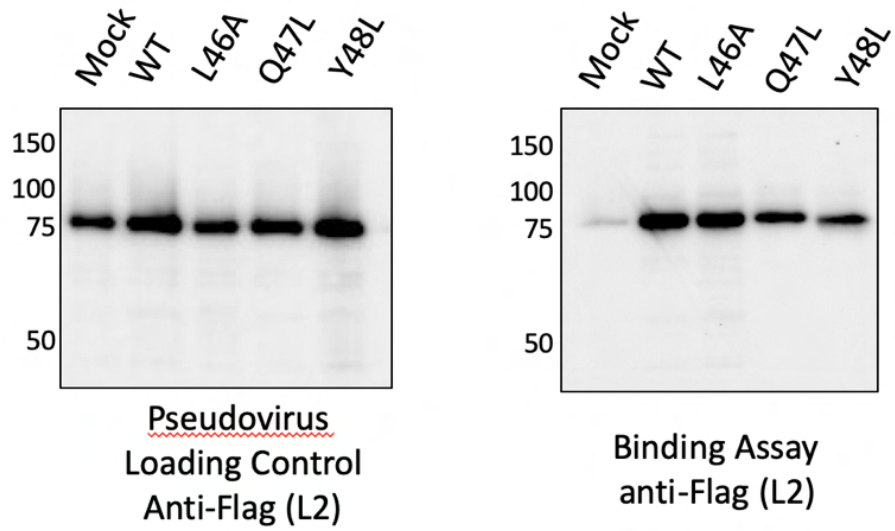


***Figure 3.28: TM mutants bind to cells***

(Left) Normalized amounts of PsV were analyzed by SDS-PAGE followed by western blotting for L2 (FLAG). (Right) HeLa S3 cells were incubated with normalized amounts of PsV for 2 hours on ice to allow binding without internalization. Samples were lysed, analyzed by SDS-PAGE and immunoblotted for L2.

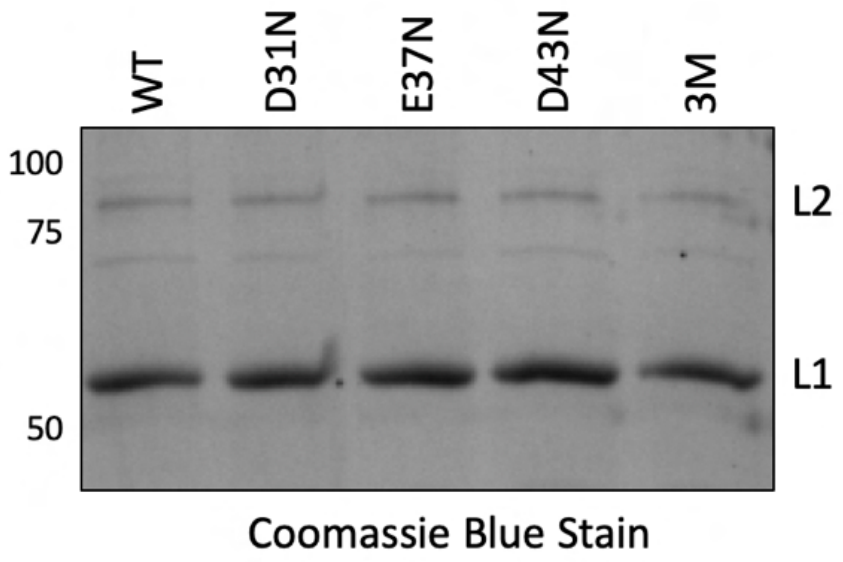


***Figure 3.29: Characterization of pH point mutants***

Purified PsV was analyzed normalized for genome content and analyzed by SDS-PAGE followed by Coomassie Blue staining. L1 = 50kDa, L2 = 75kDa

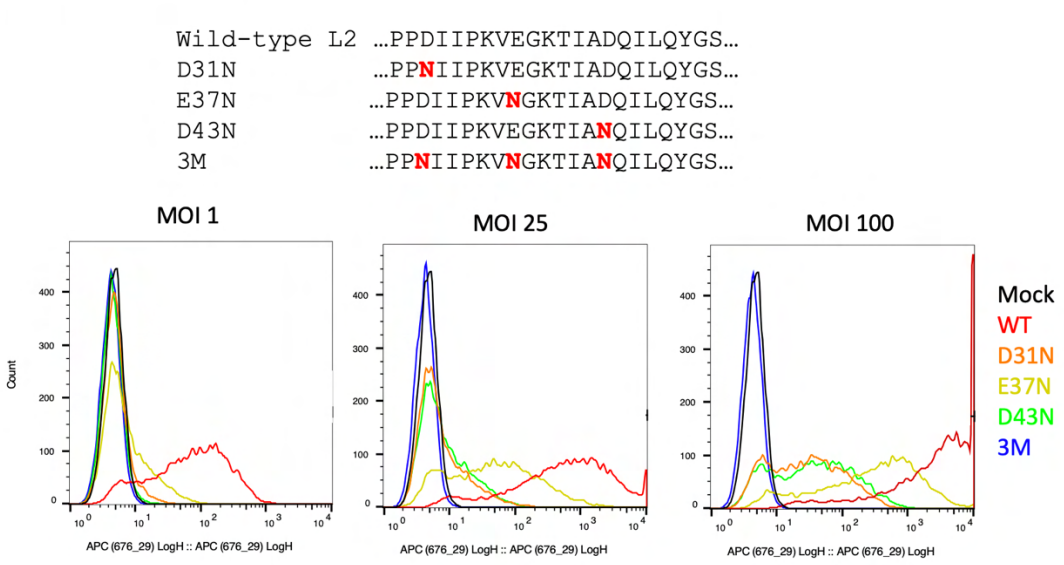


***Figure 3.30: pH point mutants have varying infectivity***

(Top) Sequence of wild-type L2 protein and mutant proteins. Mutations are highlighted in red. (Bottom) HeLa S3 cells were infected with normalized amounts of wild-type or mutant PsV at three different MOIs, as indicated. 48 hours post infection, samples were collected and analyzed for HcRed reporter gene expression. A shift to the right indicates successful infection.

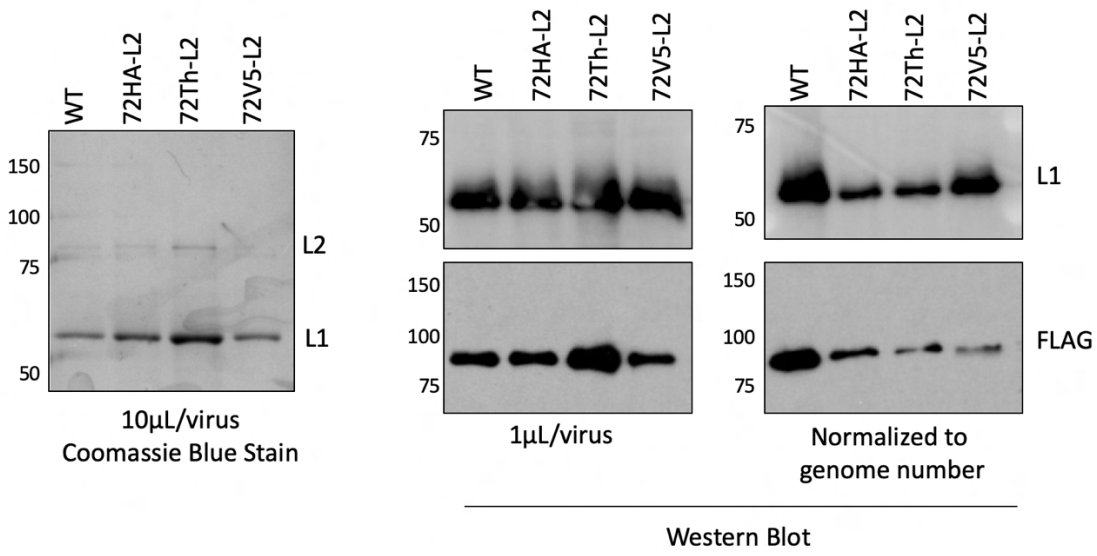


***Figure 3.31: Characterization of L2 insertion mutants***

10 µL of purified PsV was analyzed by SDS-PAGE followed by Coomassie Blue staining (left). 1µL of purified PsV (middle) or the same amount of PsV normalized to genome number (right) was analyzed by SDS-PAGE followed by immunoblotting for L1 and FLAG (L2).

WT …ADQI**LQYGSMGVFFGGLGIGTGSGTG**GRTG…
72HA-L2 …ADQI**LQYGSMGVFFGGLGIGTGSGTG**GRTGYPYDVPDYAYI
72Th-L2 …ADQI**LQYGSMGVFFGGLGIGTGSGTG**GRTGLVPRGSYI
72V5-L2 …ADQI**LQYGSMGVFFGGLGIGTGSGTG**GRTGGKPIPNPLLGLDSTYI

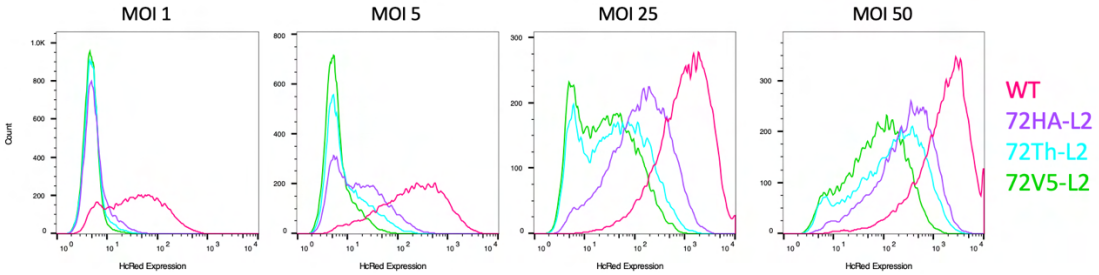


***Figure 3.32: L2 insertion mutants have varying infectivity***

(Top) Sequence of wild-type L2 protein and mutant proteins. Bold = putative TM domain, red = insertion. (Bottom) HeLa S3 cells were infected with normalized amounts of wild-type or mutant PsV at four different MOIs, as indicated. 48 hours post infection, samples were collected and analyzed for HcRed reporter gene expression. A shift to the right indicates successful infection.

# Chapter IV: Interactions between γ-secretase and retromer in HPV infection

## Introduction

Retromer is a cellular protein complex that regulates the trafficking of cellular proteins through the retrograde transport pathway [97]. The core retromer trimer includes VPS26, VPS29, and VPS35. There are also multiple sorting nexins, such as SNX17 and SNX27, that can associate with retromer in order to modulate retromer activity. Lastly, the small GTPase Rab7 regulates retromer recruitment to the endosomal membrane with its cargo, and its GTPase activating protein (GAP), TBC1D5, mediates dissociation of retromer and its cargo from the membrane [108, 114-117].

The three core retromer trimer subunits, SNX17, SNX27, Rab7, and TBC1D5 all play important roles in HPV infection to deliver the viral particle into the retrograde transport pathway [29-31, 37, 41, 42]. HPV utilizes retrograde transport to traffic from the endosome, to the trans-Golgi network, possibly the endoplasmic reticulum, and finally the nucleus. Perturbing retromer function in several ways, including retromer core subunit protein knockdowns; altering Rab7 activity through the use of catalytic mutants or protein knockdown; TBC1D5 knockdown or modulation using a small transmembrane protein; or the use of a small peptide that can bind to and sequester retromer, blocks HPV infection and causes endosomal accumulation of the incoming viral particle [37, 42, 44]. Retrograde

trafficking inhibitors, such as Retro2, also block HPV infection, although it is not known if Retro2 acts on retromer or another, retromer-independent retrograde pathway [37].

There are two retromer binding motifs (sequence FYL and YYML) in the C-terminus of HPV L2 that are required for L2 to bind directly to retromer [31]. Unpublished work has shown that L2 binds at the interface between VPS26 and SNX3, a sorting nexin very similar to SNX12 that is important for HPV infection. The retromer cargo DMT1-II, which has a similar retromer binding site as HPV L2, also binds at this interface [108]. In normal infection of culture cells, L2 associates with retromer at an early time point, around 8 hours post infection (h.p.i.) when the viral DNA and proteins are in the endosome, and disassociates from retromer by 16 h.p.i., when viral DNA and proteins are observed in the TGN [31].

Both retromer and γ-secretase act upon HPV at early steps in infection, and the action of both proteins is necessary for HPV to traffic out of the endosome and into the TGN [31, 47]. Previous investigation into interactions between these two protein complexes showed that the γ-secretase subunit PS1 and retromer subunit VPS35 interact both *in vivo* and *in vitro* [131]. Additionally, there is evidence that when cells are treated with $NH_4Cl$, a compound that blocks endosomal acidification, PS1 is found within both endosomal and Golgi/ER fractions [131]. There is evidence that γ-secretase complex components are trafficked through the retrograde transport pathway, although it is unclear if this is *via* retromer-dependent pathways, retromer-independent pathways, or both [132]. Finally, mutations within retromer and γ-secretase subunits are both associated with neurodegenerative diseases, such as Parkinson's Disease and Alzheimer's Disease [39, 119, 121].

Due to these associations between retromer and γ-secretase, we sought to determine if these two proteins acted coordinately to assist HPV in escaping the endosome and successfully infecting cells. We tested if the two proteins associated with one another in our system, and how HPV infection affects that association. We also wanted to determine how perturbing retromer function would affect γ-secretase binding and stabilization, as well as membrane association and protrusion of HPV L2. Lastly, we investigated the role of γ-secretase in retrograde trafficking of cellular cargo.

## Results

## Retromer and γ-secretase associate

Previous reports in the literature suggest that retromer and γ-secretase associate. I investigated this phenomenon by performing co-immunoprecipitation experiments. Uninfected PS1 KO and parental HeLa cells were transfected with plasmids encoding the three retromer subunits, VPS26, VPS29, and VPS35. 24 hours post transfection, uninfected cells were lysed in buffer containing 1% CHAPSO, a mild detergent, and the PS1 subunit of γ-secretase was immunoprecipitated. The samples were analyzed by western blotting for the retromer subunits VPS35 and VPS26. As is shown in Figure 4.1, the retromer subunits co-immunoprecipitated with PS1, but did not co-IP in cells where PS1 expression was knocked out, indicating that these two proteins are in a complex together in uninfected cells. To test whether γ-secretase inhibition would block this interaction, cells were transfected, as above, and then treated with the γ-secretase inhibitor XXI for one hour prior to lysis. Extracts were subjected to immunoprecipitation as above, and Figure 4.1 shows that the XXI inhibitor blocked the association between γ-secretase and retromer. This shows that γ-secretase activity is necessary for complex between retromer and γ-secretase

and further suggests that the γ-secretase/retromer interaction is real and not simply an artifact caused antibody cross reaction.

Because both γ-secretase and retromer play an important role in endosomal escape of HPV, I then asked if HPV infection affected the association between these two complexes. 293T cells were transfected to overexpress the retromer subunits, as above, and 24 hours post transfection, they were infected with HPV16 PsV at MOI 50. 16 hours post infection, cells were collected, lysed in buffer containing 1% CHAPSO, and immunoprecipitated with an antibody that recognizes PS1. HPV infection did not change the amount of VPS35 that was co-IPed by the anti-PS1 antibody, suggesting that infection did not inhibit the association between retromer and γ-secretase (Figure 4.2).

## Retromer binding is required for γ-secretase binding and stabilization

Because retromer and γ-secretase associate, we next asked how blocking binding of retromer to HPV L2 would affect the ability of HPV to bind and stabilize γ-secretase. A clonal VPS35 knock out HeLa cell line was generated by CRISPR-Cas9, and loss of VPS35 expression was confirmed in these cells (Figure 4.3). We had previously generated VPS35 knockdown (KD) cells and wanted to determine if a full knockout would decrease HPV infection further. Additionally, we can perform wild-type and mutant addbacks in the KO cells. HPV infection is substantially decreased in these KO cells (Figure 4.4), but infection is not totally blocked. This could be due to compensatory mechanisms in the VPS35 KO cells, some residual retromer function due to the location of the guide RNA in the final exon of VPS35, or potential HPV trafficking via a retromer-independent pathway.

To test γ-secretase-L2 binding and HPV-mediated γ-secretase stabilization in the absence of retromer expression, the control and retromer KO cells were infected with

HPV16 PsV for 16 hours and cell lysates were collected in 1% DDM lysis buffer. The PS1 subunit of γ-secretase was immunoprecipitated and samples were analyzed by western blotting for γ-secretase subunits and HPV L2. In cells without retromer expression, the amount of HPV L2 bound to γ-secretase decreased (Figure 4.5). γ-secretase stabilization by HPV was also decreased in these cells (Figure 4.5). These results show that retromer binding to HPV is important for both γ-secretase binding to HPV and γ-secretase stabilization by HPV.

We also used a HPV16 PsV containing L2 with a retromer binding site mutation to determine if the absence of L2-retromer binding in the VPS35 knock-out cells was responsible for the block in γ-secretase binding to HPV. This mutant (DM) cannot infect cells, bind to retromer, or traffic to the TGN at late time points, but rather accumulates in the endosome, the consistent phenotype observed when retromer does not bind to HPV L2. HeLa S3 cells were infected with wild-type HPV PsV or DM PsV for 16 hours, processed for co-immunoprecipitation using an antibody that recognizes PS1, and analyzed by western blot. As shown in Figure 4.6, wild-type L2 bound to γ-secretase but the DM L2 did not. Additionally, wild-type L2 stabilized the γ-secretase complex, as expected, but the DM PsV did not stabilize γ-secretase. This result is consistent with the result in the retromer knockdown cells and showed that binding of L2 to retromer is important for both γ-secretase binding to HPV L2 and γ-secretase stabilization by HPV. This result also indicates that the lack of γ-secretase binding and stabilization when retromer expression is decreased is not simply due to trafficking defects from a lack of retromer expression or due to some unexpected feature of the knockout cells.

Additionally, we tested whether γ-secretase was still bound to and stabilized by HPV in cell expressing Rab7 CA. Rab7 is a GTPase that recruits retromer to the endosome membrane in association with its cargo. We showed in published work that a constitutively active Rab7 (Rab7 CA) mutant recruits retromer to HPV. However, at 16 hours post infection, when retromer has typically disassociated from HPV, the Rab7 CA mutant does not allow retromer to disassociate from HPV and causes HPV accumulation in the endosome [177]. Parental cells and cells expressing Rab7 CA were infected with HPV16 PsV. 16 h.p.i., we then lysed the cells in buffer containing 1% DDM and immunoprecipitated PS1. As shown in Figure 4.7, L2 does not bind to or stabilize γ-secretase in the Rab7 CA cells. This result implies that Rab7-GTP inhibits γ-secretase binding, or that Rab7-GDP or Rab7 cycling is required for γ-secretase binding and stabilization of HPV L2.

Finally, previous experiments in the lab suggested that γ-secretase acted upstream of retromer. In cells only treated with the γ-secretase inhibitor, HPV PsV does not accumulate in the endosome at 16 h.p.i. [47]. On the other hand, the retromer binding site mutant (DM) HPV PsV accumulates in the endosome at 16 h.p.i. [31]. These two different phenotypes allowed us to perform an epistasis experiment, where cells were treated with γ-secretase inhibitor and then infected with DM PsV. The proximity ligation assay (PLA) was performed to assess proximity of L2 and an endosomal marker EEA1 to determine how the virus acted in the endosome: did it accumulate or not? In this experiment, we showed that the DM PsV did not accumulate in the endosome at 16 h.p.i., suggesting that γ-secretase acts upstream of retromer (experiment performed by Wei Zhang, Figure 4.8).

## Transient membrane association of HPV L2

We recently published that L2 transiently inserts into the membrane when retromer binding is disrupted: at 6 h.p.i., L2 is partitions equally between integral membrane and non-integral membrane fractions in both wild-type and retromer KD cells, as assessed by a carbonate extraction assay, but at 8 h.p.i., L2 is fully inserted in wild-type cells and not inserted in the retromer KD cells (Figure 4.9, [177]). This suggests that L2 is being anchored in the membrane at 8 h.p.i. by retromer binding. As an initial test whether cytoplasmic protein binding can anchor L2, I performed a split GFP assay in cells infected with HPV16 PsV containing wild-type L2 or the retromer binding site mutant (DM) L2. In this assay, GFP1-10 is expressed in the cytoplasm of cells and GFP11 is appended to the C-terminus of L2 in both wild-type and DM viral particles. When expressed individually, GFP11 and GFP1-10 do not fluoresce, but if GFP11-tagged L2 protrudes through the endosome membrane into the cytoplasm, GFP is reconstituted and fluorescence can be observed by confocal microscopy. With GFP11-tagged L2 containing an intact retromer binding site, reconstituted fluorescence is observed at both 6 and 8 h.p.i., as expected (Figure 4.10 and 4.11). A similar level of reconstituted fluorescence is also observed at both of these time points with the GFP11-tagged DM mutant, even though carbonate extraction did not detect membrane association of this mutant at 8 h.p.i. We note that the carbonate extraction experiment was performed in cells that did not express GFP1-10 infected with PsV lacking GFP11. This result raises the possibility that the DM L2 is being kept in the membrane, not by binding to retromer, but by binding to GFP1-10. Taken together, these experiments

suggest that binding of L2 to a protein in the cytoplasm, retromer during normal infection and GFP1-10 in the split GFP assay, stabilizes the association of L2 with the membrane.

## Effect of retromer mutants on infectivity

Many mutations within retromer subunits, typically VPS35, are associated with neurodegenerative diseases. One such mutation is the D620N mutation in VPS35, which is associated with Parkinson's Disease (PD). This is a rare mutation that is present in an estimated 0.3% of sporadic and 1.3% of familial PD cases and has high, but not full, penetrance [178, 179]. The D620N mutant properly associates with the other two subunits of the retromer complex (VPS26 and VPS29) and can bind to retrograde cellular cargo, but cargo does not traffic properly in cells carrying this mutation [180]. Some studies show that this mutation causes PD in a dominant gain of function manner while others report it has a loss of function, depending on context and the organism and process being studied [181]. Regardless, we can use this mutant VPS35 as an alternate method to test whether protein binding is sufficient for membrane association of L2, since this mutant is reported to bind to cargo but does not support trafficking. First, we showed that the parental cells used in the laboratory contain wild-type VPS35 (Figure 4.12). Wild-type or D620N VPS35 was introduced into the VPS35 KO cells described above, and expression of the exogenous VPS35 protein was confirmed by western blotting (Figure 4.3). These cells were infected with HPV16 PsV and infectivity was measured by flow cytometry for expression of the reporter protein. Intriguingly, HPV infectivity was much higher in cells expressing the D620N VPS35 protein than in cells transduced with wild-type VPS35 and similar to the infectivity of parental HeLa S3 cells (Figure 4.4). To test whether HPV uses a retromer-independent pathway to infect the D620N cells, I infected the wild-type, knock out, and

addback cells with the DM PsV. As shown in Figure 4.13, the DM does not infect the D620N cells, suggesting that the rescue of infection observed with the D620N mutant is through a retromer-mediated pathway.

## γ-secretase is required for retrograde trafficking of cellular cargo

The association between retromer and γ-secretase prompted us to investigate if γ-secretase activity was important for the retrograde trafficking of cellular cargo that use retromer. I examined the trafficking of DMT1-II, a cellular protein that undergoes retromer-mediated recycling from the endosome back to the TGN. If retromer activity is inhibited, DMT1-II accumulates in the endosome and is absent from the TGN. The retromer binding site of DMT1-II is similar to the L2 RBS and binds directly to the VPS26 subunit of retromer in conjunction with SNX3. I treated uninfected HeLa M cells with XXI for 1 hour and then transfected the cells with a plasmid expressing GFP-tagged DMT1-II. 24 hours post transfection, cells were fixed, permeabilized, and processed for immunofluorescence using antibodies for GFP and the cellular marker protein EEA1 or gm130, to assess endosome or TGN localization, respectively. In cells treated with the DMSO control, there is some co-localization between DMT1-II and EEA1, which is significantly increased in cells treated with XXI (Figure 4.14). This indicates that blocking γ-secretase activity causes endosomal accumulation of DMT1-II, likely because it cannot be recycled properly. Similarly, in control cells, there is readily detectable co-localization between DMT1-II and TGN46, which is significantly decreased when cells are treated with XXI (Figure 4.14). These data suggest that γ-secretase activity is important for the retrograde trafficking of cellular cargo as well as HPV.

## Discussion

These studies of the interactions between retromer and γ-secretase led to many interesting conclusions. First, γ-secretase and retromer associate with each other and this association is blocked by a γ-secretase inhibitor. When HPV infects cells, there is no obvious difference in the amount of these two proteins in association. However, it is possible that the localization of proteins is altered during infection, or that infection concentrates the two proteins to a specific area on the endosomal membrane. Further localization studies using immunofluorescence and the proximity ligation assay (PLA) can assess this possibility.

Further, in HPV infection, we show that retromer is required for stable membrane association of L2. L2 inserts into the membrane transiently when it cannot bind retromer, and this was shown both with cells that do not express retromer, and virus containing an L2 protein that cannot bind to retromer [177]. Retromer is also important for L2 to bind to and stabilize the γ-secretase complex. This was an unexpected result because of epistasis experiments performed where γ-secretase inhibition and the retromer binding site mutant were combined to determine which protein acted first in HPV infection. Wild-type L2 does not accumulate in the endosome with γ-secretase inhibition, and the DM mutant L2 does in cells not treated with the γ-secretase inhibitor. In the epistasis experiment, cells were treated with the γ-secretase inhibitor and subsequently infected with the DM, and we did not observe L2 endosomal accumulation, suggesting that γ-secretase acts before retromer binding. However, given the results that retromer binding is important for both stable membrane association of L2, and γ-secretase binding and stabilization by L2, these results need to be reexamined. Our results now suggest that these two protein complexes somehow

work together to support infection. It may not be possible to determine if γ-secretase activity is necessary before or after retromer action, since the steps appear to be intertwined. However, during infection, membrane association, γ-secretase stabilization, γ-secretase binding, and retromer binding are all clearly closely coordinated.

Our results also suggest that retromer binding to HPV is anchoring the protein in the cytoplasm. The results in the split GFP assay with the DM virus suggest that binding to a protein in the cytoplasm can anchor L2 within the membrane. In order to test this hypothesis, we want to use a carbonate extraction experiment to determine membrane association in the presence and absence of cytoplasmic protein binding to the C-terminus of L2. For example, the results of the split GFP assay suggests that we can test whether cytoplasmic GFP1-10 allows only GFP11-tagged L2 to stably associate with the membrane. The results of these and similar experiments will allow us to better understand the complex interactions between HPV L2, γ-secretase, and retromer on the endosomal membrane.

An intriguing result is that the D620N mutant version of VPS35 supports HPV infection to a similar level as the parental HeLa S3 cells. The wild-type VPS35 protein increases HPV infection in the VPS35 KO cells, but not to the same level as the parental S3's or the D620N mutant. This rescue occurs through a retromer-dependent pathway because the DM HPV mutant is not infectious in any of these cells.

The D620N VPS35 mutant has been reported to bind to cargo, but does not allow cargo to traffic properly. It is unknown if the mutant disassociates from the membrane similarly to wild-type VPS35, however this mutant does show an increased localization with EEA1, an early endosome marker, and LAMP1, a late endosome/ lysosome marker,

compared to wild-type VPS35 [180]. This suggests that the D620N mutant does not disassociate from the membrane with the same kinetics as wild-type VPS35 since it has increased colocalization with late endosome markers. Because the D620N mutant supports infection, and to a higher degree than the wild-type VPS35 protein, this suggests that only the cargo binding function of VPS35 is required for HPV infection, however this hypothesis needs to be further studied. Perhaps the D620N mutant causes there to be more retromer localized to the membrane, which allows for greater infection of HPV if the main role of retromer in HPV infection is binding to L2 and anchoring it in the membrane.

We can exploit the fact that the D620N mutant doesn't traffic properly to dissect which roles of retromer (i.e. trafficking or only cargo binding) are required for various processes in HPV infection. We can assess if L2 stably associates with the membrane in these cells, as well as test for retromer binding to L2. Because of the interactions between γ-secretase and retromer, we can also test γ-secretase association with retromer, as well as γ-secretase stabilization and binding of L2 in cells expressing the D620N mutant. If the results of these experiments show that L2 can bind to retromer and can stably associate with the membrane in these D620N cells, without trafficking cellular cargo, that would suggest that the main role of retromer in HPV infection is to bind to L2 and anchor it within the membrane, and not to necessarily traffic the viral particle. This would be a very interesting new result and would require further study to determine what cellular factors and processes HPV uses to traffic through the cell to the nucleus.

Finally, we have shown that γ-secretase activity is required for recycling of DMT1-II. This result suggests that γ-secretase and retromer may act coordinately to support normal trafficking of cellular cargo. DMT1-II is recognized by the SNX3-retromer

complex, but there are two other classes of retromer complexes: the SNX-BAR-retromer and the SNX27-retromer. It would be interesting to determine if γ-secretase activity is necessary for the trafficking of cargo that utilizes these other classes of retromer, or if γ-secretase activity is only necessary for cargo that uses the SNX3-retromer. There are also retromer-independent retrograde trafficking pathways and it could be interesting to determine if γ-secretase plays a role in general retrograde trafficking, or only in specific instances through its interaction with retromer.

## Figures

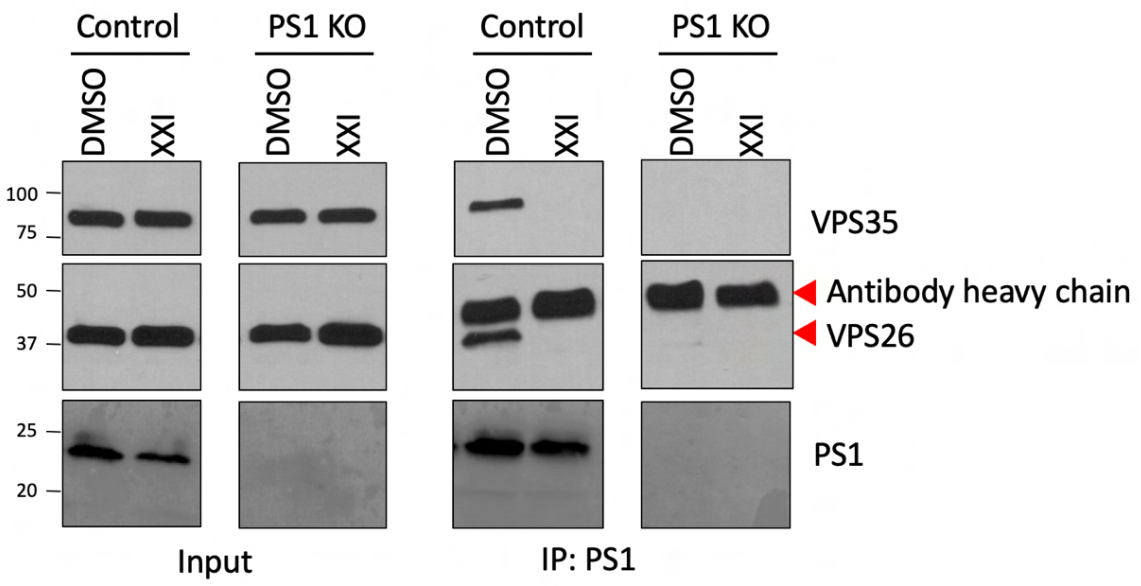


***Figure 4.1: Retromer and γ-secretase associate***

HeLa PS1 KO and parental cells were treated with 1μM XXI or DMSO vehicle for 1 hour and then transfected with plasmids encoding the three retromer subunits (VPS26, VPS29, and VPS35). 24 hours post transfection, cells were lysed in buffer containing 1% CHAPSO and immunoprecipitated with a PS1 antibody. Immunoprecipitates were incubated with protein G magnetic beads, washed in lysis buffer, eluted from the beads, and analyzed by SDS-PAGE and western blotting for PS1 or the indicated retromer subunit.

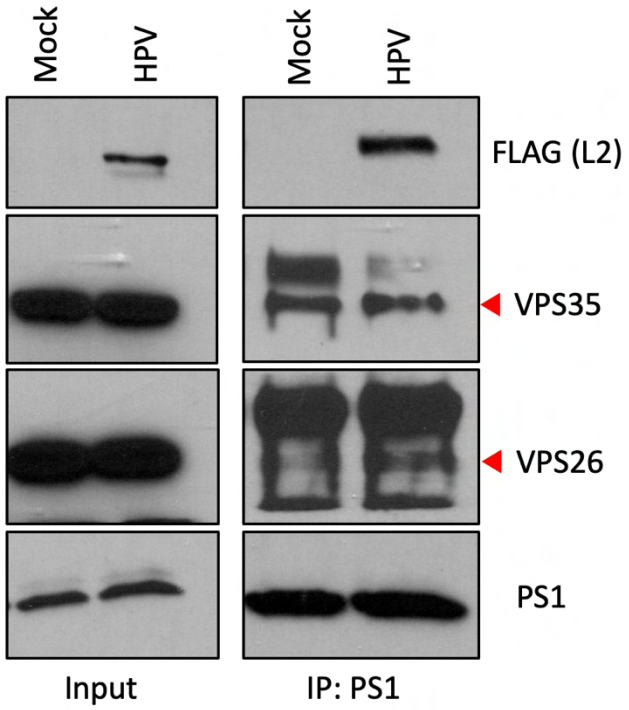


***Figure 4.2: HPV infection does not inhibit the association between retromer and γ-secretase***

293T cells were transfected with plasmids encoding the three retromer subunits (VPS26, VPS29, and VPS35). 24 hours post transfection, cells were infected with HPV16 PsV for 16 hours, lysed in buffer containing 1% CHAPSO and immunoprecipitated with a PS1 antibody. Immunoprecipitates were incubated with protein G magnetic beads, washed in lysis buffer, eluted from the beads, and analyzed by SDS-PAGE and western blotting for L2 (with the anti-FLAG antibody), PS1, or the indicated retromer subunit.

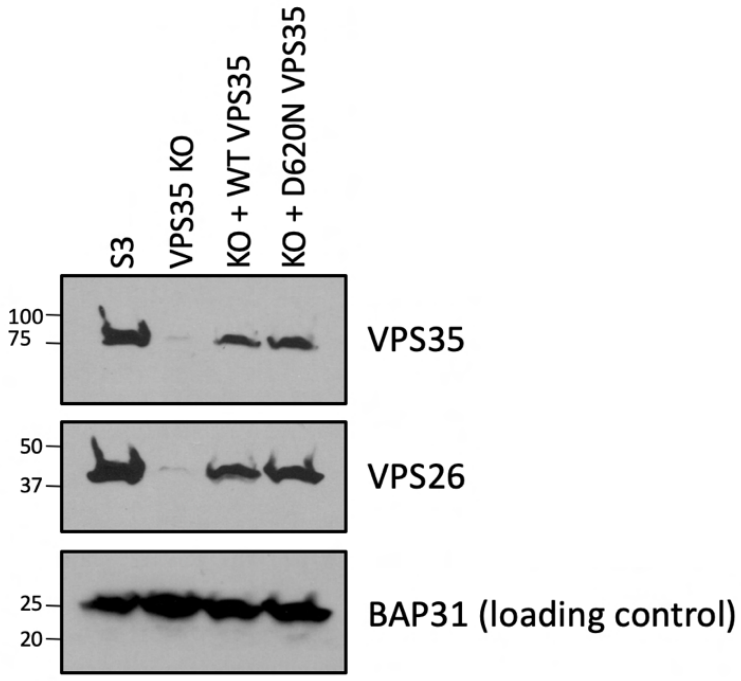


***Figure 4.3: VPS35 expression is eliminated in CRISPR-Cas9 knockout cell lines and reconstituted in the add-backs***

HeLa cells were transduced with a lentivirus containing the sgRNA targeting VPS35. Cells were selected with puromycin and single-cell cloned to generate VPS35 KO cells. The VPS35 KO cells were transduced with lentivirus containing the indicated retromer expression construct and selected with hygromycin. Cell lysates were collected and analyzed via western blotting for VPS35, VPS26, and BAP31 (as a loading control).

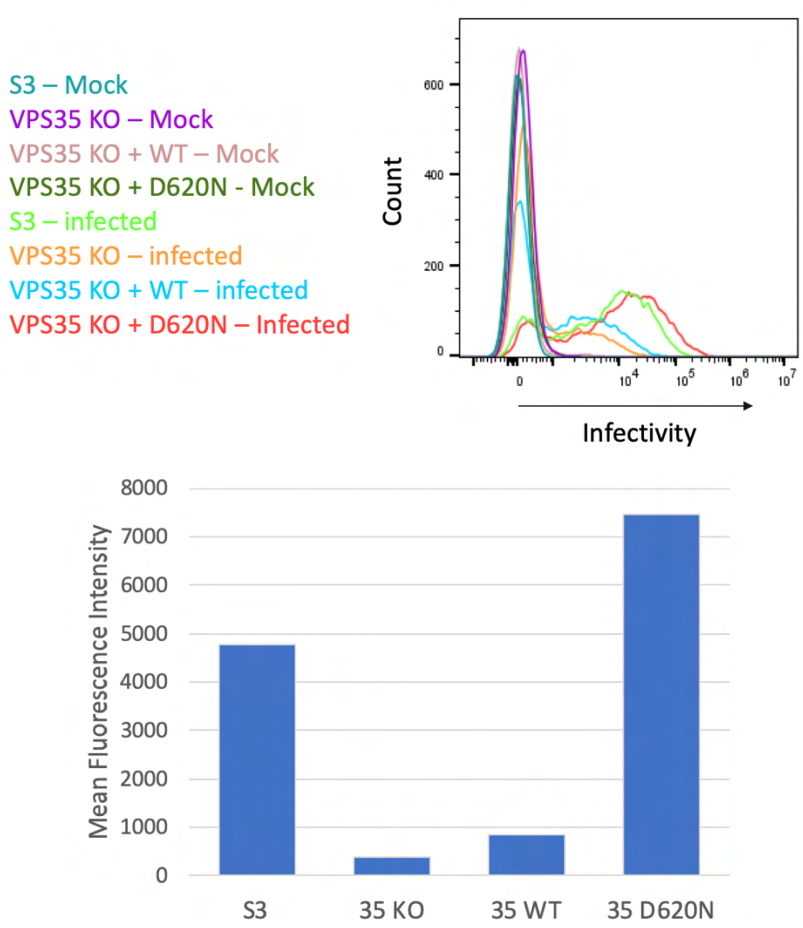


***Figure 4.4: HPV infection is decreased in VPS35 KO cells***

(Top) The indicated cells were infected with HPV PsV at an MOI of 5 or mock infected. 48 hours post infection, cells were collected and analyzed by flow cytometry for HcRed expression. A shift to the right indicates successful infection. (Bottom) Quantitated mean fluorescence intensity (MFI) for the infected cells from one experiment.

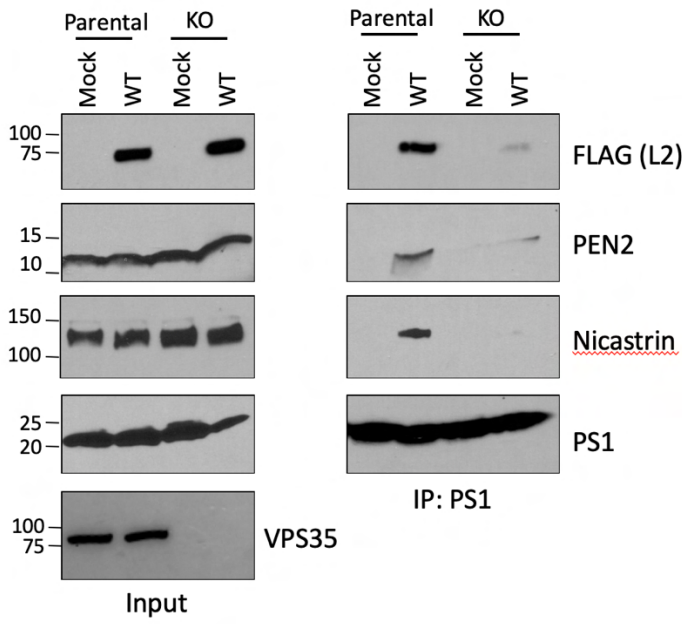


***Figure 4.5: Knocking out VPS35 reduces the ability of HPV to bind and stabilize γ-secretase***

VPS35 KO and parental HeLa cells were infected with HPV16 PsV containing FLAG-tagged L2 for 16 hours. Cells were lysed in buffer containing 1% DDM lysis buffer, immunoprecipitated with a PS1 antibody, and incubated with protein G magnetic beads. Samples were washed in TBS-T, eluted from the beads, and analyzed via western blotting for γ-secretase subunits and HPV L2.

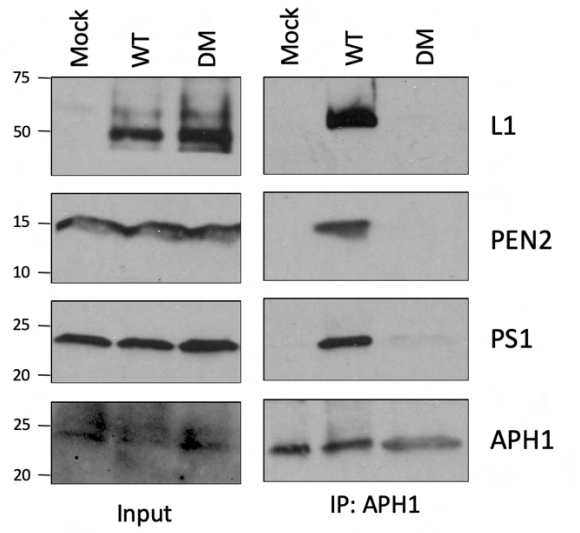


***Figure 4.6: The retromer binding site mutant HPV does not bind to or stabilize γ-secretase***

HeLa cells were infected with wild-type or double mutant (DM) HPV16 PsV for 16 hours or mock infected. Cell lysates were collected in 1% DDM lysis buffer, immunoprecipitated with APH1 antibody, and immunocomplexes were captured with protein G magnetic beads. Samples were washed in TBS-T, eluted from the beads, analyzed by SDS-PAGE, and immunoblotted for the indicated γ-secretase subunit and HPV L1.

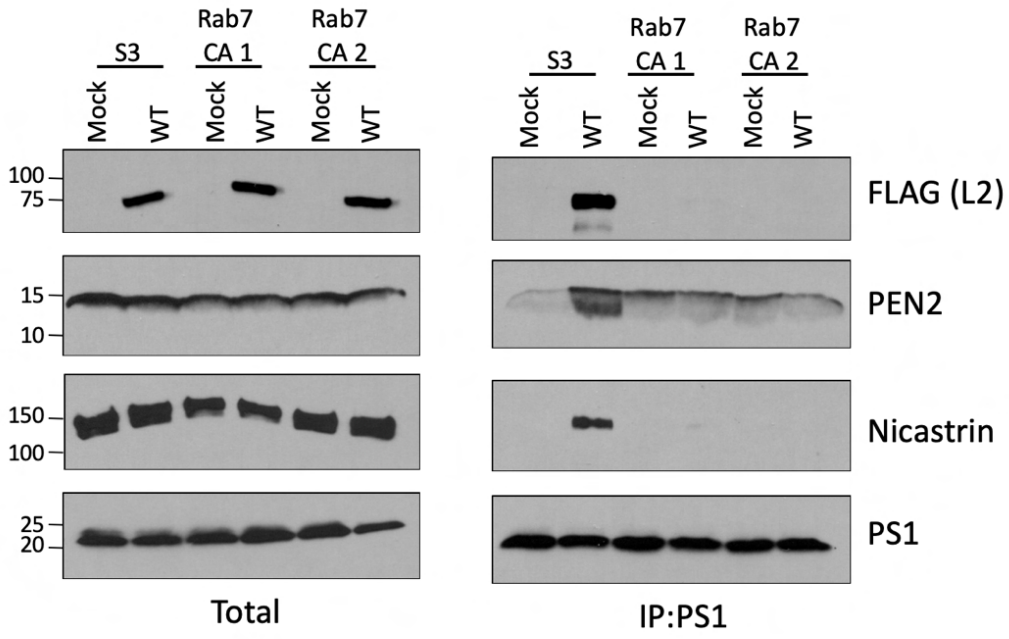


***Figure 4.7: HPV L2 does not bind to or stabilize γ-secretase in cells expressing Rab7 CA***

Parental HeLa S3 cells and cells expressing Rab7CA were infected with wild-type PsV for 16 hours. Cells lysates were collected in 1% DDM lysis buffer and incubated with an antibody recognizing the PS1 subunit of γ-secretase. Samples were incubated with protein G magnetic beads overnight and subsequently washed with TBS-T. Samples were eluted from the beads using sample buffer and analyzed via SDS-PAGE and western blotting for the indicated proteins.

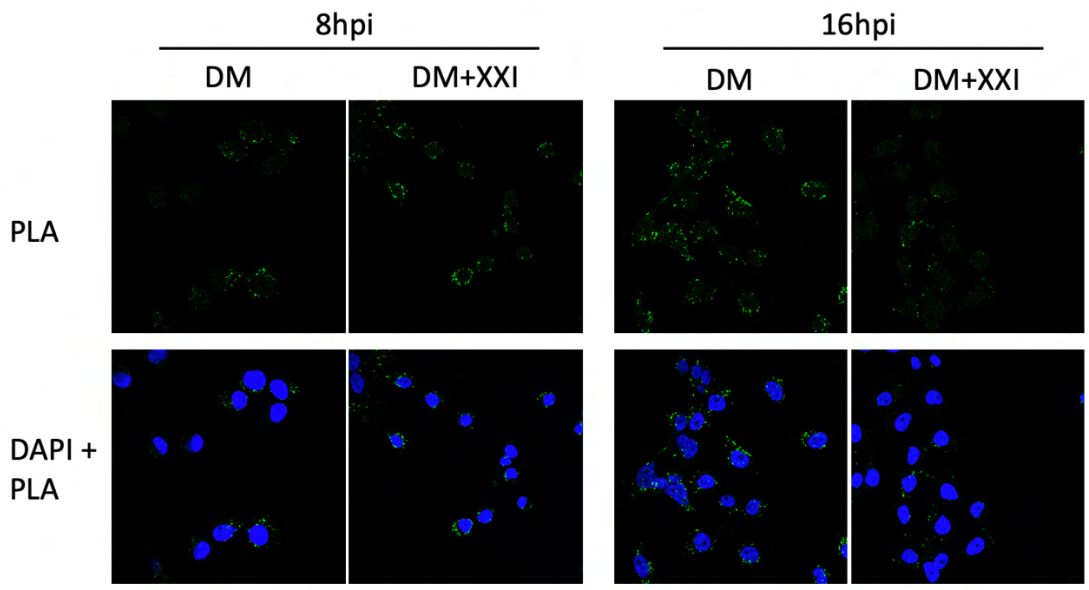


***Figure 4.8 – γ-secretase inhibition blocks endosomal accumulation of the DM***

HeLa cells were treated with XXI γ-secretase inhibitor or DMSO control and subsequently infected with the retromer binding site mutant (DM) HPV PsV. 8 or 16 h.p.i. cells were fixed, permeabilized, and processed for the proximity ligation assay for EEA1 and HPV L2 (FLAG).

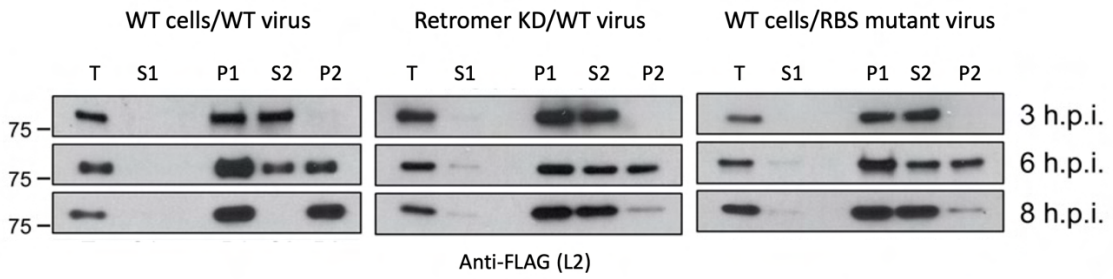


***Figure 4.9: Transient L2 insertion is stabilized by retromer binding***

HeLa cells were transfected with siRNA targeting VPS35 (middle panels) or left untreated. Forty-eight hours after transfection, cells were infected at MOI of 50 with wild-type or retromer binding site mutant HPV16 PsV. At 3, 6, or 8 h.p.i., cells were lysed, fractionated, and extracted with sodium carbonate. Fractions were analyzed by SDS-PAGE followed by immunoblotting with anti-FLAG to detect HPV L2. The experiment shown was performed by Jian Xie [177].

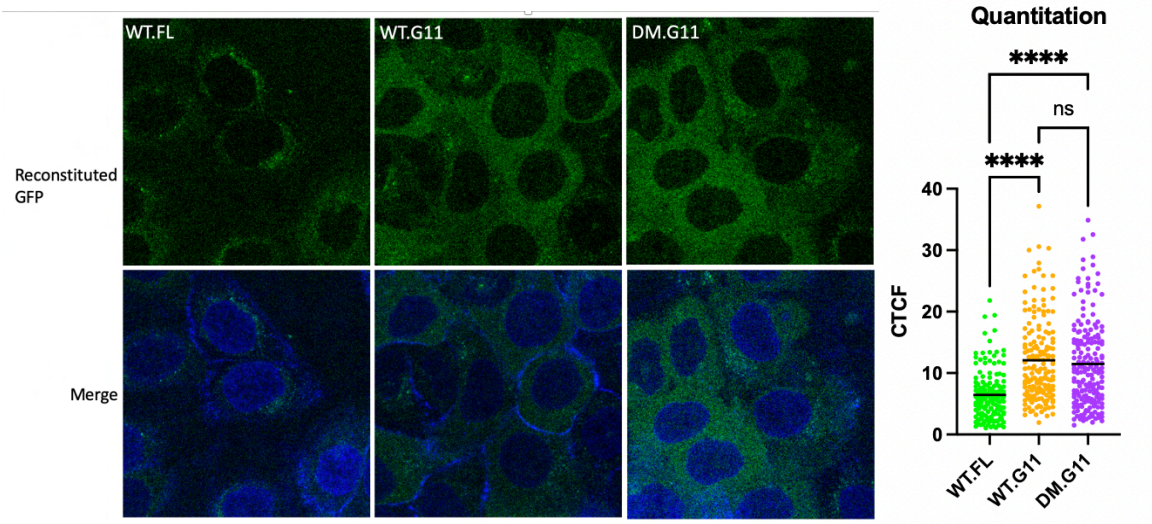


***Figure 4.10: DM L2 protrudes into the cytoplasm at 6 h.p.i.***

(Left) Clonal HaCaT cells expressing cytoplasmic GFP1-10 were infected with HPV containing FLAG-tagged L2 (WT.FL, control) or HPV16 PsV containing GFP11-tagged wild-type or DM L2. 6 h.p.i., cells were stained with Hoechest 33343 (blue), and reconstituted GFP fluorescence due to cytoplasmic protrusion of L2 (green) was observed in live cells using a Leica SP8 confocal microscope. (Right) Quantitation of corrected total cellular fluorescence (CTCF) from the left panel. CTCF = Integrated Density – (Area of selected cell X Mean fluorescence of background readings) and was calculated in ImageJ. Each symbol represents an individual cell. ns - not significant; **** $p \leq 0.0001$

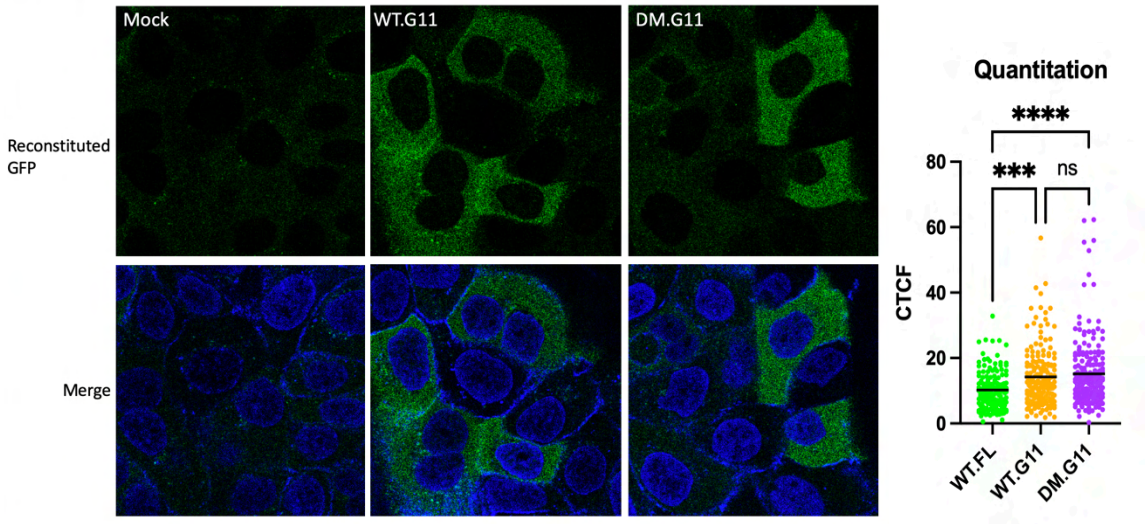


***Figure 4.11: DM L2 protrudes into the cytoplasm at 8 h.p.i.***

(Left) Experiment was conducted as in Figure 56. (Right) Quantitation of corrected total cellular fluorescence from the left panel, as above. Each symbol represents an individual cell. ns - not significant; *** $p \leq 0.001$; **** $p \leq 0.0001$

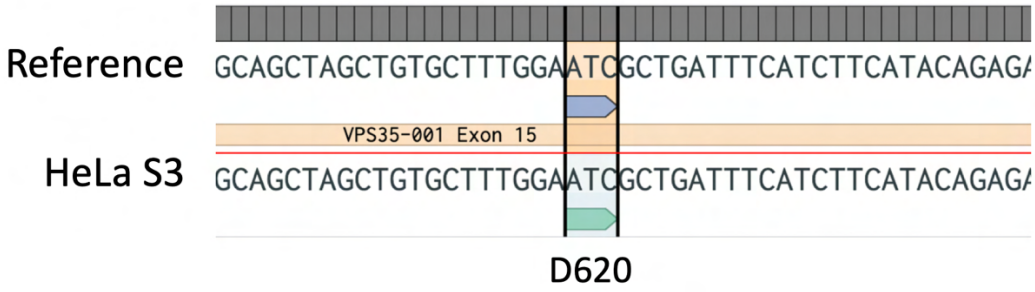


***Figure 4.12 HeLa S3 cells do not contain the D620N mutation***

A portion of the VPS35 genomic DNA was amplified from HeLa S3 cells using primers within the intergenic regions between VPS35 exons. PCR products were sequenced (Yale Keck Sequencing) and aligned to the reference VPS35 genomic DNA (top line). The position of the D620 amino acid is highlighted.

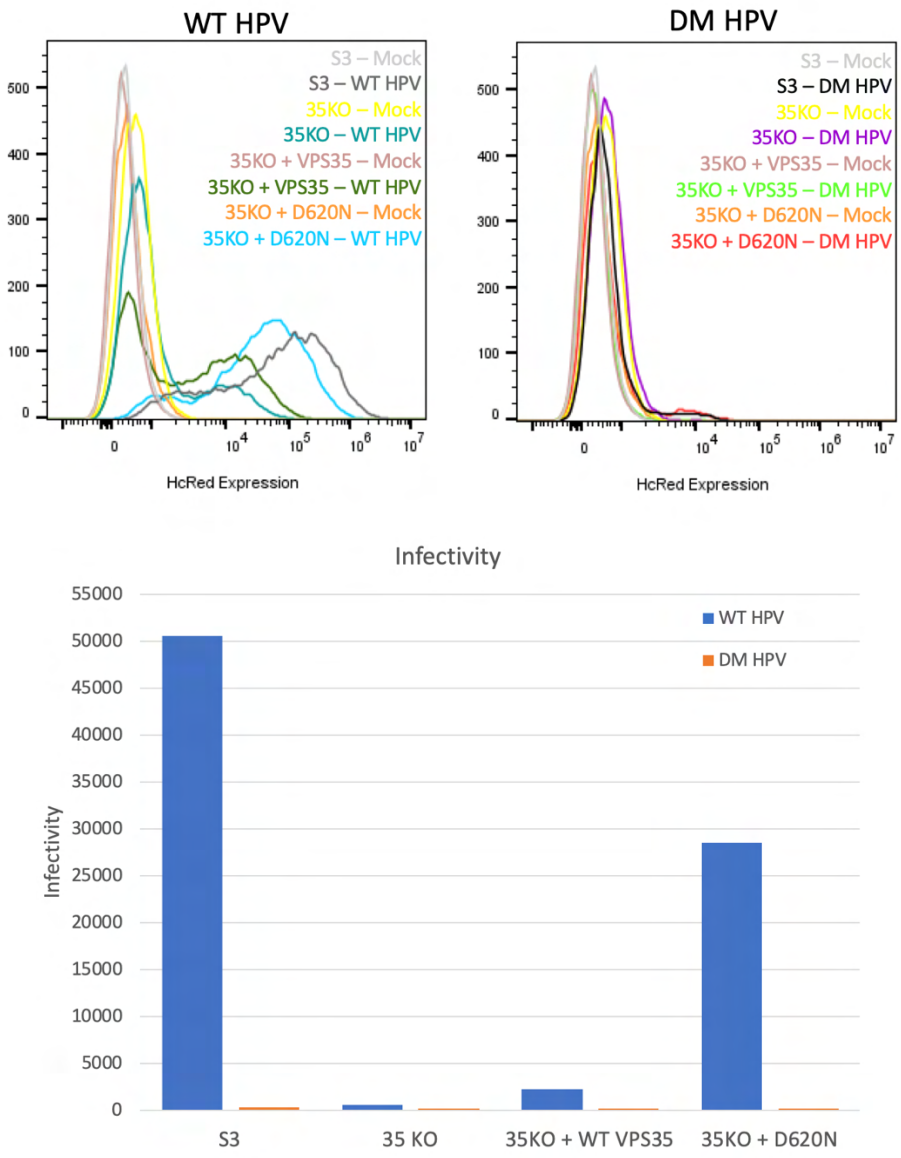


***Figure 4.13: DM HPV is not infectious in the VPS35 addback cells***

(Top) The indicated cells were infected with wild-type (left) or DM (right) mutant HPV PsV. 48 hours post infection, cells were collected and analyzed by flow cytometry for HcRed expression. A shift to the right indicates successful infection. (Bottom) Quantitated mean fluorescence intensity (MFI) for the infected cells.

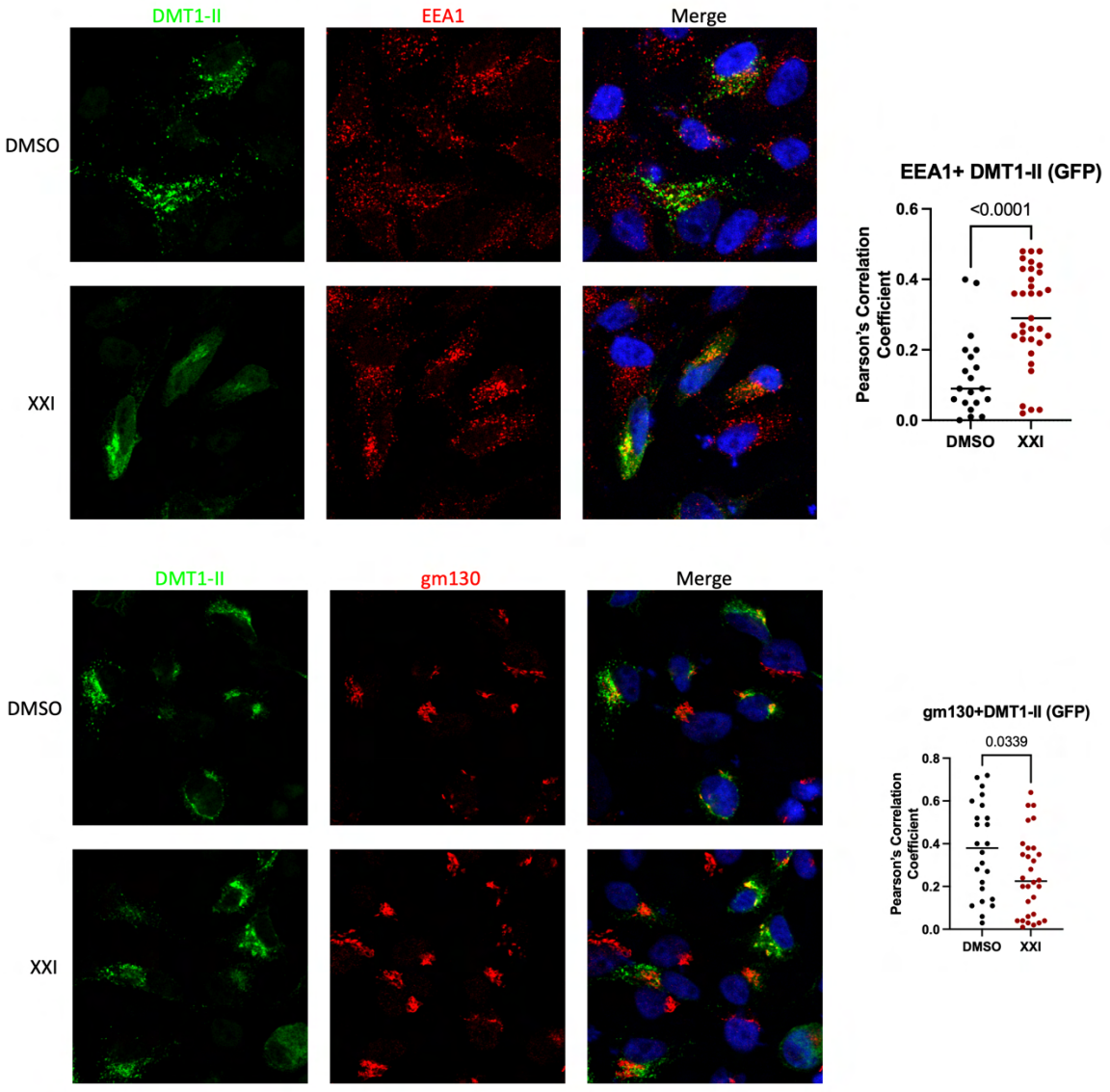


***Figure 4.14: γ-secretase activity is necessary for trafficking of DMT1-II***

HeLa M cells were treated with 1μM XXI γ-secretase inhibitor for 1 hour, followed by transfection with a plasmid expressing GFP-tagged DMT1-II. Cells were then fixed, permeabilized, and processed for immunofluorescence using antibodies for GFP (green), EEA1 (top, endosome marker, red), and gm130 (bottom, TGN marker, red). Samples were analyzed using a Leica SP5 confocal microscope for EEA1/GFP and gm130/GFP staining. Overlap is pseudocolored yellow in the Merge panel. Overlap is quantitated in right panels. Each symbol represents an individual cell.

# Chapter V: Discussion

Our study of the role of γ-secretase in HPV infection and entry led to many interesting discoveries. First, we characterized the interactions between γ-secretase and HPV and found that HPV interacts with all four subunits of the γ-secretase complex, but interacts strongly with PS1. This is consistent with published work examining the interactions between γ-secretase and its substrates, Notch and APP, in that both substrates interact with the PS1 subunit [63, 64]. The interaction of HPV with the catalytic subunit of γ-secretase appears vital for HPV entry, consistent with the fact that inhibitors of γ-secretase activity block HPV infection, even though γ-secretase protease activity is not required for successful infection.

Second, co-IP experiments with antibodies recognizing two different γ-secretase subunits showed that infection with HPV capsids containing L2 stabilizes a pre-exisiting γ-secretase complex, whereas PsV capsids devoid of L2 do not stabilize the complex. The other components of the γ-secretase complex only co-IP with PS1 in cells that are infected with complete HPV (capsids containing L1 and L2), but not in cells that are mock infected or infected with L1-only PsV. This was an unexpected result, as a stabilization phenotype of γ-secretase has not previously been reported with other γ-secretase substrates. Both α- and β-papillomaviruses stabilize the γ-secretase complex, stabilization occurs at multiple MOIs in a dose-dependent manner, and stabilization occurs in multiple relevant cell types including HeLa cervical cancer cells and HaCaT immortalized keratinocytes. Binding to γ-secretase is first seen at 4 h.p.i., followed by stabilization shortly thereafter at 6 h.p.i. These results highlight that, while we do not know the full role that γ-secretase stabilization

plays in HPV infection, it is likely an important step in infection because it is conserved among diverse papillomavirus types in multiple relevant cell lines.

Third, we found that the putative TM domain of HPV L2 cannot be replaced with TM domains that share similar features from other proteins and retain infectivity of the mutant PsV. The TM replacement mutants that I produced, including those that had TM domains from other TM proteins, those that had the TM domains from canonical γ-secretase substrates, those that had TM domains with multiple GXXXG motifs, and those that had the TM domain replaced with the fusion peptides from enveloped viruses, were infectious. We also found that the L2 TM domain is required for γ-secretase binding and stabilization, as well as membrane protrusion and insertion. Thus, the wild-type HPV16 L2 TM domain is required for infection of HPV16, presumably because there is something specific about the L2 TM domain that allows it to support infection. Indeed, mutational analysis with the point mutants revealed that single residue changes within the TM domain can have a large effect on HPV infection. Analysis of the point mutants also showed that γ-secretase stabilization by HPV L2, γ-secretase binding to HPV L2, and infectivity are highly correlated: the mutants that were the least infectious failed to bind to or stabilize the γ-secretase complex, while those that were partially infectious both bound to and stabilized γ-secretase. I did not find a mutant that could bind to γ-secretase without stabilizing it, for example. These results again show that stabilization is highly correlated with infection, and show that the wild-type HPV16 L2 TM domain is vital in the initial entry steps in order for the protein to be recognized by the γ-secretase complex.

Fourth, through examining the interactions between γ-secretase and the retromer complex, we found that retromer and γ-secretase interact with one another, regardless of

HPV infection, and that this interaction requires γ-secretase activity. This result led us to investigate the role of retromer in γ-secretase binding and stabilization, as well as in membrane association and protrusion. Intriguingly, retromer binding was required for HPV L2 to bind to and stabilize γ-secretase, and is also important for membrane association of L2. L2 inserts into the membrane transiently if it cannot bind to retromer, so we hypothesize that retromer binding anchors L2 within the membrane. Additionally, we found that DM HPV can protrude into the cytoplasm in cells expressing GFP1-10, likely due to protein (in this case GFP1-10) binding to L2. These results suggest that binding to a protein anchors L2 within the membrane: retromer in HPV infection, and GFP1-10 in the split GFP assays. Experiments are underway to clarify these results.

## The many functions of γ-secretase

The stabilization of γ-secretase when in complex with HPV L2 is intriguing. Previous research has not described any γ-secretase stabilization phenotype when the protein is associated with its other substrates. It is unclear if previous researchers have looked for this phenotype, as most studies on γ-secretase and its substrates focus on the cleavage of γ-secretase substrates and any pathogenic or other effects that incorrect cleavage produces. It is known that some γ-secretase inhibitors stabilize the γ-secretase complex through increasing interactions between γ-secretase substrates. We did not find compelling evidence that HPV acts as an inhibitor of γ-secretase, even though it stabilizes the complex, however we only investigated cleavage of one γ-secretase substrate (Notch). It will be interesting to identify other cellular proteins that stabilize γ-secretase and to determine if their TM domains can replace the L2 TM domain and support HPV infection.

The structure of the γ-secretase complex bound to its substrates provides insight into substrate recognition and potentially stabilization. Recent studies have determined the structure of the γ-secretase complex bound to either Notch or APP and have highlighted the differences in how the two substrates are recognized by PS1. Many of the residues in PS1 that contact Notch and APP differ. Notch recognition by PS1 requires 10 residues (M139, L150, I168, L173, F176, F177, I229, V236, V261, V272) in PS1 that are not required for APP recognition. On the other hand, APP recognition by PS1 requires three residues (L85, T147, and I287) in PS1 that are not required for Notch recognition. However, despite these differences, there are a few common features for recognition of both substrates. Both substrates interact with multiple TM domains of PS1 and induce the formation of two β-sheets in PS1. Additionally, both substrates contain a β-sheet C-terminal to the TM domain, and interaction between the two β-sheets of PS1 and the β-sheet of the substrate is vital to substrate cleavage. Lastly, two hydrogen bonds anchor the interaction of the substrate TM domain with S169 or G384 of PS1. These common features of the interaction between γ-secretase and either APP or Notch may be the features important for cleavage of the substrate. While the structure of HPV L2 bound to γ-secretase is unknown, L2 likely interacts with PS1 in a different way than either canonical substrate, because L2 cleavage is minimal and because of the unusual sequence of the L2 TM domain. We speculate that interactions between HPV L2 and γ-secretase produce different structural arrangements of PS1 that stabilize the complex. Alternatively, L2 itself may act as a "glue" by simultaneously contacting multiple γ-secretase subunits. Future experiments could clarify the interactions between γ-secretase and HPV L2 by determining the structure of L2 bound to the γ-secretase complex.

More generally, γ-secretase may play an important role in helping other soluble proteins become transmembrane proteins and remain stably associated with the membrane. γ-secretase could also potentially assist in retromer recognition of other retrograde cargo proteins because we see that γ-secretase is required for retrograde trafficking of DMT1-II, a protein that is retromer cargo. DMT1-II has a retromer recognition motif that is similar to L2, and it is recognized by the SNX3-retromer complex. There are two other classes of retromer complexes: the SNX-BAR retromer and the SNX27-retromer. It will be interesting to determine if γ-secretase activity is required for trafficking of other types of retromer cargo, or just those recognized by the SNX3-retromer complex. This is an exciting area of research to pursue, as little has been done to investigate the role of γ-secretase in retrograde trafficking of cellular proteins, and there are few, if any, known instances other than HPV L2 where a soluble protein becomes a TM protein during its normal function.

## The transmembrane domain of HPV L2

Through mutational analysis, we also found that the wild-type sequence of the HPV16 L2 TM domain is important to maintain infectivity, and γ-secretase recognition and stabilization. A mutant without a TM domain (Null-FL) fails to infect cells, bind to or stabilize the γ-secretase complex, and associate with and protrude through the membrane. Additionally, the TM domain cannot be replaced with those from other proteins and maintain infectivity of the viral particle, even if the TM domain shares similar features as the natural HPV L2 TM domain, such as simply being a TM domain (PDGFR-L2 mutant), γ-secretase recognition (APP-L2 and Notch-L2 mutants), GXXXG dimerization motifs (GlyA-L2 and APP-L2 mutants), or being part of a protein that requires a cellular trigger to insert into the membrane (DENV Env-L2, Flu HA-L2, and pHLiP-L2 mutants). This

suggests that the natural HPV L2 TM domain is vital for infection, not just individual features of the TM domain, such as the ability to bind γ-secretase or dimerization motifs. Perhaps if stabilization of the γ-secretase complex was understood in more detail and other proteins were found to stabilize γ-secretase, TM domains from these substrates could be used in place of the natural L2 TM domain and support HPV infection.

However, other results presented in this thesis suggest that again, it is not just specific features of the L2 TM domain that allow it to support infections; the sequence context is also important for infection. Mutations in the HPV16 L2 TM domain that alter the native residue to a residue found in other papillomavirus types, such as the G49L mutant, are less infectious than the wild-type HPV16 PsV. Perhaps the glycine residue in the context of the HPV16 L2 protein, allows the virus to properly bind to and stabilize the γ-secretase complex, but another similar residue (in this case leucine) does not allow for those same interactions. PS1 could be interacting specifically with this residue to promote infection for HPV16. This is supported by the fact that γ-secretase recognizes canonical substrates through different residues, so in a different sequence context, a leucine could allow for proper recognition of HPV L2 by γ-secretase and thus proper infection of the virus.

Our results extend the findings of others that point mutations in the L2 TM domain can inhibit infection. The Jung group found that a L46K mutant PsV was almost as infectious as wild-type PsV, whereas PsV containing a triple mutation of L46, Q47, and Y48 to alanine was essentially noninfectious. Additionally, they showed that a quintuple alanine mutation of residues 49-53 retained roughly 90% infectivity of wild-type HPV PsV. Residues other than L46 within this six-amino acid region were not tested individually.

[56]. We found that L46, G49, and S50 are critical for infection, and that mutations at Q47, Y48, and M51 moderately impaired infection. There are two key differences between the two studies that could contribute to these conflicting results. The Jung group assessed infectivity of their mutants in CHO-K1 hamster kidney cells, which is not a natural target for papillomavirus infection, whereas we studied HeLa cells, which are representative of HPV's natural target. In addition, the Jung group replaced the residues with alanine or lysine (a positively charged amino acid not typically found within TM domains), and we replaced them with leucine (the most abundant residue within TM domains [182]).

The HPV L2 protein appears to act as an inducible TM protein, adopting a soluble existence at times and at other times, a transmembrane one. There are very few examples of other naturally-occurring proteins that can be induced to become transmembrane. Most proteins with a TM domain insert in to the membrane during synthesis through co-translational insertion. In this process, as soon as a newly synthesized portion of a protein leaves the ribosome, it is immediately fed into a translocon that chaperones the insertion of the protein into the membrane [183]. Thus, these proteins are transmembrane for essentially their entire existence. There are examples of inducible viral fusion proteins that insert into the membrane. In this instance, after a distinct trigger, typically receptor binding or low pH, the hydrophobic fusion peptide becomes unmasked and can then insert into a host cell membrane, either at the surface or in the endosome, to mediate membrane fusion and viral entry [184].

The HPV L2 protein does not appear to act in either of these manners and there are still questions about how L2 becomes a TM protein. One possibility for how HPV L2 becomes a TM protein, is that first the cell penetrating peptide on the C-terminus of L2

inserts into the membrane and spools out into the cytoplasm until it reaches the TM domain. This then makes L2 a TM protein which would allow for its recognition by both γ-secretase and retromer which then bind to L2 and stabilize it within the membrane. It would be interesting to determine if recombinant L2 could insert into liposomal membranes, without γ-secretase or retromer present. This would suggest that the CPP alone is sufficient for membrane association and would clarify whether or not γ-secretase is acting as a chaperone to promote membrane insertion, or rather acting as a stabilizer to keep L2 within the membrane. It is also unclear if there is an alternate process, other than CPP insertion or γ-secretase association, for example, that triggers L2 to insert into the membrane. L2 undergoes furin cleavage at the N-terminus, and this cleavage could potentially alter the conformation of the hydrophobic TM domain, which could then support membrane insertion [16, 27]. Indeed, a furin inhibitor blocks L2 membrane insertion, but it is not known if furin cleavage is required specifically for L2 membrane insertion, or for another process that occurs before membrane insertion [49]. It is also known that HPV entry requires endosomal acidification after viral internalization. Endosomal acidification is also required for membrane insertion, and is another possible trigger that could alter the conformation of L2, since low pH is a well-known trigger of membrane insertion of fusion peptides of enveloped viruses [28]. The requirement of particular triggers such as furin cleavage and/or low pH could be investigated *in vitro* with the liposomal experiments mentioned above.

In addition to questions about how HPV L2 becomes a TM protein, there are also questions about the topography of the L2 protein. We do not know the precise portions of HPV L2 that are exposed to the cytoplasm. We believe that L2 has a type I TM

conformation, with the N-terminus in the lumen and the C-terminus in the cytoplasm, however this has not been shown definitively. The C-terminal region of L2 is likely in the cytoplasm because that is where the retromer binding site is, and selective permeabilization experiments followed by staining with specific antibodies suggest that this region is exposed [31, 55]. Additionally, the extreme N-terminus, just N-terminal to the TM domain, is likely in the lumen of the endosome, which was also shown through selective permeabilization assays [55]. We had planned to investigate the topography of the L2 protein with the L2 insertion mutants described in Chapter III, however the lower infectivity of these mutants makes their study difficult. There are other methods that could be used to study the topography of L2, such as using an enzyme to biotinylate L2 and then mapping the biotinylated segments, using protein complementation assays with one segment of a protein expressed in the cytoplasm and the other inserted in different places in L2 and monitoring reconstituted activity, or even using super-resolution microscopy techniques to directly visualize insertion in live, infected cells. Regardless of which technique is used, experiments such as these would clarify the topography of L2 and determine if L2 crosses the membrane as a single-pass or multi-pass transmembrane protein.

## Retromer and γ-secretase

Retromer and γ-secretase associate in our system, and HPV infection does not appear to affect the association between these two proteins: the same amount of retromer co-IPs with γ-secretase subunits with and without infection. This result suggests that there is a basal level of γ-secretase/retromer association within cells. Retromer binding is also required for γ-secretase binding and stabilization during HPV infection. We can dissect the

functions of γ-secretase and retromer that are required for this interaction and HPV infection utilizing PS1 KO and VPS35 KO cells and mutant protein addbacks. In PS1, there are two interesting mutants to study, the L166P and F237I mutant, both of which are deficient in the protease activity of γ-secretase and cleave substrates inefficiently. However, the F237I mutant supports HPV infection and membrane insertion, while the L166P mutant does not [49]. Thus, we originally proposed that the F237I mutant retained a hypothesized chaperone activity of γ-secretase required for L2 membrane insertion, but L166P did not. However, an alternative explanation is that the L166P affects the binding between γ-secretase and retromer, and thus blocks association between these two proteins, which is what inhibits HPV membrane insertion and infection, while the F237I mutant supports the association between γ-secretase and retromer, and thus L2 membrane insertion and infection. We can use co-IP to directly test if γ-secretase and retromer can associate in either of these mutant addback cells. If these proteins associate in cells with both PS1 mutants expressed, that result supports the existence of a chaperone function for γ-secretase, while if they only associate in the F237I cells, that might suggest that it is the retromer/γ-secretase association that is required for infectivity of HPV, not a chaperone function. In the case of VPS35, we have the D620N mutant, which supports HPV infection and allows for cargo binding, but is reported to not traffic properly. If we see association between γ-secretase and retromer in cells expressing D620N and confirm a trafficking defect of the cellular cargo, that would suggest the trafficking function of retromer was not required for their association.

We previously showed that γ-secretase activity is required for membrane insertionand in this thesis we have also shown that retromer is required for membrane

insertion of HPV L2. In the absence of retromer binding, L2 inserts into the membrane transiently. We do not yet know if L2 inserts into the membrane transiently when γ-secretase activity is inhibited and studies to assess membrane insertion in cells without γ-secretase activity, γ-secretase protein expression, and with mutant PS1 constructs are underway. We also do not see γ-secretase stabilization or association with HPV in cells expressing a constitutively active Rab7. It is possible that retromer and γ-secretase don't associate in these Rab7 CA cells, which could explain why we do not see γ-secretase binding and stabilization in these cells. We can test this hypothesis using co-IP for retromer or γ-secretase subunits.

Additionally, we have evidence that suggests protein binding to L2 anchors it within the membrane. We do not see stable membrane insertion in cells where L2 cannot bind retromer, suggesting that binding to retromer anchors L2 within the membrane. Additionally, the results of the split GFP experiments with the retromer binding site mutant (DM) also suggest that protein binding anchors L2 within the membrane. We see protrusion of DM-G11 at later time points in cells expressing G1-10, which suggests that binding to G1-10 anchors L2 within the membrane. There are two important experiments that we can use to test this hypothesis - carbonate extraction in cells infected with the DM-G11 virus expressing GFP1-10 (conditions where GFP11 or GFP1-10 is missing), and carbonate extraction in cells expressing the D620N mutant that supports cargo binding, but not trafficking. If we see membrane insertion of L2 in these experiments, that would suggest that binding to a protein in the cytoplasm anchors L2 within the membrane.

Overall, perhaps the main role of γ-secretase in HPV infection is to act as a 'bridge' between retromer and L2 until L2 can stably insert into the membrane. γ-secretase can bind

to L2 within the lumen of the endosome, and retromer on the membrane. Then, L2 inserts into the membrane transiently until retromer is recruited and able to successfully bind L2. The co-IP experiments with the various mutants of VPS35 and PS1 will allow us to begin dissecting this mechanism. If, for example, retromer and γ-secretase don't associate in the VPS35 D620N mutant cells, but retromer remains on the membrane, binds to L2, and allows for L2 membrane insertion, that would suggest that as long as retromer remains on the membrane, γ-secretase is not necessary. We could also perform γ-secretase association and stabilization experiments in the D620N cells to determine the role of γ-secretase for HPV infection in these cells. Detailed analysis of these mutants will allow for the determination of the specific roles of these proteins in HPV infection and will provide novel insights about their function.

Another aspect of our current model is that γ-secretase and retromer bind to L2 essentially simultaneously: γ-secretase in the putative TM domain at the N-terminus and retromer in the retromer binding motif at the C-terminus. We first see γ-secretase binding to L2 around 4 h.p.i., and we generally investigate retromer binding to L2 around 8 h.p.i., however we have not looked at earlier times post infection. It will be interesting to determine if the timing of binding of these two proteins to L2 aligns, which would provide some evidence in support of our hypothesis that binding of γ-secretase and retromer to L2 occur simultaneously. We typically test binding by co-IP, but the PLA assay could also be used to examine the time course of association.

Finally, I found that γ-secretase activity is required for the trafficking of the retrograde cargo, DMT1-II. To extend these results, other retrograde cargo should be tested for their dependence on γ-secretase activity to traffic properly using similar assays as those

described for DMT1-II in this thesis. We can also utilize the PS1 mutants described above to determine which activities of γ-secretase are required for trafficking of these retrograde cargo. There are three distinct classes of retromer complexes, SNX3-retromer (and its close homologue, SNX12-retromer, which appears important for HPV infection), SNX-BAR retromer, and SNX27-retromer that are recognized in different ways. We have preliminary evidence that HPV trafficking utilizes the SNX3/12-retromer. DMT1-II has a similar retromer binding motif as L2, and uses SNX3-retromer, so it will be interesting to determine if the trafficking of all retromer cargo requires γ-secretase function, or just the SNX3-retromer cargos. Additionally, there are retromer-independent retrograde transport pathways and it is possible that γ-secretase plays a role in those pathways as well, a possibility that can be investigated using both the γ-secretase inhibitor and PS1 KO cells.

Overall, my work in the DiMaio lab has revealed important aspects of HPV infection and shown that analysis of the steps in virus infection lead to intriguing discoveries that bear on cellular biology as a whole. Our results show that detailed mechanistic analysis of individual steps in viral infection lead to discoveries that can highlight novel functions of proteins that are important for cellular biology. Therefore, it is vital that we continue our study of HPV infection in order to learn more not only about the viral lifecycle, but also the biology of the host cell.

# Chapter VI: Materials & Methods

## Cell lines

HeLa S3, HeLa M, HeLa Sen2, HaCaT, 293TT, 293T, and COS7 cells were cultured at 37°C and 5% $CO_2$ in DMEM supplemented with 2% HEPES, 10% fetal bovine serum, 2mM L-glutamine, and 100 units/mL penicillin streptomycin.

## Generation of CRISPR knock-out cell lines

### sgRNA construction

sgRNAs to the relevant gene (TAP1, TAPBP, VPS35, VPS26a or VPS26b) were obtained through the CHOP CHOP program (https://chopchop.cbu.uib.no/). gRNAs were chosen based on their proximity to the first exon in the gene, number of mismatches with other genes, and rank on the CHOP CHOP.

### Oligo Annealing

Oligos were annealed in a reaction of 100μM oligo 1, 100μM oligo 2, 1μL 10x T4 DNA Ligase buffer and dH2O to 10μL. Reactions were placed in a thermocycler and annealed for 30 min at 37°C, followed by 95C for 5 minutes and ramping down by 5C/min until the final temperature of 25C was reached.

### Vector Digestion

5μg of the LentiCRISPRv2 vector was digested in a reaction using 1.5μL FastDigest BsmBI, 1.5μL FastAP, 3μL 10X FastDigest buffer, and dH2O to 30μL. The reaction was incubated at 37°C for 2 hours, run on a 1% agarose gel, and the top 11kb band was purified using the Monarch Gel Purification Kit.

**Ligation**

The ligation reaction was performed using 50ng BsmBI digested LentiCRISPR vector, 1μL annealed oligos (diluted 1:200), 1μL 10X T4 Ligase buffer, 0.5μL T4 Ligase and dH2O to 10μL. The ligation was incubated at 16C overnight.

**Transformation and Sequencing**

1μL of the ligation product was transformed into Stbl3 competent cells using the manufacturer's recommendations. The transformation was plated on LB ampicillin plates and incubated at 37°C overnight. Plasmid DNA from a few colonies was amplified using Macherey Nagel MiniPrep according to the manufacturer's instructions. Amplified DNA was sent for sequencing (Keck) to ensure proper insertion of the gRNA.

**Lentivirus Generation**

To generate lentivirus, 293T cells were plated onto 12 well plates. 2μL of Lipofectamine 200 was incubated in 100μL optiMEM for 10 minutes at room temperature. 0.8μg of the lentiCRISPR plasmid, 0.4μg of pMG2.D, and 0.4μg of psPAX2 were incubated in 100μL optiMEM for 10 minutes at room temperature. Diluted plasmids and diluted lipofectamine were mixed and incubated for a further 20 minutes at room temperature. Diluted lipofectamine/DNA mix was added to the 12 well plate without changing the growth media. 24 hours post transfection (hpt), growth media was removed and 1mL of fresh media was added. 48 hpt, the growth media containing the lentivirus was harvested and filtered through a 45μM filter.

**Target cell transduction and selection**

Fresh HeLa S3 cells were plated in 12 well plates and 1mL of the filtered virus was added to the cells, along with 4μg/mL polybrene. 24 hpi, media was removed and fresh media

was added. 48 hpi, media was removed and fresh media containing 0.5µg/mL puromycin was added to the cells every 3-4 days until all of the uninfected cells died.

**Single-cell colony generation**

After selection, surviving HeLa S3 cells were either sorted into 96 well plates using flow cytometry, such that each well would receive one cell. Alternatively, cells were diluted such that each well in a 96 well plate would receive 0.5 cells. Colonies were monitored for single colony growth, and grown in successively larger plates (96 wells to 48 wells to 24 wells to 12 wells to 6 wells to 6cm dishes), until there was enough cell material.

**CRISPR confirmation**

Selected, single-cell colonies were lysed in 2X Lamelli sample buffer and subjected to SDS-PAGE, followed by transfer to a PVDF membrane for western blotting. Membranes were blocked for 1h in 5% milk in TBST and incubated with the relevant antibody at 4°C overnight. Membranes were washed in TBST and incubated with the appropriate secondary for 1-2h at room temperature. After secondary incubation, membranes were washed again and incubated with Pico or Femto chemiluminescent substrate (Fisher) and imaged.

## Generation of mutant HPV16 pseudovirus packaging plasmids

A silent unique AvrII restriction site was inserted downstream of the putative L2 TM domain in the p16SheLL-3X FLAG vector using the Q5 site directed mutagenesis protocol and Phusion High Fidelity Polymerase. This plasmid was then used to generate the putative TM domain mutants by inserting gBlocks (IDT) containing the relevant mutation between the XbaI site upstream of the L2 start codon and AvrII restriction sites. The retromer binding site double mutant (DM) and GV mutants were previously described [31, 49]. For

split GFP experiments, seven copies of GFP11 were appended to the C-terminus of L2 in wild-type or mutant PsV preparations, as previously described [34].

## HPV pseudovirus production

293TT cells were plated into T150 flasks. The following day, polyethylene imine (PEI) was used to transfect the cells with wild-type or mutant p16L1-GFP, p16SheLL, p5SheLL, p18SheLL (12.5 μg/T150 plate) together with pCAG-HcRed or pCINeo-GFP as a reporter gene (12.5 μg/T150 plate). 24 hours post transfection, media was aspirated and fresh media was added to the cells. 72 hours post transfection, cells were washed 1X with PBS and trypsinized. Cell lysates were collected in 50mL conical tubes and slowly centrifuged at 1200 rpm. The pellet was washed in PBS and recentrifuged. The pellet was then resuspended in PBS and aliquoted into siliconized Eppendorf tubes. These were centrifuged at 0.5k xg. Pellets were resuspended in a lysis buffer containing 0.5% Triton X, 10mM $MgCl_2$, 5mM $CaCl_2$, 1μL/mL RNAse A, diluted in PBS, and incubated overnight in a 37°C water bath to allow for capsid maturation. The following morning, an iodixonol (OptiPrep) gradient was set up by first diluting the OptiPrep to 46% in DPBS supplemented with 0.8M NaCl. Three gradient steps of 27%, 33%, and 39% OptiPrep were layered. The gradient was incubated for 1-4h, but typically 1h, at room temperature to allow the gradient to diffuse. The matured PsV preps were incubated on ice for 10-15 minutes and then centrifuged for 10 minutes at 5k xg. Matured PsV capsids were loaded onto the top of the OptiPrep gradient and centrifuged at 50k xg for 4h at 4°C in a SW-55Ti Beckman Ultracentrifuge rotor. 10 ~200μL Fractions were collected in siliconized Eppendorf tubes and L1 and L2 levels of purified PsV preparations were assessed by SDS-PAGE followed

by Coomassie blue staining or by immunoblotting with antibodies recognizing L1 and L2. Fractions with the highest levels of L1 and L2 were pooled and used for subsequent studies.

## p16L1L2 PsV generation

Replicating PsV, made with the p16L1L2 plasmid, was generated similarly as above, except 25μg of p16L1L2 plasmid was transfected into 293TT cells. After capsid maturation, as above, the unpurified stock was used to infect a fresh set of 293TT cells for 48 hours. Cell lysates were again collected, as above, and matured to produce a second stock of unpurified PsV that was used to infect a fresh set of 293TT cells. After collecting cell lysates and maturing the capsids, these capsids were purified using an iodixonol gradient and assessed for L1 and L2 levels, as above.

## Infectivity

$1x10^5$ HeLa S3 or HaCaT cells were plated in 12 well plates 1 day before infection. Cells were mock-infected or infected with wild-type or mutant PsV, and flow cytometry was used to measure reporter gene expression 48 hours post infection (h.p.i.). The amount of mutant PsV used to infect cells was normalized to wild-type HPV16 PsV by using equal levels of packaged L1 and L2 of purified PsV or qRT-PCR for the reporter genome.

## qRT-PCR for PsV genomes

5μL of PsV prep was digested for 1h at 37C in a 100μL reaction with 10μL DNAse I, 65μL RDD buffer, and 20μL H2O (Qiagen DNAse Kit). The DNAse was then inactivated at 75C for 30 minutes. 120μL PBS and 20μL Proteinase K were added to the sample and incubated

for 1h at 37C. 200µL of AL buffer was added and the sample was incubated at 56C for 10 minutes. The samples were then purified using the DNeasy Blood & Tissue Kit (Qiagen). Following purification, the qRT-PCR reactions were set up using 10 µL SybrGreen, 1µL 10µM forward primer, 1µL 10µM reverse primer and 8 µL PsV digest in a clear bottom 96 well plate.

## siRNA transfections

Cells were plated such that they were 70% confluent at the time of transfection. Transfection was carried out using 10nM of the indicated siRNA and the Lipofectamine siRNAMax reagent (ThermoFisher), according to the manufacturer's details.

## Co-immunoprecipitation of HPV16-FLAG and γ-secretase

$1x10^6$ HeLa S3 cells were plated in 6 cm dishes 24 hours before infection. Cells were infected with wild-type or mutant HPV PsV at a multiplicity of infection (MOI) of 50 for 16 hours, unless otherwise indicated. Cells were scraped off the dishes and lysed in HN-DMNG lysis buffer (50mM HEPES pH 7.5, 150mM NaCl, 1% DMNG supplemented with HALT protease inhibitors) on ice for 45 min. For the co-immunoprecipitation experiment where γ-secretase subunits were stripped away from HPV using different amounts of detergents, samples were prepared the same, except HN lysis buffer with combinations of DDM and NP40 was used. Cell debris was removed from the sample by centrifuging at 16.1xg for 15 minutes at 4°C. The supernatant was incubated with anti-FLAG antibody for 4-6 hours at 4°C on a rotating tube rack. 50 µL of Protein G magnetic beads (Fisher) were washed in TBS-T, added to the lysate, and incubated at 4°C

overnight. Samples were washed with TBS-T 3X and eluted from the beads using 2X Laemmli sample buffer at 100°C. The entire sample was subjected to SDS-PAGE and immunoblotting with antibodies recognizing the FLAG tag on the C-terminus of HPV16 L2 and γ-secretase substrates.

## Assay for γ-secretase-HPV association and γ-secretase stabilization

$1x10^6$ HeLa S3 cells were plated in 6 cm dishes 24 hours before infection. Cells were infected with wild-type or mutant HPV PsV at a MOI of 50 for 16 hours. Cells were washed, scraped off the dishes, and lysed 165μL cold HN-DDM lysis buffer (50mM HEPES pH 7.5, 150mM NaCl, 1% DDM supplemented with HALT protease inhibitors) on ice for 45 min. Cell debris was removed from the sample by spinning at 16.1k xg for 15 minutes at 4°C. 15μL was removed and labelled "input." The supernatant was then incubated with 1μL of anti-PS1 or anti-APH1 antibody for 4-6 hours at 4°C on a rotating tube rack. 50μL of Protein G magnetic beads were washed, added to the lysate, and incubated at 4°C overnight. Samples were washed 3X with TBS-T and eluted from the beads using 2X Laemeli sample buffer at 100°C. The entire sample was subjected to SDS-PAGE and immunoblotting with antibodies recognizing HPV16 L1, the FLAG tag on the C-terminus of HPV16 L2 or γ-secretase subunits.

## Co-immunoprecipitation of γ-secretase subunits and retromer

293T cells were plated in 6 cm dishes such that they were 70% confluent at the time of transfection. PEI was used to transfect cells with pCINeo-VPS35, pCINeo-VPS29, and pCINeo-VPS26, or with pCINeo-GFP as a control. 24 hours post-transfection, cells were

mock-infected or infected with wild-type HPV16 PsV at a MOI of 50. Cells were washed, scraped off the dishes, and lysed in 165µL HN-CHAPSO(50mM HEPES pH 7.5, 150mM NaCl, 1% DMNG supplemented with HALT protease inhibitors)on ice for 45 min. Cell debris was removed from the sample by spinning at 16.1xg for 15 minutes at 4°C. 15µL was removed and labelled "input." The supernatant was then incubated with 1µL of anti-PS1 antibody for 4-6 hours at 4°C on a rotating tube rack. 50µL of Protein G magnetic beads were washed, added to the lysate, and incubated at 4°C overnight. Samples were washed 3X using cold lysis buffer and eluted from the beads using 2X Laemmli sample buffer at 100°C. The entire sample was subjected to SDS-PAGE and immunoblotting using the indicated antibodies for HPV and γ-secretase.

## Carbonate extraction

1.5 million HeLa S3 cells were plated in 6cm dishes. 24 hours later, cells were infected with wild-type or mutant HPV at an MOI of 50 for the indicated time. Following infection, cells were homogenized to ~80% lysed using a dounce homogenizer with the "B" pestle, or using a ball-bearing homogenizer (Isobiotec) with a 6µM clearance. Samples were centrifuged at 16.1xg for 15 minutes, and 30µL of the supernatant was removed and labeled as the total fraction. The rest of the supernatant was centrifuged in a SW55Ti rotor at 50,000 rpm for 30 minutes at 4C to give the S1 and P1 fractions. The P1 pellet was then resuspended in Tris buffer (composition) for 30 minutes on ice and 30µL were taken out as the P1 fraction. The rest of the sample was incubated with 0.1M $Na_2CO_3$ (pH 11.5) and 4.2M urea for 30 minutes to an hour on ice. The sample was then centrifuged at 50,000 rpm for 30 minutes at 4C to give the supernatant (S2) and pellet (P2) fractions. The S1 an

S2 fractions were concentrated using Amicon Centricons with a 3kDa cutoff until the sample was 40μL. Total, S1, P1, S2, and P2 fractions were then analyzed by SDS-PAGE, followed by immunoblotting with the indicated antibodies for PDI (luminal proteins), VPS26 (peripheral membrane proteins), BAP31 (TM proteins), and HPV L2.

## Generation of GFP1-10 cells

HaCaT or HeLa M cells expressing GFP1-10NES were generated by transducing the cells with lentivirus expressing GFP1-10NES, as above, and selecting with puromycin. Puromycin-resistant single cell clones were obtained by plating single cells into 96 well plates and expanding. Alternatively, the pTight system was used to express GFP1-10, as previously described [177].

## Split GFP Assay

$2.5x10^4$ GFP1-10NES expressing cells were plated in eight-chambered glass slides overnight. Cells were infected with wild-type HPV16 PsV with a FLAG tag (negative control) or with seven copies of GFP11 fused to the C-terminus of L2, or with mutant HPV PsV with seven copies of GFP11 fused to the C-terminus of L2. All PsVs were infected at a MOI of 1,500 to 2,000. 3, 6, or 8 hours post infection, live cells were stained with Hoescht 33342 for 15 minutes at 37°C to visualize DNA. Live cells were analyzed for reconstituted GFP fluorescence using a Leica SP5 or SP8 confocal microscope.

## Immunofluorescence

Typically, $3.5x10^4$ HeLa Sen2, or $2.5x10^4$ HaCaT or HeLa M cells were plated in 24 well plates on cover slips. Cells were manipulated as indicated in the figure legends, either by infection, typically at an MOI of 25-50; transfected with plasmids expressing γ-secretase or retromer components for 24 hours; treated with inhibitors; or left untreated. Cells were then fixed with 10% formalin (Formaldefresh) for 10 minutes at room temperature. Following fixation, cells were washed with PBS at least three times and then permeabilized with 1% saponin for 1h at room temperature or 0.5% Triton X for 30 minutes at room temperature. Permeabilized cells were blocked using 5% FBS in PBS, 5% BSA in PBS, or 10% FBS in DMEM for 1-2 hours at room temperature. Primary antibody, diluted in blocking buffer, was added to cells at varying dilutions, and allowed to incubate overnight at 4°C. The following morning, cells were washed 3X for 10 minutes each with PBS and then incubated with a 1:200 dilution of an AlexaFluor conjugated secondary antibody for 1 hour at 37°C. Cells were washed 3 more times with PBS for 10 minutes and mounted on glass slides using a mounting medium that contained DAPI (FluorShield with DAPI). Mounting media was allowed to dry for 1-2 hours and slides were sealed using fingernail polish and stored at 4°C (short term) or -20°C (long term), until imaging with a Leica SP5 confocal microscope.

## Trafficking assay of DMT1-II and CIMPR

$2.5x10^4$ HeLa-M cells were seeded on coverslips in 24-well plates. 24 hours later, cells were treated with 1μM XXI γ-secretase inhibitor or left untreated, and then transfected with 1μg GFP-DMT1-II plasmid using the Trans-IT HeLaMONSTER reagent. 24 hours

post transfection cells were fixed for 15 minutes using 4% paraformaldehyde, permeabilized for 1 hour using 0.5% triton X, blocked for 1 hour using 5% normal donkey serum, and incubated with anti-GFP mouse antibody and anti-EEA1 rabbit antibody over night. The following day, the samples were incubated with AlexaFluor-conjugated secondary antibodies at 37C for 1 hour. Slides were mounted and images were acquired with a Leica SP5 or SP8 confocal microscope.

## Proximity Ligation Assay

$2.5x10^4$ HeLa Sen2 cells were plated on coverslips in 24 well plates. The following day, cells were infected with wild-type or mutant HPV PsV at an MOI of 50, or mock infected. Cells were then fixed with 10% formalin (Formaldefresh) for 10 minutes at room temperature. Following fixation, cells were washed with PBS at least three times and then permeabilized with 1% saponin for 1h at room temperature. Cells were blocked with 10% FBS in DMEM for 1-2h at room temperature. Blocked cover slips were incubated overnight at 4°C with a primary antibody to a cellular marker (EEA1 or TGN46) and HPV (FLAG for L2 or L1), diluted in blocking buffer. The following morning, cells were washed 3X for 5 minutes with PBS. Cover slips were moved to the top of a humidity chamber that had been prewarming at 37°C. PBS was aspirated and 40µL PLA probe was added to each well individually (PLA Probe: 24µL blocking buffer, 8µL Anti-Rabbit Minus PLA Probe, 8µL Anti-Mouse Plus PLA probe). Samples were incubated at 37°C for 1.5h. Cover slips were washed 2X with 50µL of PLA Wash Buffer A for 5 minutes each. Wash Buffer A was aspirated and 40µL of ligation mix was added to each over slip (Ligation mix: 8µL ligation buffer, 31µL H2O, 1µL ligase). Cover slips were incubated at 37°C for 1h. After 1h, cover slips were washed 2X with 50µL wash buffer A for 2 minutes each and then

incubated with 40µL of amplification buffer (Amplification mix: 8µL amplification buffer, 31.5µL H2O, 0.5µL polymerase) for at least 3 hours at 37°C. If needed, 5-10µL of H2O was added to the coverslips 1.5 hours into the incubation to prevent drying out. After 3h, cover slips were washed with PLA Wash Buffer B 2X for 10 minutes each wash, followed by a wash with 0.01X Wash Buffer B for 1 minute. After this wash, cover slips were mounted on glass slides using Fluroshield Mounting Media with DAPI and allowed to dry 1-2 hours. Slides were sealed using fingernail polish and stored at 4°C (short term) or -20°C (long term), until imaging with a Leica SP5 confocal microscope.

## Antibody staining for flow cytometry

For cells that were treated with siRNAs, siRNA transfection was performed as described above. 48 hours post transfection, or one day after plating, cells were washed 3X with cold PBS. 500µL of PBS + 0.5mM EDTA was added to the cells and they were incubated for 15 minutes to detach the cells. 1mL of cold PBS was added and cells were transferred to XX tubes. Cells were centrifuged at 1300rpm for 5 minutes. Cells were then washed 2X with cold PBS. Cells were then fixed in 10% formalin (Formaldefresh) for 10 minutes at room temperature, and then washed in cold PBS 2X. Cells were blocked using 5% Normal Goat Serum for 30 minutes on ice. Following blocking, cells were centrifuged, as above, and incubated with either an unconjugated primary antibody, or a conjugated primary antibody for 30 minutes. After incubation, cells were washed 2X with cold PBS, as above, and if the primary antibody was conjugated to a fluorophore, samples were resuspended in 5% NGS and analyzed as below. If an unconjugated primary antibody was used, cells were incubated with an AlexaFluor secondary antibody at a dilution of 1:2000 for 30 minutes in

the dark. Following this incubation, cells were washed 2X with cold PBS, as above, and resuspended in 5% NGS. All samples were filtered and analyzed on a Stratedigm 13 flow cytometer.

# Appendix I: Spatially restricted tagging method to identify HPV interactors

## Introduction

Viral entry is a complex process that we seek to understand using a variety of methods. Numerous screens for HPV entry factors have been undertaken in order to identify proteins necessary for HPV entry [37, 52]. Many of these screens are protein knockdown based, via the use of siRNA or shRNA libraries. Our lab identified the retromer and γ-secretase complex as being important in HPV entry through a siRNA screen, so these are valuable tools in dissecting the complex entry process of HPV and other viruses [37]. However, with protein knockdown or knockout screens, the removal of an essential proteins will cause cellular death, so the function of essential proteins in entry cannot be assessed. Additionally, many cellular processes can compensate for each other so it is possible that if the expression of a protein essential for HPV entry was decreased or removed, another protein could perform the same function. We chose to undertake a screen utilizing spatially restricted protein tagging in order to identify the cellular factors that are near and interact with HPV on its journey to the nucleus.

Ascorbic peroxidase (APEX) is an enzyme that can biotinylate proteins in close proximity to it [185]. Upon the addition of biotin phenol and hydrogen peroxide to intact cells, APEX catalyzes the formation of phenoxyl radicals that can then covalently react with specific amino acids in proteins to label them with a biotin molecule. APEX is advantageous due to its small labelling radius (approximately 20nm) and the very short lifespan of these radicals. Other protein labelling enzymes such as biotin ligase, require

long labelling reactions (~24h) in comparison to APEX, which can label cells for as little as 1 minute [160, 186, 187]. APEX also is active in the mammalian cytosol, unlike the horseradish peroxidase (HRP) labelling enzyme [188, 189]. HRP is inactive in the mammalian cytosol likely due to the fact that the protein has four disulfide bonds that are critical for its structure and these bonds would be unable to form in the reducing environment of the cytosol [189]. APEX was first engineered and used to identify proteins within human mitochondria [185, 189]. In this study, the Ting lab used a mitochondria-targeted APEX enzyme to biotinylate proteins in a short, 1-minute labelling reaction. They then purified these biotinylated proteins using streptavidin beads, digested the peptides with trypsin, and performed MS/MS to identify the proteins. This method identified 495 mitochondrial proteins, 464 of which had already been identified as mitochondrial proteins, indicating this method's specificity and use for future studies.

## Results

## APEX-L2 Screen

An APEX-L2 construct was created by a postdoctoral associate in the lab, Teymur Kazakhov, in which APEX was fused to the C terminus of L2. When PsV is made using this construct, APEX decorates the outside of the HPV pseudovirion. This APEX-PsV was then used to infect cells and the biotinylation reaction was performed at 8 h.p.i. Cells were lysed and biotinylated proteins were pulled down using streptavidin and identified through MS/MS. A "mock" sample infected with PsV containing a FLAG tag (instead of APEX) as a control, was treated in the same way. 775 proteins were identified in the mock sample to have an expectation value under 0.05, only 67 of which were unique to the mock sample and not found in the infected sample. 1415 proteins were identified in the infected sample

and 598 of these proteins were not found in the mock infected sample. Multiple previously identified interacting partners of HPV, such as components of the retromer complex (VPS26 and VPS35) [37, 47], the dynein light chain (DYL1) [32, 33], and the epidermal growth factor receptor (EGFR) [190], were identified from the MS data, confirming the validity of the screen (selected hits in Figure A1.1).

One of the most interesting hits from the APEX screen is the transporter associated with antigen processing, TAP1, protein. The TAP complex is an ATP-binding cassette (ABC) transporter, composed of a heterodimer of TAP1 and TAP2 [191-194]. It utilizes conformational changes as a result of peptide binding and ATP hydrolysis to translocate peptides across the ER membrane into the ER lumen [195, 196]. TAP is associated with the larger peptide loading complex (PLC) through tapasin (TAPBP) which recruits the remainder of the PLC [197, 198] (Figure A1.2). The peptides that TAP transports are then edited and loaded onto MHC Class I molecules by TAPBP and the ER chaperone Erp57 [199]. Once loaded with a high affinity peptide, the MHC class I molecules leave the ER and traffic through the Golgi to the cell surface, where they are recognized by cytotoxic CD8+ T-cells which can subsequently induce apoptosis [200]. TAP1 was particularly interesting to us to study as it is localized to ER membranes. The later trafficking steps of HPV infection are poorly characterized, but it has been reported that HPV traffics through both the TGN and ER. Thus, a possible role for TAP1 and the PLC is to help HPV translocate into the ER, where it could remain in a membrane-bound compartment until the onset of mitosis when it enters the nucleus. Additionally, we chose TAP1 to study as this protein was not found in the control sample, and multiple other components of the PLC, such as calnexin and calreticulin were found in the HPV-APEX infected sample.

## TAP1 and TAPBP in HPV infection

To assess the relevance of TAP1 and TAPBP in HPV infection, we first performed siRNA knockdowns in HaCaT and HeLa S3 cells. Either cell type was transfected with a siRNA targeted to either TAP1 or TAPBP. 48 hours post transfection (h.p.t.), cells were infected with HPV PsV containing a GFP or RFP reporter gene. 48 hours post infection (h.p.i.), cells were collected and processed for flow cytometry. A VPS29 knockdown was used as a negative control and a RISC-free siRNA was used a control for the presence of a siRNA. Multiple individual siRNAs were used to limit the likelihood of off-target effects, and efficient protein knockdown was confirmed via western blot (Figure A1.3). siRNAs to TAP1 and TAPBP potently blocked HPV infection in HaCaT (Figure A1.4) and HeLa (Figure A1.5), similar to the block in infection we see in cells treated with a siRNA to VPS29.

We also used a pull-down experiment to assess binding between HPV and TAP using peptides. Three biotinylated peptides were generated that have different segments of HPV L2 appended to biotin [31]. One is in the N-terminus of L2 (aa 13-45), upstream of the putative TM domain, the second is in the middle of L2 (aa 240-267) and has the SNX binding site, NPAY, and the third is in the C-terminus of L2 (aa 434-461) and has both retromer binding sites as well as the cell penetrating peptide. The biotinylated peptides were incubated with HeLa cell lysates, pulled down via streptavidin, electrophoresed on SDS-PAGE gels and immunoblotted for TAP1 (Figure A1.6). The peptide that corresponds to the C-terminus of L2 bound to TAP1 the most. We also saw a small amount binding between TAP1 and the peptide containing residues in the middle of L2. These preliminary data suggested that the interaction between HPV and TAP1 could be direct. However, it is

important to note that TAP1 binds to and edits peptides from many proteins, so this result needs to be analyzed with these caveats.

To confirm the relevance of TAP1 and TAPBP in HPV infection, I then generated CRISPR knock out cells. Two separate sgRNAs were generated using the CHOP CHOP online tool [201-203] and chosen due to their proximity at the N-terminus of the protein, lack of predicted off-target effects, and self-complementary rankings from the tool. Two sgRNAs were used for each protein to increase the likelihood that the protein would be knocked out in one of the cell lines. DNA encoding these sgRNAs was cloned into the lenticrispr v2 plasmid [204], which produces high titer lentivirus, and the resulting lentivirus was used to transduce HeLa S3 cells with a sgRNA to either TAP1 or TAPBP. Transduced cells were then selected with puromycin and plated at clonal cell density into 96 well plates once antibiotic selection was completed. Single cell clones were grown out and then tested for TAP1 or TAPBP protein expression via western blot (Figure A1.7 and A1.8). Multiple individual clones had no TAP1 or TAPBP expression. We confirmed the gene disruption with CRISPR sequencing and found that, although the single cell clones had accumulated more mutations and thus weren't homogeneous, there were mutations in the genes encoding for TAP1 and TAPBP where the guide RNAs targeted, and the wild-type sequence for these genes was absent in these clones, again confirming knockout (Figure A1.9 and A1.10). Finally, I used human leukocyte antigen (HLA) staining to determine if TAP1 and TAPBP were functionally knocked out in these cell lines. As the expression of MHC Class I molecules, and thus the HLA proteins, on the surface of cells depends on functional TAP1 and TAPBP proteins, a decrease in the expression of HLA would indicate that TAP1 and TAPBP were knocked out. I stained non-permeabilized

CRISPR KO cells for HLA on the surface and saw a decrease in HLA staining, suggesting that the proteins were non-functional (Figure A1.11).

I then tested these cell lines for defects in HPV infection. CRISPR KO TAP1 or TAPBP cells were freshly thawed, plated, and infected with HPV PsV at a variety of MOIs. As shown in Figure A1.12, there was no difference in HPV infection in cells with or without TAP1 or TAPBP expression for multiple individual clones. This was a surprising result given that the siRNAs had a drastic effect on infection. To determine which phenotype was correct and whether or not TAP1 or TAPBP was important for HPV infection, I turned to a final method of generating knockdown cells, shRNAs. I used multiple shRNAs to either protein and generated stable cell lines expressing each individual shRNA. I confirmed protein knockdown via western blot (Figure A1.13 and A1.14). I then infected these stable cell lines with HPV PsV and measured reporter gene expression 48 hours post infection. In agreement with the results from the CRISPR KO cells, there was no defect in infectivity in response to any of the shRNAs used (Figure A1.15). This convinced us that TAP1 and TAPBP expression were not important for HPV entry and we turned to other results from the original APEX screen.

I spent a significant amount of time trying to determine which protein to investigate next. However, it became apparent that the original screen did not have the proper controls and I had many problems analyzing the data, as described below. I was not able to quantitate the amount of the protein for each hit; I could only look at the expectation value to determine how confident we were that the protein labeled by APEX was actually in the sample. I tried to rank the samples by determining which proteins had a biotinylated peptide by looking through each peptide individually and determining if it was biotinylated.

Unfortunately, biotinylated peptides are difficult to detect using mass spectrometry, and thus there were few biotinylated peptides and none that were of high enough confidence that we thought they were real. I also compared the results from the APEX screen with those from two other siRNA screens [37, 52]. There was little overlap between the results from any of the three screens: 11 proteins were shared between the Lipovsky and Aydin siRNA screens, three proteins were shared between the Lipovsky screen and the APEX screen, and five proteins were shared between the Aydin and APEX screens [37, 52]. There were no proteins shared between all three screens. It was thus impossible to rank the 598 unique hits without redoing the screen with proper controls, and/or have a biological readout of the relevance of the hits. Therefore, I decided to abandon this project in favor of the experiments that were producing interesting results, such as the γ-secretase stabilization and retromer + γ-secretase interactions, described in the main text of this thesis.

## Discussion

Ascorbic peroxidase (APEX), an enzyme that can biotinylate proteins within a short distance, is a useful biological tool. The applications of this enzyme are far-reaching and will allow dissection of complex biological processes spatially and in intact cells. Unfortunately for the purposes of studying HPV infection in this way, APEX did not prove useful. There are likely many useful hits in the screen that could be further studied, but because of methodological problems, it was not possible to extract much useful information from the screen. The main way to determine the biological relevance of these proteins is using knockdowns, either through siRNAs or shRNAs. As is apparent from this study, an effect from a knockdown is not always an accurate measure of whether a protein is vital to HPV infection. Likely, the use of these siRNAs caused a global anti-viral effect that

decreased HPV infection, instead of a specific effect from knocking down the targeted protein. Indeed, the fact that TAP1 and TAPBP are part of the immune surveillance system could explain why knocking down their protein expression transiently caused a general decrease in infection. Additionally, in looking at the data more rigorously in retrospect, we should have been more cautious in our interpretation of the data. We attributed some of the variation in effect to the reagents, when in reassessing the data with the entire story in mind, it is likely that the phenotype caused by siRNA knockdown was not strong or stable. This variation in effect of the "knockdown" again points to a global anti-viral effect from the use of these siRNAs.

Despite our experience, an APEX screen could still be beneficial to the study of HPV infection. The ability to perform the biotinylation reaction at essentially any timepoint is a powerful tool that has not been fully utilized. We could potentially perform screens at different times after infection to pinpoint cellular factors that are in proximity to the virus and potentially important at particular stages in infection, such as the elusive later steps involving the TGN and the ER. Additionally, targeting the APEX reaction to a particular region of the cell, such as the endosome or the TGN would likely give a more manageable list of proteins that interact with HPV in particular cellular compartments. To accomplish this, we could use mutants or treatments that cause the viral particles to accumulate in particular compartments. Proteins that interact with the viral particles in the endosome could be identified using the retromer binding site double mutant attached to APEX, or any one of a number of cellular manipulations that affect retromer binding to L2, such as retromer knockdown, expressing a constitutively active Rab7 mutant, or using a short transmembrane protein to regulate Rab7 cycling, because they all cause HPV to accumulate

in the endosome [31, 37, 42]. TGN localization could be assessed using the R302 mutant that accumulates in the TGN, or an inhibitor of cell cycle progression, such as aphidicolin, which also causes HPV TGN accumulation [50]. Utilizing the right combination of the proper controls, such as using cells with and without APEX, with and without the biotinylation reaction, uninfected cells, cells infected with FLAG-tagged HPV or various mutant HPVs, and/or cells treated with various inhibitors, would allow the results from such a screen to be properly quantitated and utilized to the highest degree.

## Figures

| | Expectation | |
|---|---|---|
| | PsV-FLAG | PsV-APEX |
| TAP1 | - | 1.7E-16 |
| TAP2 | - | 0.07 |
| TAPBP | - | - |
| Calnexin | 1.5E-23 | 3.4E-29 |
| Calreticulin | 9.4E-06 | 3.8E-06 |
| $B_2M$ | - | - |
| Erp57 | - | - |
| HLA-A A68 | 6.2E-15 | 8.5E-46 |
| HLA-A A69 | - | 3.5E-41 |
| HLA-A A34 | 1.0E-15 | 2.1E-29 |
| HLA-A A23 | - | 1.4E-26 |
| HLA-C Cw16 | - | 8.2E-22 |
| HLA-B B46 | - | 7.8E-20 |
| VPS26 | - | 1.2E-11 |
| VPS35 | 8.5E-09 | 1.6E-27 |
| EGFR | - | 2.3E-10 |
| DYL1 | 6.2E-11 | 1.5E-15 |

***Figure A1.1: Selected APEX screen hits***

Samples were infected with PsV-FLAG with a FLAG tag on the C-terminus of L2 or with PsV-APEX with both a FLAG tag and the APEX enzyme on the C-terminus of L2. 8 hours post infection, the biotinylation reaction was performed using biotin phenol and hydrogen peroxide. Cells were lysed, biotinylated proteins were pulled down using streptavidin, digested off of the beads, and identified through MS. The expectation value refers to the confidence that the protein of interest is present in the sample.

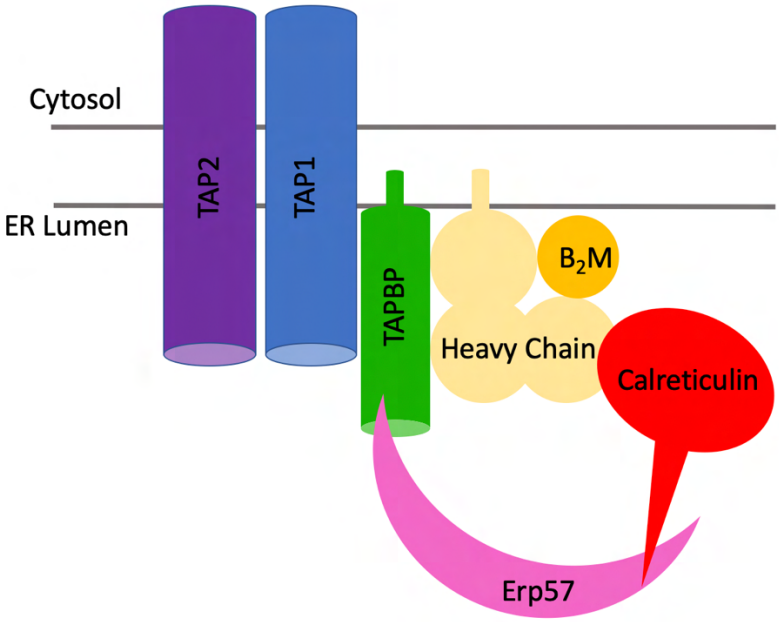


***Figure A1.2: The peptide loading complex***

The TAP1 and TAP2 heterodimer associates with the rest of the PLC through TAPBP. The entire PLC is localized to the ER membrane and is necessary for loading peptides onto MHC Class I molecules which are then presented at the surface of the cell for immune surveillance. Calreticulin – red, $\beta_2$Microglobulin – Orange, Heavy Chain of MHC – Pale yellow, Erp57 – pink, TAPBP – green, TAP1 – blue, TAP2 – purple

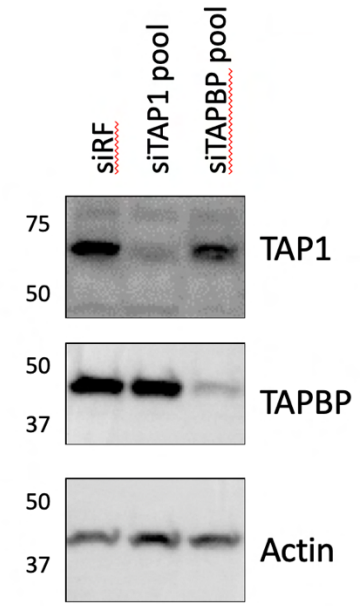


***Figure A1.3: siRNAs to TAP1 and TAPBP decrease protein expression***

HeLa S3 cells were transfected with the indicated siRNA for 48 hours using lipofectamine siRNA Max. Cell lysates were collected, run on SDS-PAGE gels, and western blotted with the indicated antibody.

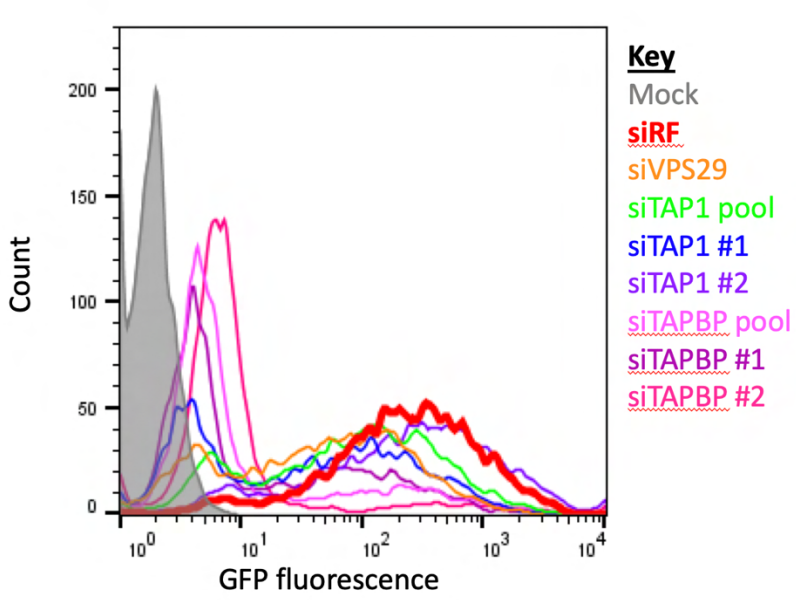


***Figure A1.4: siRNAs to TAP1 and TAPBP decrease HPV infection in HaCaT cells***

HaCaT cells were transfected with the indicated siRNA for 48 hours and subsequently infected with HPV PsV containing a GFP reporter plasmid for an additional 48 hours. Infection was quantified by counting the fraction of infected cells through flow cytometry for reporter gene expression. A decrease in infection is exemplified by a shift in fluorescence to the left.

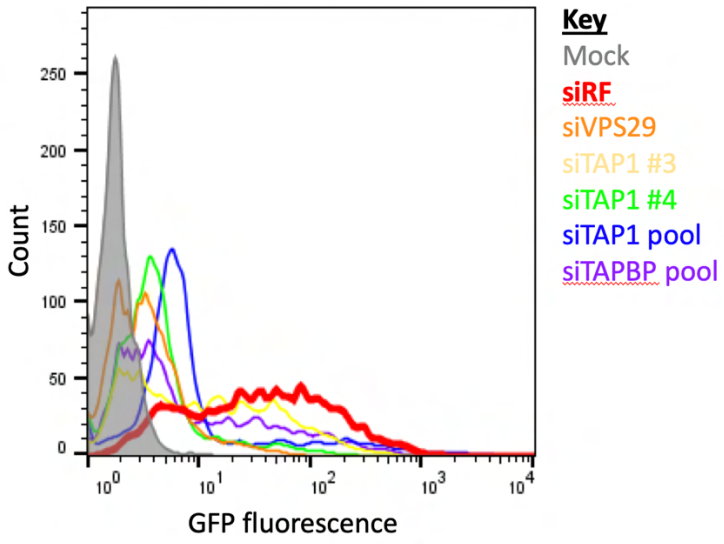


***Figure A1.5: siRNAs to TAP1 and TAPBP decrease HPV infection in HeLa cells***

HeLa cells were transfected with the indicated siRNA for 48 hours and subsequently infected with HPV PsV containing a GFP reporter plasmid for an additional 48 hours. Infection was quantified by counting the fraction of infected cells through flow cytometry for reporter gene expression. A decrease in infection is exemplified by a shift in fluorescence to the left.

L2-N ASATQLYKTCKQAGTCPPDIIPKVEGKTIADQK-B
L2-M B-PAFVTTPTKLITYDNPAYEGIDVDNTLY
L2-C B-SPQYTIIADAGDFYLHPSYYMLRKRRKR

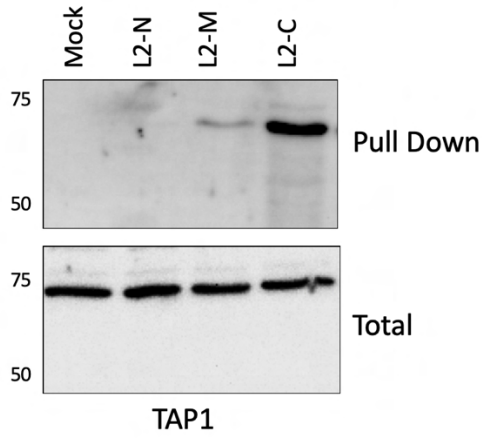


***Figure A1.6: Biotinylated peptides derived from HPV L2 bind to TAP1 in HeLa cell lysates***

(Top) Sequences of the biotinylated peptides that were incubated with HeLa cells. B – biotin. (Bottom) HeLa cell lysates were incubated with the indicated peptide, or no peptide (mock) for 2h at 4°C. The lysates were then incubated with streptavidin beads for 1h at 4°C, and subsequently washed with HEPES buffer to remove any unbound peptide. Samples were subjected to SDS-PAGE and immunoblotting for TAP1.

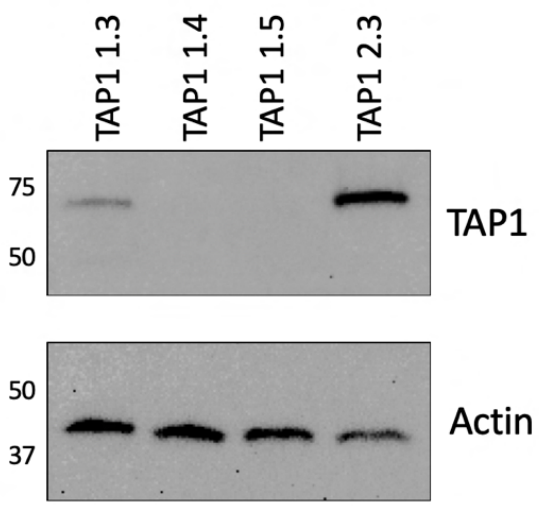


***Figure A1.7: TAP1 expression is knocked out in CRISPR/Cas9 cell lines***

HeLa cells were transduced with a lentivirus containing the indicated sgRNA. Cells were selected with puromycin and single-cell cloned. Cell lysates were collected and analyzed via western blotting for TAP1 and actin (as a loading control).

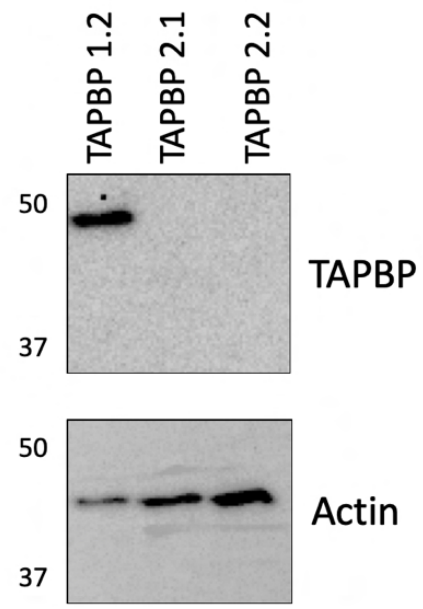


***Figure A1.8: TAPBP expression is knocked out in CRISPR/Cas9 cell lines***

HeLa cells were transduced with a lentivirus containing the indicated sgRNA. Cells were selected with puromycin and single-cell cloned. Cell lysates were collected and analyzed via western blotting for TAPBP and actin (as a loading control).


***Figure A1.9: There are mutations in TAP1 near the sgRNA binding site***

A region surrounding the sgRNA targeting site was amplified by PCR and analyzed by deep sequencing (Harvard MGH Core). For each set of sequences, the top line represents the TAP1 gene sequence and the lines below represent single sequences that were obtained from the sequencing.


***Figure A1.10: There are mutations in TAPBP near the sgRNA binding site***

A region surrounding the sgRNA targeting site was amplified by PCR and analyzed by deep sequencing (Harvard MGH Core). For each set of sequences, the top line represents the TAPBP genomic sequence and the lines below represent single sequences that were obtained from the sequencing.

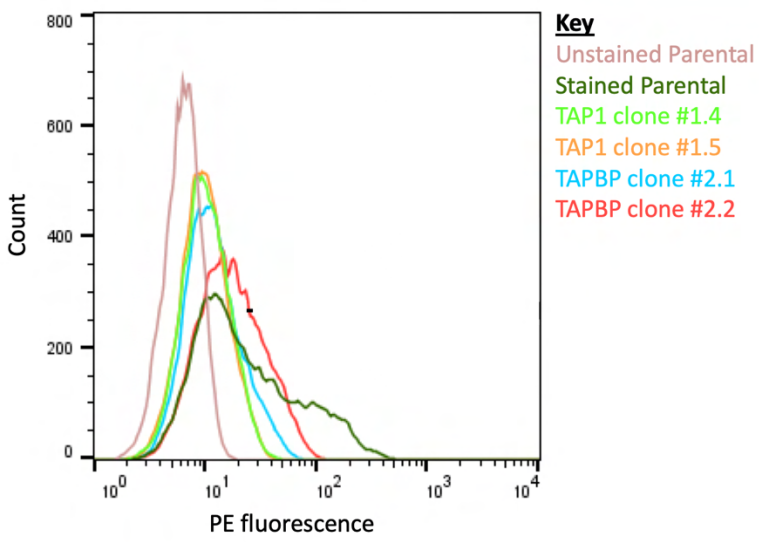


***Figure A1.11: HLA expression is decreased in TAP1 and TAPBP knockout cell lines***

Parental or CRISPR KO cells were trypsinized, washed, blocked, and incubated with an antibody to HLA-ABC conjugated to PE. Samples were then washed to remove unbound antibody, resuspended in 5% NGS, filtered, and analyzed via flow cytometry.

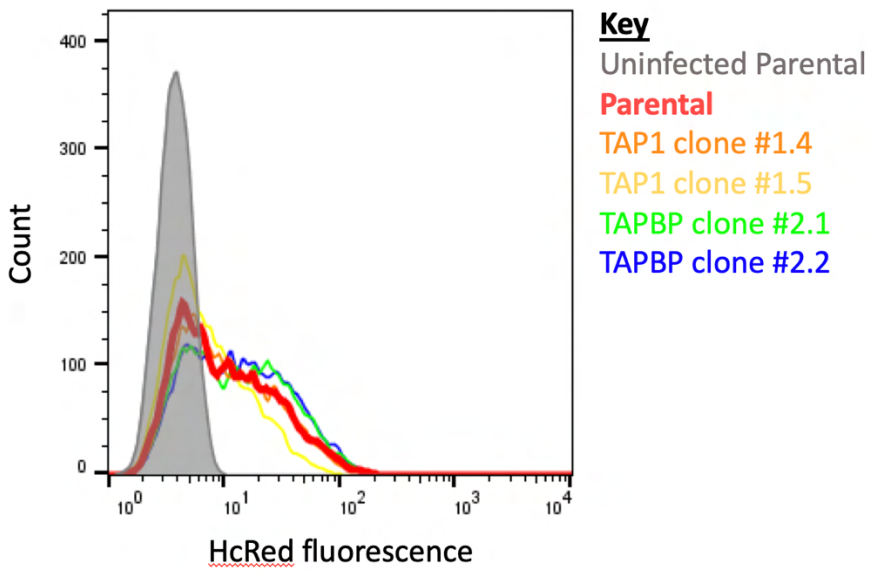


***Figure A1.12: HPV infection is not decreased in TAP1 or TAPBP knockout cell lines***

Parental or knockout HeLa cells were infected with HPV PsV for 48 hours and infection was quantified through flow cytometry for reporter gene fluorescence.

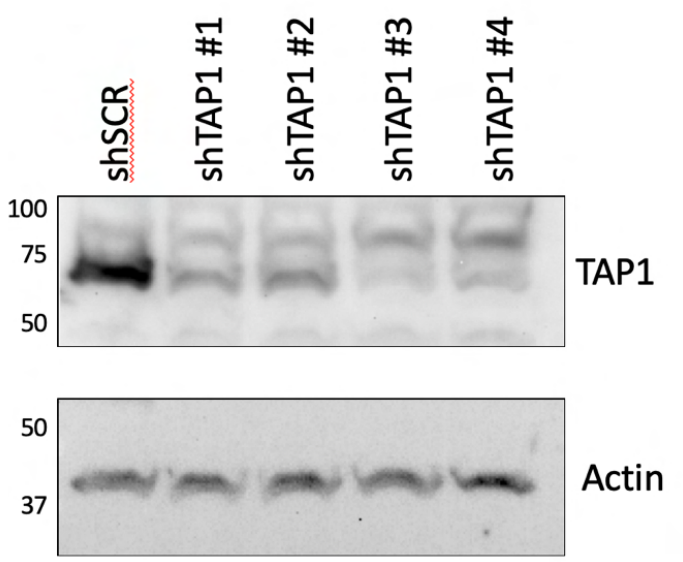


***Figure A1.13: TAP1 expression is decreased in shRNA knockdown cells***

shRNA cell lines were generated by transducing HeLa cells with lentivirus encoding the individual shRNAs to TAP1. Cell lysates were collected and analyzed via Western blotting for the indicated protein.

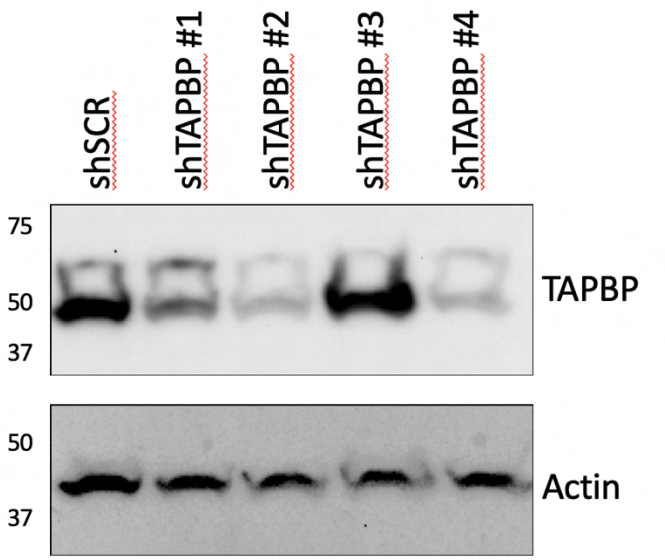


***Figure A1.14: TAPBP expression is decreased in most shRNA knockdown cells***

shRNA cell lines were generated by transducing HeLa cells with lentivirus encoding the individual shRNAs to TAPBP. Cell lysates were collected and analyzed via Western blotting for the indicated protein.

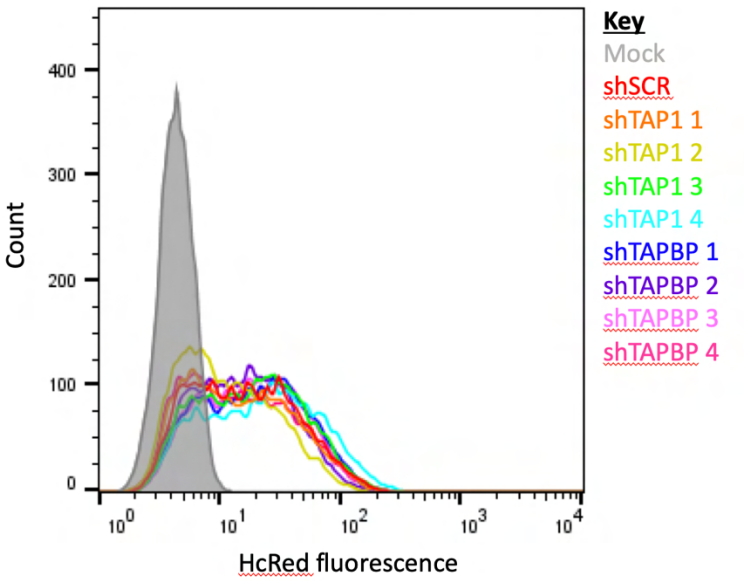


***Figure A1.15: HPV infection is not decreased in TAP1 or TAPBP shRNA cell lines***

shRNA cell lines were generated by transducing HeLa cells with lentivirus encoding the individual shRNAs. The shRNA cell lines were infected with HPV PsV for 48h and infection was assessed by flow cytometry for reporter gene expression.

# Appendix II: A screen for HPV mutants using a novel replicating virus system

## Introduction

There are multiple viral production systems in place that can be used to study HPV [205]. There are four different types of particles that can be studied, each of which has distinct advantages and disadvantages. Native virions are produced in an organotypic raft culture system and contain the full HPV capsid and genome [206-208]. The organotypic raft culture system allows for the production of HPV particles in their native environment of a differentiating epithelium. Producing particles this way is the closest to the particles that would be produced in an active infection. This system also allows genetic mutants of the virus to go through the entire HPV lifecycle, from the initial infection through genome replication, virion assembly and cellular egress. However, this system is expensive and cumbersome, and the production of particles takes 10 to 20 days which is much slower than the other three types of particles.

The other three types of particles are produced in transfection-based systems, where plasmids encoding the viral capsid proteins and possibly a genome of interest are transfected into a production cell line and particles are harvested and purified a few days later [205]. These systems rely on the fact that L1 and L2 self-assemble into capsids. HPV particles can package essentially any DNA under 8kb, and the HPV genome does not have a packaging signal. Virus Like Particles (VLPs) can be assembled using only L1 or L1 and L2 and lack encapsidated DNA [209-213]. Pseudovirions (PsVs) have L1 and L2 as well as a reporter gene of interest, such as one encoding RFP or GFP [18, 168, 169, 214]. This

small reporter gene of interest is packaged as the viral genome and allows HPV infection to be easily assessed through measuring reporter gene expression, but these particles lack the genes encoding L1 and L2 and are therefore only useful to study the entry process of HPV. Quasivirions (QVs) are the closest to native virions, and have L1, L2, and the full HPV genome. They have many of the same epitopes exposed on the surface of capsids as native virions [215, 216]. The quick production of VLPs, PsVs, and QVs is a clear advantage for these three particle types over the native virions, as particles are produced within three to four days and can then be harvested, purified, and/or concentrated. This transfection-based system is much less expensive than the production of native virions and allows for large amounts of particles to be produced. Additionally, the non-pathogenic nature of these particles, as well as the ease with which viral mutants can be made and studied, makes them attractive systems to use to study HPV. However, all of the recombinant particles are produced in non-relevant cell lines, like 293TT cells, and could undergo different modifications that would not occur during a normal infection [217]. While these particles all require maturation like native virions, this maturation occurs by incubating the particles in a 37°C water bath overnight, as opposed to maturation that occurs as host keratinocytes differentiate [18, 169]. Most of the work in this thesis has been done using the PsV system.

In the standard PsV production system, the large p16SheLL (10.8kb) packaging plasmid that encodes L1 and L2 is transfected into 293TT cells along with a small plasmid containing a reporter gene of interest, such as RFP or GFP [168, 169]. Because human papillomavirus particles can package any DNA under 8kb they will encapsidate the

reporter gene, but not the large packaging plasmid [168, 169]. Reporter gene expression is then used as a proxy for infection.

In addition to the standard PsV production system, Buck and colleagues described a replicating virus system which can be used to generate high titer viral stocks through successive rounds of infection [168]. In this system, the small p16L1L2 (6.3kb) plasmid both encodes L1 and L2, replicates to high copy number in response to SV40 large T antigen, and can be packaged as the viral genome. This plasmid is transfected into 293TT cells (which express T antigen), the PsV particles are harvested, and then this resulting vector stock can be used to infect fresh 293TT cells where it will replicate to high titers. Stocks can continually be passaged and amplified, collected, and eventually purified to produce PsV stocks with very high titers. In this system, the L1 and L2 proteins in the capsid can be linked to the genes encoded by the p16L1L2 plasmid (Figure A2.1). Therefore, we hypothesized that we could mutagenize the capsid gene of interest and generate stocks where the gene in the PsV particle encodes the amino acid sequence of the L1 or L2 protein on the capsid. We could then impose any number of selections, such as γ-secretase or retromer inhibition, to select for mutants with interesting phenotypes. However, the selections need to be developed and the generation of these mutant viral stocks needs to be validated.

## Results

## Virus generation and titer

In order to utilize this system, we first had to generate PsV using the new protocol and plasmids. 293TT cells were transfected with the small p16L1L2 plasmid that can be packaged as the genome, using PEI. 72 hours post transfection, cells were harvested using

the typical protocol, where cells are washed, trypsinized, and collected. The cells were lysed in lysis buffer containing 1X PBS, 0.5% Triton X, 100mM $MgCl_2$, 50mM $CaCl_2$, and ~5 U RNAse A/mL, and incubated in a 37°C water bath overnight. The following morning, the cell lysate was stored at -80°C and labelled as the initial vector stock. This stock can then be used to infect new cells and produce a higher titer virus. This vector stock was used to infect a fresh set of 293TT cells, allowed to infect and produce new virus for 72 hours, and collected as above, as a second vector stock. A second infection was performed from this vector stock and the cells were harvested as above. This second cell lysate was purified using a 27/33/39% optiprep gradient and fractions were collected, using the same method as for standard PsV. Those fractions were analyzed by SDS-PAGE, stained with Coomassie Brilliant Blue, and compared to virus produced under the standard single-transfection protocol. As can be seen in Figure A2.2, virus produced from the replicating system had much higher levels of both L1 and L2.

We then wanted to ensure that the replicating virus was actually replicating in cells. I infected Cos7 or 293TT cells, both of which have the SV40 large T antigen to drive L1 and L2 expression from the SV40 *ori* in the p16L1L2 plasmid and incubated the cells for 24 or 48 hours. I stained the infected cells with an L1 antibody and performed flow cytometry to determine if L1 levels increased after the initial infection event. As is shown in Figure A2.3 and A2.4, L1 levels increased from the 24-hour time point to the 48-hour time point in both COS7 and 293TT cells, indicating that new L1, and thus new PsV, was being produced. This validates the system as efficient at producing high titer virus. It also shows that the high titer virus can infect new cells and produce more virus in those infected cells, as long as they express the SV40 large T antigen.

## HPV Plaque Assay

An entry screen could be performed using a plaque-based screening method. We needed to determine, however, if the replicating HPV PsV could form plaques. Viral plaques form as a result of localized cell death and virus spread after infection from a virus that kills cells. If the assay is set up correctly, each plaque will arise from a single infected cell. This would be beneficial for screening mutants in the replicating system because, at a low enough MOI, any individual plaque would be caused by a single viral mutant, after imposing some selection on the cells, such as γ-secretase or furin inhibition. Clonal virus could then be isolated from the plaque, sequenced, and used directly to characterize the new mutant virus. It may also be possible to isolate plaque morphology or temperature sensitive mutants easily. HPV does not typically form plaques upon infection, as it does not typically kill the cells that it infects. However, with a high titer, replicating virus, it's possible that plaques will form after infection due to the ability of this virus to replicate to high viral loads in cells, which could potentially kill infected cells.

I first attempted the plaque assay in 293TT and Cos7 cells, since they overexpress large T which is required for the production of new virus from the p16L1L2 plasmid. Cells were plated in 60mm dishes and infected with replicating virus generated from the p16L1L2 plasmid as described above at 10-fold dilutions in order to achieve a low enough MOI such that individual plaques could be isolated. SV40 was used as a positive control, as this virus is known to form plaques. Cells were overlaid with multiple different types of semi-solid medium, to hopefully find one that would allow for plaque formation. I used methylcellulose, low melting point agar, normal melting point agar, and Avicel as separate overlays. The goal of the overlay is to limit viral diffusion through the medium because the

overlays are viscous. I also tried using both MEM and DMEM as media for the plaque assay. Unfortunately, there were no conditions under which I saw plaque formation, either for the replicating HPV virus, or for SV40. I also did not see clear cell death or lysis from these plaque assays after staining with Neutral Red, a dye that has to be imported into cells and thus only stains living cells.

## Generation of mutant p16L1L2 plasmid

Although a plaque assay presents an attractive system to screen mutants with, there are other screening methods that can be used. Regardless of the screening method used, viral mutants need to be generated such that the mutant L1 and L2 proteins are encoded by the p16L1L2 plasmid that the PsV packages. These "oligoclonal stocks" can then be used to infect cells such that each cell only receives a single viral particle. A selection would be imposed, such as γ-secretase inhibition, or growth at permissive and non-permissive temperatures (to generate temperature sensitive mutations), after the cells were infected with the mutagenized oligoclonal PsV stocks. Viral mutants that are able to overcome the imposed selection would expand and the DNA of PsVs that can overcome the selection would be recovered and sequenced. First, the generation of the oligoclonal stocks needs to be validated. In order to do this, we wanted to clone a FLAG or HA tag on the C-terminus of L2 in the p16L1L2 plasmid. We chose these tags because PsV produced with either tag in the standard system remains infectious. Both plasmids would then be co-transfected into 293TT cells, and PsV will be collected. In this initial seed stock, any one capsid would likely have both FLAG- and HA-tagged L2 molecules, and either the FLAG- or HA-tagged genome. We would then use this seed stock to infect new 293TT cells, or other cells that express T antigen at low MOI. It is vital that in this infection, there is only one replicating

viral particle per cell. Thus, any PsV produced from that cell will have either a FLAG-tagged L2 protein and corresponding DNA or a HA-tagged L2 protein and corresponding DNA. We wanted to test this by using this oligoclonal stock to infect new cells at low multiplicity in microtiter plates. Viral genomes and viral proteins from these wells would be collected and PCR or Western blots, respectively, would be performed to confirm that the proteins and genomes match. We would systematically vary the conditions of PsV production, infection, and collection until oligoclonal stock generation can be confirmed.

Unfortunately, through multiple cloning methods including restriction digests, PCR amplification with primers, gBlocks including the full L2 protein, and Gibson assembly, these mutants could not be generated. This project was therefore abandoned in favor of experiments that were producing interesting results as described in the main body of this thesis.

## Discussion

The replicating virus system is an attractive PsV production system that produces high titer virus. This has been confirmed by comparing L1 and L2 levels after PsV production using both methods and observing higher levels of L1 and L2 in the replicating virus system. It has also been confirmed that the replicating virus can replicate in cells expressing SV40 large T. Unfortunately, the optimization of the plaque assay and my inability to clone the FLAG or HA tag on the C-terminus of L2 in the p16L1L2 plasmid hampered the progress of this project and screen. It is likely that the old viral stock of SV40 that I was using was non-infectious, and thus a new stock needs to be used to optimize the plaque assay for HPV16. The SV40 control stock should also be tested for infection in permissive cells before being used as a control for the HPV plaque assay. It's also possible

that the replicating virus will not produce plaques upon infection, so other mutant screening methods should be developed if this project is pursued further. Cloning the FLAG or HA tag onto the end of L2 in this plasmid is likely achievable because we have constructed other mutations in this segment of L2. Regardless, the replicating PsV system has been validated and can be used to produce high titer virus for relevant applications, such as *in vivo* studies or electron microscopy, which both require high amounts of virus.

## Figures

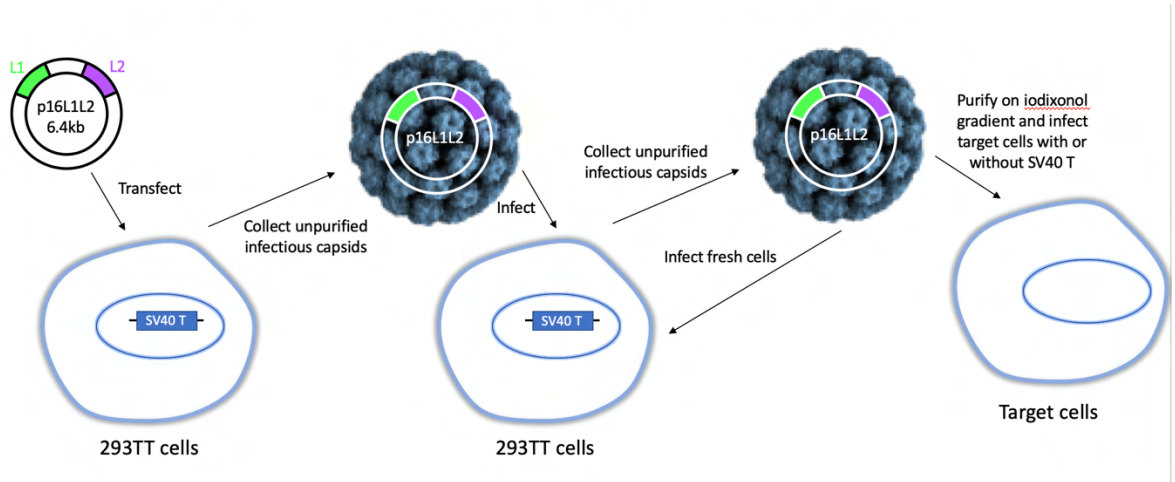


***Figure A2.1: The replicating viral system***

p16L1L2 PsV was produced by transfecting 293TT cells with the p16L1L2 plasmid as both the packaging plasmid and genome. 72h post transfection, cell lysates were collected and matured overnight. The initial vector stock was then used to subsequently infect a fresh set of 293TT cells and the harvesting process was repeated. This infection can be repeated multiple times. After the final infection, PsV is purified using a 27/33/39% iodixanol gradient.

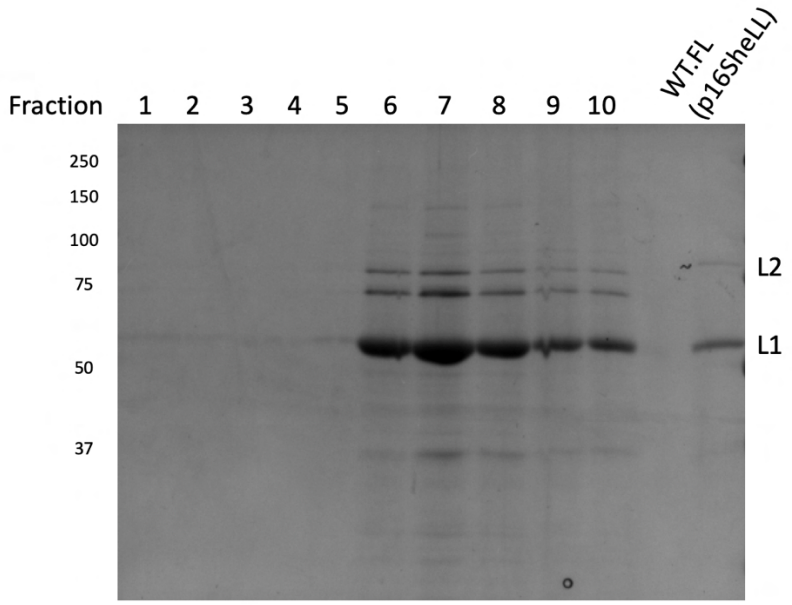


***Figure A2.2: The replicating viral system produces PsV with higher levels of L1 and L2 than the standard PsV production system***

Fractions of purified p16L1L2 virus were collected and 10µL of the fractions were analyzed via SDS-PAGE and Coomassie Brilliant Blue staining. 10µL of wild-type PsV made with the p16SheLL plasmid was analyzed in the final lane for comparison of L1 and L2 levels.

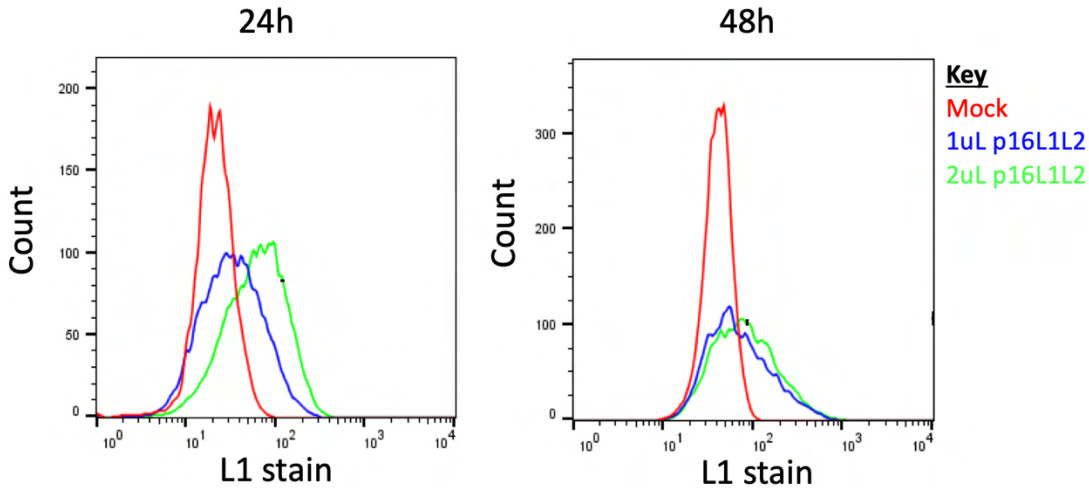


***Figure A2.3: p16L1L2 infection in 293TT cells***

293TT cells were infected with the indicated volume of p16L1L2 PsV for 24h (left) or 48h (right), or mock infected. After 24 or 48h, viral particles were stained with an antibody recognizing L1, conjugated to FITC. Samples were analyzed through flow cytometry to assess the amount of L1 in the cells. The shift to the right in the 48h graph indicates that new virus is being made in these cells.

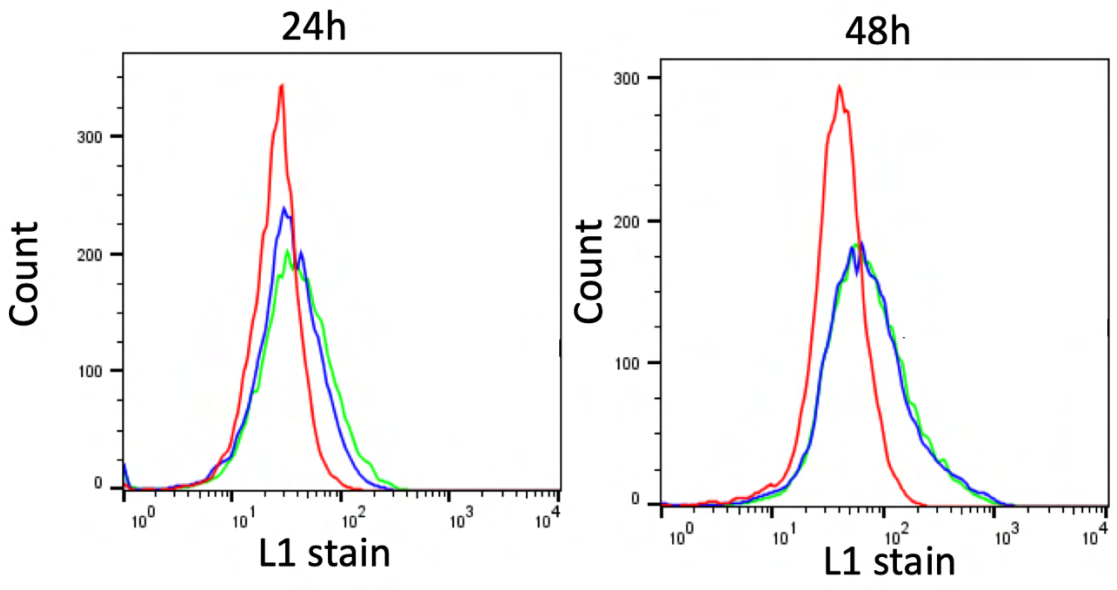


***Figure 2.4: p16L1L2 infection in Cos7 cells***

Cos7 cells were infected with the indicated volume of p16L1L2 PsV for 24h (left) or 48h (right), or mock infected. After 24 or 48h, viral particles were stained with an antibody recognizing L1, conjugated to FITC. Samples were analyzed through flow cytometry to assess the amount of L1 in the cells. The shift to the right in the 48h graph indicates that new virus is being made in these cells.

# References


1. Wildly, P., *Classification and Nomenclature of Viruses*, in *Monographs in Virology*, J.L. Melnick, Editor. 1971.
2. van Regenmortel, M.H.V., et al., *Seventh report of the INternational Committee on Taxonomy of Viruses*, in *Virus Taxonomy*. 2000: San Diego. p. 1162.
3. Moens, U., et al., *ICTV Virus Taxonomy Profile: Polyomaviridae.* J Gen Virol, 2017. **98**(6): p. 1159-1160.
4. Van Doorslaer, K., et al., *ICTV Virus Taxonomy Profile: Papillomaviridae.* J Gen Virol, 2018. **99**(8): p. 989-990.
5. Van Doorslaer, K., et al., *The Papillomavirus Episteme: a major update to the papillomavirus sequence database.* Nucleic Acids Res, 2017. **45**(D1): p. D499-d506.
6. Bzhalava, D., C. Eklund, and J. Dillner, *International standardization and classification of human papillomavirus types.* Virology, 2015. **476**: p. 341-344.
7. de Villiers, E.M., et al., *Classification of papillomaviruses.* Virology, 2004. **324**(1): p. 17-27.
8. Bernard, H.U., et al., *Classification of papillomaviruses (PVs) based on 189 PV types and proposal of taxonomic amendments.* Virology, 2010. **401**(1): p. 70-9.
9. Saraiya, M., et al., *US assessment of HPV types in cancers: implications for current and 9-valent HPV vaccines.* J Natl Cancer Inst, 2015. **107**(6): p. djv086.
10. de Martel, C., *Worldwide burden of cancer attributable to HPV by site, country, and HPV type.* Int J Cancer, 2017.
11. Koutsky, L.A., et al., *A controlled trial of a human papillomavirus type 16 vaccine.* N Engl J Med, 2002. **347**(21): p. 1645-51.
12. Gillison, M.L., A.K. Chaturvedi, and D.R. Lowy, *HPV prophylactic vaccines and the potential prevention of noncervical cancers in both men and women.* Cancer, 2008. **113**(10 Suppl): p. 3036-46.
13. Chaturvedi, A.K., et al., *Human papillomavirus and rising oropharyngeal cancer incidence in the United States.* J Clin Oncol, 2011. **29**(32): p. 4294-301.
14. Reagan-Steiner, S., D. Yankey, and J. Jeyarajah, *National, Regional, State, and Selected Local Area Vaccination Coverage Among Adolescents Aged 13-17 Years - United States, 2015.* MMWR Morb Mortal Wkly Rep, 2016. **65**: p. 850-858.
15. Buck, C.B., et al., *Arrangement of L2 within the papillomavirus capsid.* J Virol, 2008. **82**(11): p. 5190-7.
16. Richards, R.M., et al., *Cleavage of the papillomavirus minor capsid protein, L2, at a furin consensus site is necessary for infection.* Proc Natl Acad Sci U S A, 2006. **103**(5): p. 1522-7.
17. Day, P.M., et al., *Mechanisms of human papillomavirus type 16 neutralization by l2 cross-neutralizing and l1 type-specific antibodies.* J Virol, 2008. **82**(9): p. 4638-46.
18. Buck, C.B. and C.D. Thompson, *Production of papillomavirus-based gene transfer vectors.* Curr Protoc Cell Biol, 2007. **Chapter 26**: p. Unit 26.1.

19. Campos, S.K., *Subcellular Trafficking of the Papillomavirus Genome during Initial Infection: The Remarkable Abilities of Minor Capsid Protein L2.* Viruses, 2017. **9**(12).
20. Holmgren, S.C., et al., *The minor capsid protein L2 contributes to two steps in the human papillomavirus type 31 life cycle.* J Virol, 2005. **79**(7): p. 3938-48.
21. Giroglou, T., et al., *Human papillomavirus infection requires cell surface heparan sulfate.* J Virol, 2001. **75**(3): p. 1565-70.
22. Johnson, K.M., et al., *Role of heparan sulfate in attachment to and infection of the murine female genital tract by human papillomavirus.* J Virol, 2009. **83**(5): p. 2067-74.
23. Joyce, J.G., et al., *The L1 major capsid protein of human papillomavirus type 11 recombinant virus-like particles interacts with heparin and cell-surface glycosaminoglycans on human keratinocytes.* J Biol Chem, 1999. **274**(9): p. 5810-22.
24. Cagno, V., et al., *Heparan Sulfate Proteoglycans and Viral Attachment: True Receptors or Adaptation Bias?* Viruses, 2019. **11**(7).
25. Rusnati, M., et al., *Sulfated K5 Escherichia coli polysaccharide derivatives: A novel class of candidate antiviral microbicides.* Pharmacol Ther, 2009. **123**(3): p. 310-22.
26. Cerqueira, C., et al., *Kallikrein-8 Proteolytically Processes Human Papillomaviruses in the Extracellular Space To Facilitate Entry into Host Cells.* J Virol, 2015. **89**(14): p. 7038-52.
27. Bronnimann, M.P., et al., *Furin Cleavage of L2 during Papillomavirus Infection: Minimal Dependence on Cyclophilins.* J Virol, 2016. **90**(14): p. 6224-34.
28. Schelhaas, M., et al., *Entry of human papillomavirus type 16 by actin-dependent, clathrin- and lipid raft-independent endocytosis.* PLoS Pathog, 2012. **8**(4): p. e1002657.
29. Bergant Marusic, M., et al., *Human papillomavirus L2 facilitates viral escape from late endosomes via sorting nexin 17.* Traffic, 2012. **13**(3): p. 455-67.
30. Pim, D., et al., *A Novel PDZ Domain Interaction Mediates the Binding between Human Papillomavirus 16 L2 and Sorting Nexin 27 and Modulates Virion Trafficking.* J Virol, 2015. **89**(20): p. 10145-55.
31. Popa, A., et al., *Direct binding of retromer to human papillomavirus type 16 minor capsid protein L2 mediates endosome exit during viral infection.* PLoS Pathog, 2015. **11**(2): p. e1004699.
32. Florin, L., et al., *Identification of a dynein interacting domain in the papillomavirus minor capsid protein l2.* J Virol, 2006. **80**(13): p. 6691-6.
33. Schneider, M.A., et al., *Identification of the dynein light chains required for human papillomavirus infection.* Cell Microbiol, 2011. **13**(1): p. 32-46.
34. Zhang, P., et al., *Cell-penetrating peptide mediates intracellular membrane passage of human papillomavirus L2 protein to trigger retrograde trafficking.* Cell, 2018.
35. Frankel, A.D. and C.O. Pabo, *Cellular uptake of the tat protein from human immunodeficiency virus.* Cell, 1988. **55**(6): p. 1189-93.

36. Vivès, E., P. Brodin, and B. Lebleu, *A truncated HIV-1 Tat protein basic domain rapidly translocates through the plasma membrane and accumulates in the cell nucleus.* J Biol Chem, 1997. **272**(25): p. 16010-7.
37. Lipovsky, A., et al., *Genome-wide siRNA screen identifies the retromer as a cellular entry factor for human papillomavirus.* Proc Natl Acad Sci U S A, 2013. **110**(18): p. 7452-7.
38. Zhang, H., et al., *The Retromer Complex and Sorting Nexins in Neurodegenerative Diseases.* Front Aging Neurosci, 2018. **10**: p. 79.
39. Siegenthaler, B.M. and L. Rajendran, *Retromers in Alzheimer's disease.* Neurodegener Dis, 2012. **10**(1-4): p. 116-21.
40. Wen, L., et al., *VPS35 haploinsufficiency increases Alzheimer's disease neuropathology.* J Cell Biol, 2011. **195**(5): p. 765-79.
41. Day, P.M., et al., *Identification of a role for the trans-Golgi network in human papillomavirus 16 pseudovirus infection.* J Virol, 2013. **87**(7): p. 3862-70.
42. Xie, J., et al., *TBC1D5-Catalyzed Cycling of Rab7 Is Required for Retromer-Mediated Human Papillomavirus Trafficking during Virus Entry.* Cell Rep, 2020. **31**(10): p. 107750.
43. Young, J.M., et al., *The Known and Potential Intersections of Rab-GTPases in Human Papillomavirus Infections.* Front Cell Dev Biol, 2019. **7**: p. 139.
44. Zhang, P., et al., *Cell-penetrating peptide inhibits retromer-mediated human papillomavirus trafficking during virus entry.* Proc Natl Acad Sci U S A, 2020. **117**(11): p. 6121-6128.
45. Huang, H.S., C.B. Buck, and P.F. Lambert, *Inhibition of gamma secretase blocks HPV infection.* Virology, 2010. **407**(2): p. 391-6.
46. Karanam, B., et al., *Papillomavirus infection requires gamma secretase.* J Virol, 2010. **84**(20): p. 10661-70.
47. Zhang, W., et al., *Vesicular trafficking of incoming human papillomavirus 16 to the Golgi apparatus and endoplasmic reticulum requires gamma-secretase activity.* MBio, 2014. **5**(5): p. e01777-14.
48. Bronnimann, M.P., et al., *A transmembrane domain and GxxxG motifs within L2 are essential for papillomavirus infection.* J Virol, 2013. **87**(1): p. 464-73.
49. Inoue, T., et al., *Gamma-secretase acts dually as a chaperone and protease on the L2 capsid protein of Human Papillomavirus to promote infection.* Mol Cell, 2017.
50. Calton, C.M., et al., *Translocation of the papillomavirus L2/vDNA complex across the limiting membrane requires the onset of mitosis.* PLoS Pathog, 2017. **13**(5): p. e1006200.
51. Laniosz, V., et al., *Human papillomavirus type 16 infection of human keratinocytes requires clathrin and caveolin-1 and is brefeldin a sensitive.* J Virol, 2009. **83**(16): p. 8221-32.
52. Aydin, I., et al., *Large scale RNAi reveals the requirement of nuclear envelope breakdown for nuclear import of human papillomaviruses.* PLoS Pathog, 2014. **10**(5): p. e1004162.
53. DiGiuseppe, S., M. Bienkowska-Haba, and M. Sapp, *Human Papillomavirus Entry: Hiding in a Bubble.* J Virol, 2016. **90**(18): p. 8032-5.

54. DiGiuseppe, S., et al., *Incoming human papillomavirus type 16 genome resides in a vesicular compartment throughout mitosis.* Proc Natl Acad Sci U S A, 2016. **113**(22): p. 6289-94.
55. DiGiuseppe, S., et al., *Topography of the Human Papillomavirus Minor Capsid Protein L2 during Vesicular Trafficking of Infectious Entry.* J Virol, 2015. **89**(20): p. 10442-52.
56. Yan, H., et al., *Efficient Inhibition of Human Papillomavirus Infection by L2 Minor Capsid-Derived Lipopeptide.* mBio, 2019. **10**(4).
57. Wolfe, M.S., et al., *Are presenilins intramembrane-cleaving proteases? Implications for the molecular mechanism of Alzheimer's disease.* Biochemistry, 1999. **38**(35): p. 11223-30.
58. Wolfe, M.S. and R. Kopan, *Intramembrane proteolysis: theme and variations.* Science, 2004. **305**(5687): p. 1119-23.
59. Edbauer, D., et al., *Reconstitution of gamma-secretase activity.* Nat Cell Biol, 2003. **5**(5): p. 486-8.
60. Kimberly, W.T., et al., *Gamma-secretase is a membrane protein complex comprised of presenilin, nicastrin, Aph-1, and Pen-2.* Proc Natl Acad Sci U S A, 2003. **100**(11): p. 6382-7.
61. Takasugi, N., et al., *The role of presenilin cofactors in the gamma-secretase complex.* Nature, 2003. **422**(6930): p. 438-41.
62. Bai, X.C., et al., *An atomic structure of human γ-secretase.* Nature, 2015. **525**(7568): p. 212-217.
63. Yang, G., et al., *Structural basis of Notch recognition by human γ-secretase.* Nature, 2019. **565**(7738): p. 192-197.
64. Zhou, R., et al., *Recognition of the amyloid precursor protein by human γ-secretase.* Science, 2019. **363**(6428).
65. Yamasaki, A., et al., *The GxGD motif of presenilin contributes to catalytic function and substrate identification of gamma-secretase.* J Neurosci, 2006. **26**(14): p. 3821-8.
66. Dries, D.R. and G. Yu, *Assembly, maturation, and trafficking of the gamma-secretase complex in Alzheimer's disease.* Curr Alzheimer Res, 2008. **5**(2): p. 132-46.
67. Shah, S., et al., *Nicastrin functions as a gamma-secretase-substrate receptor.* Cell, 2005. **122**(3): p. 435-47.
68. Arawaka, S., et al., *The levels of mature glycosylated nicastrin are regulated and correlate with gamma-secretase processing of amyloid beta-precursor protein.* J Neurochem, 2002. **83**(5): p. 1065-71.
69. Gu, Y., et al., *APH-1 interacts with mature and immature forms of presenilins and nicastrin and may play a role in maturation of presenilin.nicastrin complexes.* J Biol Chem, 2003. **278**(9): p. 7374-80.
70. Lee, S.F., et al., *Mammalian APH-1 interacts with presenilin and nicastrin and is required for intramembrane proteolysis of amyloid-beta precursor protein and Notch.* J Biol Chem, 2002. **277**(47): p. 45013-9.
71. Watanabe, N., et al., *Pen-2 is incorporated into the gamma-secretase complex through binding to transmembrane domain 4 of presenilin 1.* J Biol Chem, 2005. **280**(51): p. 41967-75.

72. Fraering, P.C., et al., *Detergent-dependent dissociation of active gamma-secretase reveals an interaction between Pen-2 and PS1-NTF and offers a model for subunit organization within the complex.* Biochemistry, 2004. **43**(2): p. 323-33.
73. Hu, Y. and M.E. Fortini, *Different cofactor activities in gamma-secretase assembly: evidence for a nicastrin-Aph-1 subcomplex.* J Cell Biol, 2003. **161**(4): p. 685-90.
74. Luo, W.J., et al., *PEN-2 and APH-1 coordinately regulate proteolytic processing of presenilin 1.* J Biol Chem, 2003. **278**(10): p. 7850-4.
75. Prokop, S., et al., *Requirement of PEN-2 for stabilization of the presenilin N-/C-terminal fragment heterodimer within the gamma-secretase complex.* J Biol Chem, 2004. **279**(22): p. 23255-61.
76. Steiner, H., et al., *PEN-2 is an integral component of the gamma-secretase complex required for coordinated expression of presenilin and nicastrin.* J Biol Chem, 2002. **277**(42): p. 39062-5.
77. Shiraishi, H., et al., *PEN-2 enhances gamma-cleavage after presenilin heterodimer formation.* J Neurochem, 2004. **90**(6): p. 1402-13.
78. Capell, A., et al., *Gamma-secretase complex assembly within the early secretory pathway.* J Biol Chem, 2005. **280**(8): p. 6471-8.
79. Kim, S.H., et al., *Evidence that assembly of an active gamma-secretase complex occurs in the early compartments of the secretory pathway.* J Biol Chem, 2004. **279**(47): p. 48615-9.
80. Fukumori, A., L.P. Feilen, and H. Steiner, *Substrate recruitment by γ-secretase.* Semin Cell Dev Biol, 2020. **105**: p. 54-63.
81. Hitzenberger, M., et al., *The dynamics of γ-secretase and its substrates.* Semin Cell Dev Biol, 2020. **105**: p. 86-101.
82. Meyer, E.L., et al., *Glutamate receptor subunit 3 is modified by site-specific limited proteolysis including cleavage by gamma-secretase.* J Biol Chem, 2003. **278**(26): p. 23786-96.
83. Nakahara, S., et al., *A secreted type of beta1,6 N-acetylglucosaminyltransferase V (GnT-V), a novel angiogenesis inducer, is regulated by gamma-secretase.* Faseb j, 2006. **20**(14): p. 2451-9.
84. Beel, A.J. and C.R. Sanders, *Substrate specificity of gamma-secretase and other intramembrane proteases.* Cell Mol Life Sci, 2008. **65**(9): p. 1311-34.
85. Haapasalo, A. and D.M. Kovacs, *The many substrates of presenilin/γ-secretase.* J Alzheimers Dis, 2011. **25**(1): p. 3-28.
86. Struhl, G. and A. Adachi, *Requirements for presenilin-dependent cleavage of notch and other transmembrane proteins.* Mol Cell, 2000. **6**(3): p. 625-36.
87. Funamoto, S., et al., *Substrate ectodomain is critical for substrate preference and inhibition of γ-secretase.* Nat Commun, 2013. **4**: p. 2529.
88. Bolduc, D.M., et al., *Nicastrin functions to sterically hinder γ-secretase-substrate interactions driven by substrate transmembrane domain.* Proc Natl Acad Sci U S A, 2016. **113**(5): p. E509-18.
89. Laurent, S.A., et al., *γ-Secretase directly sheds the survival receptor BCMA from plasma cells.* Nat Commun, 2015. **6**: p. 7333.
90. Sun, L., et al., *Structural basis of human γ-secretase assembly.* Proc Natl Acad Sci U S A, 2015. **112**(19): p. 6003-8.

91. Hemming, M.L., et al., *Proteomic profiling of gamma-secretase substrates and mapping of substrate requirements.* PLoS Biol, 2008. **6**(10): p. e257.
92. Kukar, T.L., et al., *Lysine 624 of the amyloid precursor protein (APP) is a critical determinant of amyloid β peptide length: support for a sequential model of γ-secretase intramembrane proteolysis and regulation by the amyloid β precursor protein (APP) juxtamembrane region.* J Biol Chem, 2011. **286**(46): p. 39804-12.
93. Harwood, M.C., et al., *p120 catenin recruits HPV to γ-secretase to promote virus infection.* PLoS Pathog, 2020. **16**(10): p. e1008946.
94. Barthet, G., A. Georgakopoulos, and N.K. Robakis, *Cellular mechanisms of γ-secretase substrate selection, processing and toxicity.* Prog Neurobiol, 2012. **98**(2): p. 166-75.
95. Kiss, A., R.B. Troyanovsky, and S.M. Troyanovsky, *p120-catenin is a key component of the cadherin-gamma-secretase supercomplex.* Mol Biol Cell, 2008. **19**(10): p. 4042-50.
96. Kouchi, Z., et al., *p120 catenin recruits cadherins to gamma-secretase and inhibits production of Abeta peptide.* J Biol Chem, 2009. **284**(4): p. 1954-61.
97. Burd, C. and P.J. Cullen, *Retromer: a master conductor of endosome sorting.* Cold Spring Harb Perspect Biol, 2014. **6**(2).
98. Seaman, M.N., J.M. McCaffery, and S.D. Emr, *A membrane coat complex essential for endosome-to-Golgi retrograde transport in yeast.* J Cell Biol, 1998. **142**(3): p. 665-81.
99. Seaman, M.N., et al., *Endosome to Golgi retrieval of the vacuolar protein sorting receptor, Vps10p, requires the function of the VPS29, VPS30, and VPS35 gene products.* J Cell Biol, 1997. **137**(1): p. 79-92.
100. Gokool, S., et al., *Identification of a conserved motif required for Vps35p/Vps26p interaction and assembly of the retromer complex.* Biochem J, 2007. **408**(2): p. 287-95.
101. Hierro, A., et al., *Functional architecture of the retromer cargo-recognition complex.* Nature, 2007. **449**(7165): p. 1063-7.
102. Lucas, M., et al., *Structural Mechanism for Cargo Recognition by the Retromer Complex.* Cell, 2016. **167**(6): p. 1623-1635.e14.
103. Seaman, M.N., *Cargo-selective endosomal sorting for retrieval to the Golgi requires retromer.* J Cell Biol, 2004. **165**(1): p. 111-22.
104. Kvainickas, A., et al., *Retromer- and WASH-dependent sorting of nutrient transporters requires a multivalent interaction network with ANKRD50.* J Cell Sci, 2017. **130**(2): p. 382-395.
105. Simonetti, B., et al., *Sequence-dependent cargo recognition by SNX-BARs mediates retromer-independent transport of CI-MPR.* J Cell Biol, 2017. **216**(11): p. 3695-3712.
106. Restrepo, R., et al., *Structural features of vps35p involved in interaction with other subunits of the retromer complex.* Traffic, 2007. **8**(12): p. 1841-53.
107. Harterink, M., et al., *A SNX3-dependent retromer pathway mediates retrograde transport of the Wnt sorting receptor Wntless and is required for Wnt secretion.* Nat Cell Biol, 2011. **13**(8): p. 914-923.
108. Harrison, M.S., et al., *A mechanism for retromer endosomal coat complex assembly with cargo.* Proc Natl Acad Sci U S A, 2014. **111**(1): p. 267-72.

109. Tabuchi, M., et al., *Retromer-mediated direct sorting is required for proper endosomal recycling of the mammalian iron transporter DMT1.* J Cell Sci, 2010. **123**(Pt 5): p. 756-66.
110. Chen, C., et al., *Snx3 regulates recycling of the transferrin receptor and iron assimilation.* Cell Metab, 2013. **17**(3): p. 343-52.
111. Steinberg, F., et al., *A global analysis of SNX27-retromer assembly and cargo specificity reveals a function in glucose and metal ion transport.* Nat Cell Biol, 2013. **15**(5): p. 461-71.
112. Gallon, M., et al., *A unique PDZ domain and arrestin-like fold interaction reveals mechanistic details of endocytic recycling by SNX27-retromer.* Proc Natl Acad Sci U S A, 2014. **111**(35): p. E3604-13.
113. Ghai, R., et al., *Structural basis for endosomal trafficking of diverse transmembrane cargos by PX-FERM proteins.* Proc Natl Acad Sci U S A, 2013. **110**(8): p. E643-52.
114. Priya, A., et al., *Molecular insights into Rab7-mediated endosomal recruitment of core retromer: deciphering the role of Vps26 and Vps35.* Traffic, 2015. **16**(1): p. 68-84.
115. Jimenez-Orgaz, A., et al., *Control of RAB7 activity and localization through the retromer-TBC1D5 complex enables RAB7-dependent mitophagy.* Embo j, 2018. **37**(2): p. 235-254.
116. Seaman, M.N., et al., *Membrane recruitment of the cargo-selective retromer subcomplex is catalysed by the small GTPase Rab7 and inhibited by the Rab-GAP TBC1D5.* J Cell Sci, 2009. **122**(Pt 14): p. 2371-82.
117. Seaman, M.N.J., A.S. Mukadam, and S.Y. Breusegem, *Inhibition of TBC1D5 activates Rab7a and can enhance the function of the retromer cargo-selective complex.* J Cell Sci, 2018. **131**(12).
118. Sullivan, C.P., et al., *Retromer disruption promotes amyloidogenic APP processing.* Neurobiol Dis, 2011. **43**(2): p. 338-45.
119. Klein, C. and A. Westenberger, *Genetics of Parkinson's disease.* Cold Spring Harb Perspect Med, 2012. **2**(1): p. a008888.
120. Bekris, L.M., et al., *Genetics of Alzheimer disease.* J Geriatr Psychiatry Neurol, 2010. **23**(4): p. 213-27.
121. Tanzi, R.E., *The genetics of Alzheimer disease.* Cold Spring Harb Perspect Med, 2012. **2**(10).
122. Selkoe, D.J., *The cell biology of beta-amyloid precursor protein and presenilin in Alzheimer's disease.* Trends Cell Biol, 1998. **8**(11): p. 447-53.
123. Spillantini, M.G., et al., *Alpha-synuclein in Lewy bodies.* Nature, 1997. **388**(6645): p. 839-40.
124. Vilariño-Güell, C., et al., *VPS35 mutations in Parkinson disease.* Am J Hum Genet, 2011. **89**(1): p. 162-7.
125. Zimprich, A., et al., *A mutation in VPS35, encoding a subunit of the retromer complex, causes late-onset Parkinson disease.* Am J Hum Genet, 2011. **89**(1): p. 168-75.
126. Small, S.A., et al., *Model-guided microarray implicates the retromer complex in Alzheimer's disease.* Ann Neurol, 2005. **58**(6): p. 909-19.

127. Zhang, H., et al., *The Retromer Complex and Sorting Nexins in Neurodegenerative Diseases.* Frontiers in Aging Neuroscience, 2018. **10**(79).
128. Wang, X., et al., *Sorting nexin 27 regulates Aβ production through modulating γ-secretase activity.* Cell Rep, 2014. **9**(3): p. 1023-33.
129. Huang, T.Y., et al., *SNX27 and SORLA Interact to Reduce Amyloidogenic Subcellular Distribution and Processing of Amyloid Precursor Protein.* J Neurosci, 2016. **36**(30): p. 7996-8011.
130. Lee, J., et al., *Adaptor protein sorting nexin 17 regulates amyloid precursor protein trafficking and processing in the early endosomes.* J Biol Chem, 2008. **283**(17): p. 11501-8.
131. Ueda, N., et al., *Retromer and Rab2-dependent trafficking mediate PS1 degradation by proteasomes in endocytic disturbance.* J Neurochem, 2016. **137**(4): p. 647-58.
132. Kanatsu, K., et al., *Retrograde transport of γ-secretase from endosomes to the trans-Golgi network regulates Aβ42 production.* J Neurochem, 2018. **147**(1): p. 110-123.
133. Joliot, A., et al., *Antennapedia homeobox peptide regulates neural morphogenesis.* Proc Natl Acad Sci U S A, 1991. **88**(5): p. 1864-8.
134. Derossi, D., et al., *Cell internalization of the third helix of the Antennapedia homeodomain is receptor-independent.* J Biol Chem, 1996. **271**(30): p. 18188-93.
135. Quartararo, J.S., et al., *A bicyclic peptide scaffold promotes phosphotyrosine mimicry and cellular uptake.* Bioorg Med Chem, 2014. **22**(22): p. 6387-91.
136. Peraro, L. and J.A. Kritzer, *Emerging Methods and Design Principles for Cell-Penetrant Peptides.* Angew Chem Int Ed Engl, 2018. **57**(37): p. 11868-11881.
137. Joliot, A., et al., *Antennapedia homeobox peptide regulates neural morphogenesis.* Proceedings of the National Academy of Sciences, 1991. **88**(5): p. 1864-1868.
138. Faust, T.B., et al., *Making Sense of Multifunctional Proteins: Human Immunodeficiency Virus Type 1 Accessory and Regulatory Proteins and Connections to Transcription.* Annual review of virology, 2017. **4**(1): p. 241-260.
139. Kurrikoff, K., M. Gestin, and Ü. Langel, *Recent in vivo advances in cell-penetrating peptide-assisted drug delivery.* Expert Opin Drug Deliv, 2016. **13**(3): p. 373-87.
140. Nakase, I., et al., *Accumulation of arginine-rich cell-penetrating peptides in tumors and the potential for anticancer drug delivery in vivo.* J Control Release, 2012. **159**(2): p. 181-8.
141. Löfgren, K., et al., *Antiprion properties of prion protein-derived cell-penetrating peptides.* Faseb j, 2008. **22**(7): p. 2177-84.
142. Pei, D. and M. Buyanova, *Overcoming Endosomal Entrapment in Drug Delivery.* Bioconjug Chem, 2019. **30**(2): p. 273-283.
143. Richard, J.P., et al., *Cell-penetrating peptides. A reevaluation of the mechanism of cellular uptake.* J Biol Chem, 2003. **278**(1): p. 585-90.
144. Hällbrink, M., et al., *Uptake of cell-penetrating peptides is dependent on peptide-to-cell ratio rather than on peptide concentration.* Biochim Biophys Acta, 2004. **1667**(2): p. 222-8.

145. Hirose, H., et al., *Transient focal membrane deformation induced by arginine-rich peptides leads to their direct penetration into cells.* Mol Ther, 2012. **20**(5): p. 984-93.
146. Palm-Apergi, C., P. Lönn, and S.F. Dowdy, *Do cell-penetrating peptides actually "penetrate" cellular membranes?* Mol Ther, 2012. **20**(4): p. 695-7.
147. Deprey, K., et al., *Trapped! A Critical Evaluation of Methods for Measuring Total Cellular Uptake versus Cytosolic Localization.* Bioconjug Chem, 2019. **30**(4): p. 1006-1027.
148. Fuchs, S.M. and R.T. Raines, *Pathway for polyarginine entry into mammalian cells.* Biochemistry, 2004. **43**(9): p. 2438-44.
149. Qian, Z., et al., *Discovery and Mechanism of Highly Efficient Cyclic Cell-Penetrating Peptides.* Biochemistry, 2016. **55**(18): p. 2601-12.
150. Danielsen, E.M. and G.H. Hansen, *Impact of cell-penetrating peptides (CPPs) melittin and Hiv-1 Tat on the enterocyte brush border using a mucosal explant system.* Biochim Biophys Acta Biomembr, 2018. **1860**(8): p. 1589-1599.
151. Vermeulen, L.M.P., et al., *Endosomal Size and Membrane Leakiness Influence Proton Sponge-Based Rupture of Endosomal Vesicles.* ACS Nano, 2018. **12**(3): p. 2332-2345.
152. Walker, L.R., H.A. Hussein, and S.M. Akula, *Subcellular fractionation method to study endosomal trafficking of Kaposi's sarcoma-associated herpesvirus.* Cell Biosci, 2016. **6**: p. 1.
153. Lee, Y.H., H.T. Tan, and M.C. Chung, *Subcellular fractionation methods and strategies for proteomics.* Proteomics, 2010. **10**(22): p. 3935-56.
154. Murphy, R.F., S. Powers, and C.R. Cantor, *Endosome pH measured in single cells by dual fluorescence flow cytometry: rapid acidification of insulin to pH 6.* J Cell Biol, 1984. **98**(5): p. 1757-62.
155. Qian, Z., P.G. Dougherty, and D. Pei, *Monitoring the cytosolic entry of cell-penetrating peptides using a pH-sensitive fluorophore.* Chem Commun (Camb), 2015. **51**(11): p. 2162-5.
156. Zhou, Z., G. Bi, and J.M. Zhou, *Luciferase Complementation Assay for Protein-Protein Interactions in Plants.* Curr Protoc Plant Biol, 2018. **3**(1): p. 42-50.
157. Cabantous, S., T.C. Terwilliger, and G.S. Waldo, *Protein tagging and detection with engineered self-assembling fragments of green fluorescent protein.* Nat Biotechnol, 2005. **23**(1): p. 102-7.
158. Johnsson, N. and A. Varshavsky, *Split ubiquitin as a sensor of protein interactions in vivo.* Proc Natl Acad Sci U S A, 1994. **91**(22): p. 10340-4.
159. Falnes, P.O., et al., *Farnesylation of CaaX-tagged diphtheria toxin A-fragment as a measure of transfer to the cytosol.* Biochemistry, 1995. **34**(35): p. 11152-9.
160. Beckett, D., E. Kovaleva, and P.J. Schatz, *A minimal peptide substrate in biotin holoenzyme synthetase-catalyzed biotinylation.* Protein Sci, 1999. **8**(4): p. 921-9.
161. Schatz, P.J., *Use of peptide libraries to map the substrate specificity of a peptide-modifying enzyme: a 13 residue consensus peptide specifies biotinylation in Escherichia coli.* Biotechnology (N Y), 1993. **11**(10): p. 1138-43.
162. Chen, I., et al., *Site-specific labeling of cell surface proteins with biophysical probes using biotin ligase.* Nat Methods, 2005. **2**(2): p. 99-104.

163. Fairhead, M. and M. Howarth, *Site-specific biotinylation of purified proteins using BirA.* Methods Mol Biol, 2015. **1266**: p. 171-84.
164. Kämper, N., et al., *A membrane-destabilizing peptide in capsid protein L2 is required for egress of papillomavirus genomes from endosomes.* J Virol, 2006. **80**(2): p. 759-68.
165. Milech, N., et al., *GFP-complementation assay to detect functional CPP and protein delivery into living cells.* Sci Rep, 2015. **5**: p. 18329.
166. Chen, A.C., et al., *Aph-1 associates directly with full-length and C-terminal fragments of gamma-secretase substrates.* J Biol Chem, 2010. **285**(15): p. 11378-91.
167. Barthet, G., et al., *Inhibitors of γ-secretase stabilize the complex and differentially affect processing of amyloid precursor protein and other substrates.* Faseb j, 2011. **25**(9): p. 2937-46.
168. Buck, C.B., et al., *Generation of HPV pseudovirions using transfection and their use in neutralization assays.* Methods Mol Med, 2005. **119**: p. 445-62.
169. Buck, C.B., et al., *Maturation of papillomavirus capsids.* J Virol, 2005. **79**(5): p. 2839-46.
170. Lemmon, M.A., et al., *Glycophorin A dimerization is driven by specific interactions between transmembrane alpha-helices.* J Biol Chem, 1992. **267**(11): p. 7683-9.
171. Tamm, L.K., et al., *Structure and function of membrane fusion peptides.* Biopolymers, 2002. **66**(4): p. 249-60.
172. Cross, K.J., et al., *Composition and functions of the influenza fusion peptide.* Protein Pept Lett, 2009. **16**(7): p. 766-78.
173. Lorieau, J.L., J.M. Louis, and A. Bax, *The complete influenza hemagglutinin fusion domain adopts a tight helical hairpin arrangement at the lipid:water interface.* Proc Natl Acad Sci U S A, 2010. **107**(25): p. 11341-6.
174. Hunt, J.F., et al., *Spontaneous, pH-dependent membrane insertion of a transbilayer alpha-helix.* Biochemistry, 1997. **36**(49): p. 15177-92.
175. Weerakkody, D., et al., *Family of pH (low) insertion peptides for tumor targeting.* Proceedings of the National Academy of Sciences, 2013. **110**(15): p. 5834.
176. Szaruga, M., et al., *Alzheimer's-Causing Mutations Shift Aβ Length by Destabilizing γ-Secretase-Aβn Interactions.* Cell, 2017. **170**(3): p. 443-456.e14.
177. Xie, J., et al., *Retromer stabilizes transient membrane insertion of L2 capsid protein during retrograde entry of human papillomavirus.* Sci Adv, 2021. **7**(27).
178. Ando, M., et al., *VPS35 mutation in Japanese patients with typical Parkinson's disease.* Mov Disord, 2012. **27**(11): p. 1413-7.
179. Fujioka, S., et al., *Update on novel familial forms of Parkinson's disease and multiple system atrophy.* Parkinsonism Relat Disord, 2014. **20 Suppl 1**(0 1): p. S29-34.
180. Follett, J., et al., *The Vps35 D620N mutation linked to Parkinson's disease disrupts the cargo sorting function of retromer.* Traffic, 2014. **15**(2): p. 230-44.
181. Mohan, M. and G.D. Mellick, *Role of the VPS35 D620N mutation in Parkinson's disease.* Parkinsonism & Related Disorders, 2017. **36**: p. 10-18.

182. Baker, J.A., et al., *Charged residues next to transmembrane regions revisited: "Positive-inside rule" is complemented by the "negative inside depletion/outside enrichment rule".* BMC Biol, 2017. **15**(1): p. 66.
183. Cymer, F., G. von Heijne, and S.H. White, *Mechanisms of integral membrane protein insertion and folding.* J Mol Biol, 2015. **427**(5): p. 999-1022.
184. White, J.M., et al., *Structures and mechanisms of viral membrane fusion proteins: multiple variations on a common theme.* Crit Rev Biochem Mol Biol, 2008. **43**(3): p. 189-219.
185. Rhee, H.-W., et al., *Proteomic Mapping of Mitochondria in Living Cells via Spatially-Restricted Enzymatic Tagging.* Science (New York, N.Y.), 2013. **339**(6125): p. 1328-1331.
186. Cronan, J.E., Jr., *Biotination of proteins in vivo. A post-translational modification to label, purify, and study proteins.* J Biol Chem, 1990. **265**(18): p. 10327-33.
187. Roux, K.J., et al., *A promiscuous biotin ligase fusion protein identifies proximal and interacting proteins in mammalian cells.* J Cell Biol, 2012. **196**(6): p. 801-10.
188. Kotani, N., et al., *Biochemical visualization of cell surface molecular clustering in living cells.* Proc Natl Acad Sci U S A, 2008. **105**(21): p. 7405-9.
189. Martell, J.D., et al., *Engineered ascorbate peroxidase as a genetically encoded reporter for electron microscopy.* Nat Biotechnol, 2012. **30**(11): p. 1143-8.
190. Surviladze, Z., A. Dziduszko, and M.A. Ozbun, *Essential Roles for Soluble Virion-Associated Heparan Sulfonated Proteoglycans and Growth Factors in Human Papillomavirus Infections.* PLoS Pathogens, 2012. **8**(2): p. e1002519.
191. Deverson, E.V., et al., *MHC class II region encoding proteins related to the multidrug resistance family of transmembrane transporters.* Nature, 1990. **348**(6303): p. 738-41.
192. Monaco, J.J., S. Cho, and M. Attaya, *Transport protein genes in the murine MHC: possible implications for antigen processing.* Science, 1990. **250**(4988): p. 1723-6.
193. Spies, T., et al., *A gene in the human major histocompatibility complex class II region controlling the class I antigen presentation pathway.* Nature, 1990. **348**(6303): p. 744-7.
194. Trowsdale, J., et al., *Sequences encoded in the class II region of the MHC related to the 'ABC' superfamily of transporters.* Nature, 1990. **348**(6303): p. 741-4.
195. Neefjes, J.J., F. Momburg, and G.J. Hammerling, *Selective and ATP-dependent translocation of peptides by the MHC-encoded transporter.* Science, 1993. **261**(5122): p. 769-71.
196. Androlewicz, M.J., et al., *Characteristics of peptide and major histocompatibility complex class I/beta 2-microglobulin binding to the transporters associated with antigen processing (TAP1 and TAP2).* Proc Natl Acad Sci U S A, 1994. **91**(26): p. 12716-20.
197. Sadasivan, B., et al., *Roles for calreticulin and a novel glycoprotein, tapasin, in the interaction of MHC class I molecules with TAP.* Immunity, 1996. **5**(2): p. 103-14.
198. Ortmann, B., et al., *A critical role for tapasin in the assembly and function of multimeric MHC class I-TAP complexes.* Science, 1997. **277**(5330): p. 1306-9.

199. Wearsch, P.A. and P. Cresswell, *Selective loading of high-affinity peptides onto major histocompatibility complex class I molecules by the tapasin-ERp57 heterodimer.* Nat Immunol, 2007. **8**(8): p. 873-81.
200. Hulpke, S. and R. Tampe, *The MHC I loading complex: a multitasking machinery in adaptive immunity.* Trends Biochem Sci, 2013. **38**(8): p. 412-20.
201. Montague, T.G., et al., *CHOPCHOP: a CRISPR/Cas9 and TALEN web tool for genome editing.* Nucleic Acids Res, 2014. **42**(Web Server issue): p. W401-7.
202. Labun, K., et al., *CHOPCHOP v2: a web tool for the next generation of CRISPR genome engineering.* Nucleic Acids Res, 2016. **44**(W1): p. W272-6.
203. Labun, K., et al., *CHOPCHOP v3: expanding the CRISPR web toolbox beyond genome editing.* Nucleic Acids Res, 2019. **47**(W1): p. W171-w174.
204. Sanjana, N.E., O. Shalem, and F. Zhang, *Improved vectors and genome-wide libraries for CRISPR screening.* Nat Methods, 2014. **11**(8): p. 783-784.
205. Biryukov, J. and C. Meyers, *Papillomavirus Infectious Pathways: A Comparison of Systems.* Viruses, 2015. **7**(8): p. 4303-25.
206. McLaughlin-Drubin, M.E., N.D. Christensen, and C. Meyers, *Propagation, infection, and neutralization of authentic HPV16 virus.* Virology, 2004. **322**(2): p. 213-9.
207. McLaughlin-Drubin, M.E., et al., *Human papillomavirus type 45 propagation, infection, and neutralization.* Virology, 2003. **312**(1): p. 1-7.
208. Meyers, C., et al., *Biosynthesis of human papillomavirus from a continuous cell line upon epithelial differentiation.* Science, 1992. **257**(5072): p. 971-3.
209. Chen, X.S., et al., *Structure of small virus-like particles assembled from the L1 protein of human papillomavirus 16.* Mol Cell, 2000. **5**(3): p. 557-67.
210. Hagensee, M.E., N. Yaegashi, and D.A. Galloway, *Self-assembly of human papillomavirus type 1 capsids by expression of the L1 protein alone or by coexpression of the L1 and L2 capsid proteins.* J Virol, 1993. **67**(1): p. 315-22.
211. Kirnbauer, R., et al., *Papillomavirus L1 major capsid protein self-assembles into virus-like particles that are highly immunogenic.* Proc Natl Acad Sci U S A, 1992. **89**(24): p. 12180-4.
212. Kirnbauer, R., et al., *Efficient self-assembly of human papillomavirus type 16 L1 and L1-L2 into virus-like particles.* J Virol, 1993. **67**(12): p. 6929-36.
213. Rose, R.C., et al., *Expression of human papillomavirus type 11 L1 protein in insect cells: in vivo and in vitro assembly of viruslike particles.* J Virol, 1993. **67**(4): p. 1936-44.
214. Buck, C.B., et al., *Efficient intracellular assembly of papillomaviral vectors.* J Virol, 2004. **78**(2): p. 751-7.
215. Embers, M.E., et al., *Differential antibody responses to a distinct region of human papillomavirus minor capsid proteins.* Vaccine, 2004. **22**(5-6): p. 670-80.
216. Gambhira, R., et al., *A protective and broadly cross-neutralizing epitope of human papillomavirus L2.* J Virol, 2007. **81**(24): p. 13927-31.
217. Fang, N.X., I.H. Frazer, and G.J. Fernando, *Differences in the post-translational modifications of human papillomavirus type 6b major capsid protein expressed from a baculovirus system compared with a vaccinia virus system.* Biotechnol Appl Biochem, 2000. **32**(1): p. 27-33.